STRESS-DEPENDENT REGULATION OF A MAJOR NODE OF THE INSULIN-LIKE PEPTIDE NETWORK THAT MODULATES SURVIVAL

by

RASHMI CHANDRA

DISSERTATION

Submitted to the Graduate School

of Wayne State University,

Detroit, Michigan

in partial fulfillment of the requirements

for the degree of

DOCTOR OF PHILOSOPHY

2019

MAJOR: BIOLOGY

Approved By:

_____

Advisor Date

_____

_____

_____

DEDICATION

For Dr. Joy Alcedo,

Without whom this thesis would not have begun at all,

And who turned this adventure into a journey of discoveries

For all the teachers who helped me improve each day,

Beginning with my parents, grandparents, Bharati di, and the rest of the family

&

For Dr. Subrata Ghosh, Sensei, and Professor Shonku

Who made learning an adventure through fictions and facts

To Gargi and Amrita,

My 3 AM friends with a plan

In loving memory of Pisha and Bordadu,

Who are the light of my life and the shadows of my soul

ACKNOWLEDGEMENTS

During this journey of PhD, I found a teacher, friend, philosopher and a wise pillar of support in the form of Dr. Joy Alcedo. I acknowledge her mentorship with my sincerest gratitude. Her allowance for scientific freedom has led to this thesis, therefore, I will always miss the libertarian air of Science wafting in the Alcedo lab.

I express my sincere appreciation for all the lab members of the Alcedo lab for their valuable comments, timely support, and frank criticisms that made this project better each day. A special shout-out to Zahabiya Husain for her contributions. Beside his support, Shashwat Mishra's gift minutes before my first talk in *CeNeuro* will always remain precious. I thank Deniz Sifoglu and Lisa Li for their help in my papers. I would like to cheer and thank the brilliant undergraduates of Alcedo lab: Sean Shephard, Ian Clark and Tiffany Burris, for showing indomitable spirit in tackling questions fearlessly. I would like to acknowledge Kelsey Marbach for the good times spent together, and for the day when we dropped-out from the grid of telecommunications. Since Bianca Pereira is inheriting the perils of my projects, I wish her all my best and thank her for being a part of this journey.

I extend my gratefulness to my thesis committee members: Dr. David Njus, Dr. Markus Friedrich and Dr. Sokol Todi. Their support, advice and constructive criticisms made my thesis better each day, and therefore, their help cannot be penned down in words. I will always cherish the discussions that followed after each committee meeting, those discussions drove this thesis.

I would like to recognize the positive impact of few thoughtful discussions with Dr. Martin Chalfie, whose comments turned one data into an entire chapter of this thesis. I would like to acknowledge our collaborators Dr. Queelim Ch'ng, Dr. Yun Zhang, Dr. Piali Sengupta, Dr. Miriam Goodman, Dr. Stephen Eimer, Dr. Shohei Mitani and and the tight-knit *C. elegans* community for all their help in my projects. I would like to take this opportunity to thank Dr. Miriam Greenberg and Dr. Timothy Stemmler for their constant

encouragement and inspiring advice that made life better in many aspects. I will be thankful to Dr. Lori Pile and Dr. Victoria Meller for providing help during the difficult times. The constant encouragement from all the teachers of this department was very welcoming and helpful. At the end of the day, it was always a pleasure to walk home with Dr. Ann Sodja (pronounced Sodya) with discussions strictly non-scientific. I would like to express my gratitude for Linda Van Thiel, Michelle Serryn and Krystyn Purvis for all their help during teaching to accommodate the diverse need of students, and for making 'teaching' fun. The entire crew of OISS, Science Stores, Graduate School and the Biological Sciences Office deserve a standing ovation for keeping the experiments rolling and the paperwork updated for all of us. Rick Lilich and Rob Patten will be always appreciated as the 'Microscope Guys' who made Science possible microscopically, on a 'one day every day' belief.

I take pride in acknowledging the friends I made during this journey. Satarupa, Nirmalya, and master Evaan, will always remain exceptional in making this journey thrilling. Thanking Valerie Barnes and her family will not suffice for her generosities during my PhD. I would also like to thank the kind parents of my friends for replenishing my life with food and love during dire times. Poorna, Anura, Rania, Heather, Pablo, Praneet, Manish and Keanna will always remain close to my heart for the beautiful friendship that burgeoned from this journey. Though we are friends for an epoch, this is my first opportunity to thank Arkopaul a.k.a MOM (Move-Out Master), for his never-ending wisecracks bringing comic relief and smiles. Thanking Nivedita for her unconditional support and love will be an injustice to an elder sister, therefore, I dare not try. I am lucky to have Tanni Mandal and Aramita Dutta Banerjee in my life, they always inspire me to stretch for the extra mile, which matters at the end. I thank all my friends whom I met every day during work or otherwise, those five-minute respites were amazingly refreshing while juggling experiments and teaching.

When my father R. P. Chandra, reads this thesis, I am sure I will have a final count on how many framing rules of photography I broke, in the name of Science. Last but not the least, I am able to complete this thesis because of the sacrifices made by my mother Bandana Chandra. In a way, my mother and I grew up together, we both learned to live independently during my PhD. This thesis is an earnest attempt to recognize all her sacrifices, love, and respect for my choices.

PREFACE

You have made your way from worm to man,

and much within you is still worm

---- F. Nietzsche, Thus Spoke Zarathustra, Prologue ----

TABLE OF CONTENTS

LIST OF TABLES

LIST OF FIGURES

Supplemental figures

CHAPTER 1 INTRODUCTION

A brief history of neuroscience

In the ancient Indian Vedic texts, the human mind is described to be the source of consciousness necessary to assess 'self' in response to the environment. The arguments postulated in the second of the four Vedas, known as the *Rigveda*, were pioneering work in human civilization that philosophically described the existence of our mind controlling our body through five senses (in the following order): touch, vision, hearing, smell, and taste (Campbell, 2002; Chandler, 2011; Kak, 1997). The philosophical concept of consciousness or mindfulness gave birth to meditation, a technique developed to coordinate our mind and body, and became a feature of many civilizations over the history of humanity, even though the biological basis of consciousness was unknown (Chandler, 2011).

Centuries later in the Hellenistic era around 5th Century BC, highlighted for its contribution to medicine and philosophy, the Hippocratic texts described the ancient link between our mind and body. They were the first to coin the term "neuron", meaning tendon or sinew that tied our body together. About 2500 years later, after persistent efforts and differing views of numerous philosophers and scientists and with the advancement of technology, it is now known that the human brain makes conscious choices, about which we deliberate every day. These choices depend on the neuronal circuitry of the brain; and for each response we derive, there is a circuit of neurons behind it (Cajal, 1906; Crick and Koch, 1990; Crick and Koch, 1998). Since antiquity, the search for insights into our mind and the dissection of our brain has been a quest for many civilizations. Hence, it is crucial to understand the reason for which this pursuit enjoys scientific attention and the present perspective on how the experiments on animal consciousness, physiology and behavior are combined to gain insight into our minds.

At the crossroad of consciousness

One of the most challenging questions that has intrigued many scientists is how we make a conscious choice. Since the brain controls our choices, contemporary neuroscience has focused on dissecting the circuits required to produce specific behaviors (Crick and Koch, 1990; Crick and Koch, 1998). This is because of the general premise that our voluntary and involuntary behaviors are the reflection of the neural connections and their activities in our brain. Therefore, behavior becomes a good read-out of the conscious mind that modulates our physiology (Edelman et al., 2011; National_Research_Council, 1989).

For instance, visual consciousness, which is described as the ability to pay attention to visual cues and adjust to the environment, is a classic example that shows how multiple inputs culminate to form a pattern of behavior (Crick and Koch, 1995; Crick and Koch, 1998). Let us suppose, we want to avoid a puddle on the street. The information from the primary and accessory visual cortices will be processed in the limbic system and communicated to the motor cortex. Finally, through the activities of our peripheral nerves, muscles and bones, we will avoid the puddle. Similarly, if we want to ignore the puddle, then another set of reflexes will allow us to walk through the puddle. Therefore, Hamlet's '*to be or not to be'* is a reflex question, evaluating a choice that involves neural circuit activities and communication between neurons and the rest of the body.

The next question is whether other animals also have consciousness. '*The problem of other minds*' (Crick and Koch, 1990; Crick and Koch, 1998; De Sousa, 2013) is a highly debated topic because animal consciousness differs from human consciousness in many different ways. This debate arises because without the human mind as a reference, it is difficult to ascertain animal consciousness. If we account for human consciousness as a reference point of comparison for animal consciousness, then consciousness becomes a subjective matter (Crick and Koch, 1990; Crick and Koch,

1998; De Sousa, 2013; Edelman et al., 2011; Koch et al., 2016). Nonetheless, one cannot deny that a behavioral response to food or adverse environment is a reflection of what an animal is thinking at a specific time and context and not subject to human bias (Koch et al., 2016; Seth et al., 2008). Since behavior is an output of conscious thoughts established by specific neurons that communicate with each other to pass a chain of commands to the rest of the body, it is safe to assume that there is a circuit of neurons behind animal consciousness (Crick and Koch, 1998). Therefore, any behaviors and consequent physiological changes undertaken by animals to adapt to the given environment is a result of conscious choice directed by neurons.

As studies with humans, non-human primates and rodents have already elaborated on conscious behavioral choices (Boly et al., 2017; Edelman et al., 2011; Koch et al., 2016; Rees et al., 2002; Tiengo, 2003; Tononi and Koch, 2008), I consider insects, worms and elephants for further illustrations of animal consciousness. Dragonflies use their exquisite sense of selective attention to navigate themselves precisely through diverse environments in search of food as a flock (Frye, 2013). However, honey bees, despite being social creatures, lack empathic understanding while collecting flower nectars for storage in their hives (Tie, 1997). Therefore, the different types of food-seeking techniques adopted by dragonflies and honey bees are conscious choices of behavior (Frye, 2013; Tie, 1997; Tononi and Koch, 2008; Wiederman and O'Carroll, 2013).

Another display of conscious choice in invertebrates is learning to avoid the food that makes the worm *C. elegans* ill (Zhang et al., 2005) or adopting a different physiological state when the worm faces adverse conditions (Cassada and Russell, 1975; Golden and Riddle, 1984). For instance, in response to decreasing food and increasing population density or high temperatures, *C. elegans* becomes a dauer, a growth-arrested form that represents a resilient physiological state (Cassada and Russell, 1975; Golden and Riddle, 1984). When environments improve, dauers become adults to resume their reproductive

physiological form. This set of decisions, which is only undertaken by a major subset, but not all, of *C. elegans* under a given environment, is a model of objective requirement, *i.e.*, survival during stress, and is again independent of human bias.

In experiments that explore animal consciousness from a psychological perspective, elephants showed self-awareness in front of mirrors, because their behavior primarily focused on impersonating themselves or the creature they saw in the mirror (Plotnik et al., 2010; Plotnik et al., 2006). This also holds true for cats and dogs (Cazzolla Gatti, 2016). Therefore, animal consciousness can be measured by behavioral outputs, which are a culmination of psychological, molecular and physiological changes within the animals (Bickle, 2007; Hameroff, 1994).

Many animals exhibit conscious behaviors, but not all animals can appropriately evaluate all aspects of conscious choices. It is advantageous to study the psychological basis of consciousness in humans, but it is also very difficult to explore its molecular basis in us. Non-human primates are highly informative in understanding the psychological basis of social or collective conscious decisions in adverse situations, but again the cellular and molecular circuits for such conscious decisions are easier to explore in simpler animals, like flies and worms. Due to the ease of its culture conditions, largely mapped nervous system, the similarity to other animals of its neural communication processes and the existence of an excellent genetic toolkit, I chose the worm *C. elegans* to understand how an animal consciously decides to become a dauer and exit from dauer (Fig. 1.1).

Dauers

The nematode *C. elegans* develops through four successive larval stages to become an adult, which will lay eggs that will continue through the life cycle of the animal (Fig. 1.1). However, when the worms face adverse environmental situations during development, they decide to become dauers (Cassada and Russell, 1975). The conscious choice of being a dauer largely occurs in the first larval stage, L1, and depends on

environmental stress cues, such as a combination of food scarcity and increased population density or high temperatures (Cassada and Russell, 1975; Golden and Riddle, 1984). The harsh environmental cues are interpreted by sensory neurons that direct the L1s to molt into pre-dauers and dauers (Bargmann and Horvitz, 1991; Riddle et al., 1981). However, it should be noted that not all L1s choose to become dauers. About seventy percent of the L1 population enters the dauer program, whereas the rest starve and arrest as L1 or continue development to L2 (Golden and Riddle, 1984; Riddle et al., 1981). Since not all L1s switch into the dauer program under adverse conditions, it is safe to assume that L1s exhibit a conscious choice of molting into a dauer versus staying as a non-dauer larva (Fig 1.1).

Dauer pheromone, which is a mixture of ascarosides and other glycosidic molecules, is secreted throughout an animal's life and indicates the density of the population (Butcher et al., 2007; Jeong et al., 2005; Riddle et al., 1981). When the ratio of dauer pheromone to food increases, L1s make the choice to develop into dauers and retain this arrested physiology until conditions again improve (Golden and Riddle, 1984). When food becomes abundant and the level of dauer pheromone decreases or temperature becomes optimal, dauers molt into the last larval stage, L4, which will develop further into adulthood. The L1 transition into dauer and dauer transition into L4 are developmental choices that reflect the perception of changing environmental cues that influence physiology.

Dauers are distinct in many different ways from their developmental counterpart, L3 (Fig. 1.1), since dauers need to endure stressful environments. Dauers have a mouth that remains plugged, which means they do not eat; dauers are also radially constricted and thinner than L3 (Cassada and Russell, 1975). Since dauer mouths are plugged, their pharynges are remodeled and inactive, and thus do not pump to grind any bacterial food that would normally have been delivered to the intestine (Cassada and Russell, 1975;

Riddle et al., 1981). In addition, dauers develop a special cuticle structure called alae, which are secreted from epithelial tissues (Johnstone, 2000; Singh and Sulston, 1978). The alar ridges run longitudinally and span the entire length of the worm and are believed to help the worms move faster in harsh environments (Cassada and Russell, 1975). Dauer metabolism is also different from L3s: dauers have a higher rate of the glyoxalate cycle, which utilizes lipid sources to provide energy during quiescence, whereas L3s and older animals have higher rates of aerobic respiration and TCA cycle (Wadsworth and Riddle, 1989). Therefore, it is not surprising to find that dauers are radially constricted, because lipid stores in dauers provide energy for survival, which likely leads to the leanness of dauers versus non-dauers. However, it is interesting to note that despite the radial shrinkage of the dauer body, there is no shrinkage in the volume of the nervous system in dauers as compared to those in non-stressed larval stages or adults (http.www.wormatlas/dauer.org). Finally, dauers are also reported to have a global reduction in transcription, which highlights the importance of efficient use of already existing mRNAs in these animals in the effort to conserve energy for survival (Dalley and Golomb, 1992; Snutch and Baillie, 1983). Thus, all these transformations indicate that dauers are very different from the other larval stages or adult worms.

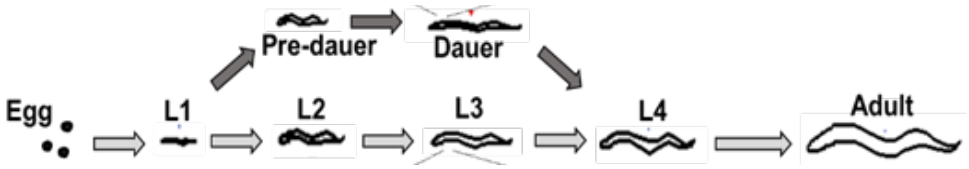

Fig. 1.1: *C. elegans* development. *C. elegans* develops through four larval stages—L1 to L4—to become a reproductive adult. Under stress, such as low food or overcrowding, L1s undergo an alternative developmental pathway—the formation of stress-resistant dauers, instead of L3s. Dauers have an altered metabolism that uses less energy, allowing it to survive until conditions improve. The return of ideal conditions causes dauers to exit to L4s and resume reproductive development (Burnell et al., 2005; Erkut and Kurzchalia, 2015; Feller, 1999; Golden and Riddle, 1984; Wang et al., 2009).

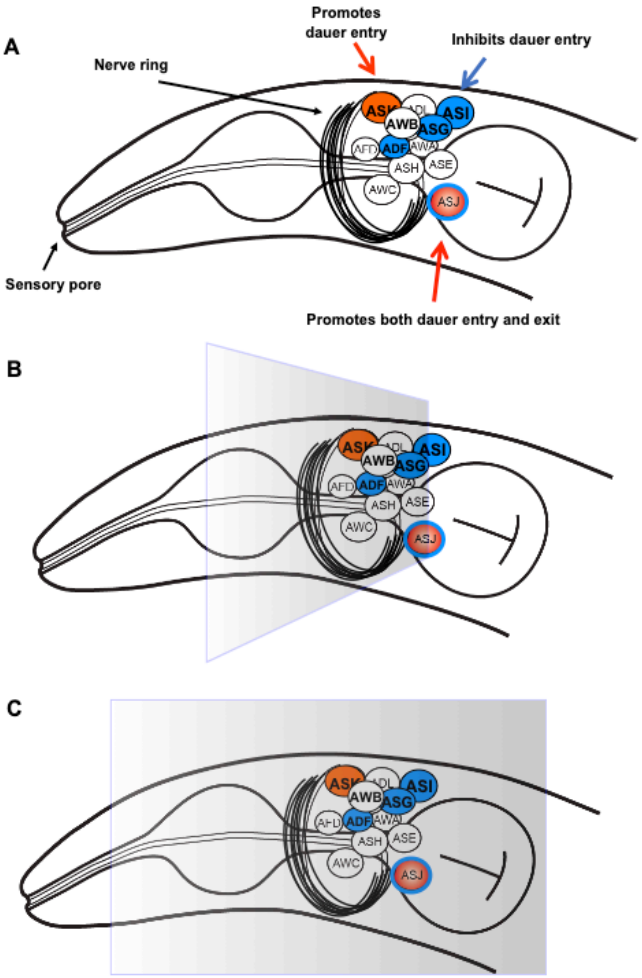

Fig. 1.2: A schema of the *C. elegans* head. (A) The small circles are cell bodies of amphid neurons. Open circles do not participate in the dauer paradigm. Blue neurons inhibit, red neurons promote dauer entry. ASJ is a neuron that has two opposing functions, by stimulating dauer entry and exit. The band-like structure has the axons that represent the nerve ring, while the dendrites are exposed to the environment through the sensory pore, also known as the nose. (B) Cartoon of a transverse section of the worm head. The electron micrographs of the nerve ring (NR) are reported through this angle (White et al, 1986). (C) The longitudinal section shown in this figure should yield transverse sections of the NR, which can depict the gaps between the axonal trajectories and the patterns of the axonal tracts.

If dauers have an altered state of physiology, then do dauers have an altered mind to counter stressful environments? Yes, indeed. The mind of a worm, which encompasses the amphid sensilla and the nerve ring, has been extensively investigated for structural changes; and electron microscopy reveals that the amphid sensilla change in structure when the animals are in dauer (Albert et al., 1981; Albert and Riddle, 1983; White et al., 1986). However, the mapping of the structure of the dauer nerve ring has yet to be completed. Therefore, to understand the structural and molecular bases of the stress-altered worm mind and their implications in the decision to recover from stress has been the aim of my thesis research.

The nervous system of *C. elegans*

C. elegans have two sexes: males and hermaphrodites. The hermaphrodite nervous system has 302 neurons and 56 glial cells, which are connected through chemical and electrical synapses (Shaham, 2006; Ward et al., 1975; White et al., 1986). Males have a larger nervous system with an additional 79 neurons and 36 glial cells, raising their total to 381 neurons and 92 glial cells (Shaham, 2006; Ward et al., 1975; White et al., 1986). The larger nervous system in males provide sensory connections to the male-mating apparatus and to the posterior part of the body. However, most of the neurons in the head region remain similar for both sexes. Out of 302 neurons in hermaphrodites and 381 neurons in males, only eight neurons are hermaphrodite-specific, namely the HSN pair and the VC1-VC6 neurons, and only four neurons are male-specific, namely the head CEM neurons (Albert and Riddle, 1983; Chen et al., 2006; Ward et al., 1975; White et al., 1986).

Amphid sensillum

To achieve complex behavioral outputs from a simple nervous system, *C. elegans* has developed several small sensilla, which include a pair of amphid sensilla, whose neuronal somas are situated adjacent and posterior to the nerve ring [NR; Fig. 1.2; (Ware

et al., 1975; White et al., 1986)]. The amphid somas have dendrites and axons and are thus bipolar in nature [Fig. 1.2A; (Ware et al., 1975; White et al., 1986)]. The amphid somas send (i) axons to the NR, where the axons synapse with other axons, and (ii) dendrites to the amphid pore, where the cilia at the dendritic tips sense the environment near the mouth of the worm [Fig. 1.2A;(White et al., 1978; White et al., 1986)]. The amphid ganglion, situated juxta-posterior to the NR, refers to the group of amphid neuronal cell bodies that have a scant number of synapses, but which remain sheathed in a pouch-like basal lamina of the hypodermis, consistent with the definition of a neural ganglion (Albert and Riddle, 1983; Ward et al., 1975; Ware et al., 1975; White et al., 1986).

The amphid ganglion forms the largest chemosensory organ of the worm. It is comprised of 12 sets of bilaterally symmetrical sensory neurons belonging to at least three different classes of sensory modalities: gustation (ADF, ADL, ASE, ASG, ASI, ASJ and ASK neurons), olfaction (AWA, AWB and AWC neurons), thermosensation (the neuron AFD and, to a minor extent, AWC) and nociception [ASH neurons; (Ware et al., 1975; White et al., 1986)]. These amphid neurons participate in controlling a multitude of physiological pathways, such as the decision to form dauers or avoid harmful odors or food that make the worms sick (Bargmann and Horvitz, 1991; Chalasani et al., 2007).

Interestingly, not all amphid neurons have been shown to participate in different physiological processes, such as the dauer program, longevity or olfactory learning (Fig. 1.2A) (Alcedo and Kenyon, 2004; Bargmann and Horvitz, 1991; Chalasani et al., 2007; Chen et al., 2013). However, multiple amphid neurons can be grouped together based on their functions to form a *'neural code'*. For instance, dauer formation and dauer exit require different sets of amphid neurons. Through the systematic ablations of amphid neurons, ASI, ADF and ASG were shown to inhibit entry into the dauer stage, whereas ASJ and ASK promote dauer entry (Bargmann and Horvitz, 1991; Schackwitz et al., 1996). Since ablation of the ASJ neuron also prevents dauers from exiting, this means that ASJ

promotes exit from dauers (Bargmann and Horvitz, 1991). Besides dauer formation, amphid neurons also participate in other physiological processes. The ablation of ASI, ASG, ASJ and ASK can impact worm longevity (Alcedo and Kenyon, 2004). Loss of ASI or ASG increases survival, whereas loss of ASJ or ASK can decrease survival (Alcedo and Kenyon, 2004). In addition to inhibiting longevity, the amphid neurons AWA and AWC participate in olfaction (Alcedo and Kenyon, 2004; Chalasani et al., 2007). Therefore, there are specific neurons designed to perform specific functions at any given period of time. In other words, the *'neural code'* that controls physiological responses is a possibility, because one particular amphid neuron can perform multiple functions during the lifetime of a worm. This is nicely exemplified by ASJ, which promotes longevity in well-fed adults at 20^{o}C, but it inhibits longevity in food-deprived adults at lower temperatures (Alcedo and Kenyon, 2004; Artan et al., 2016). Moreover, ASJ promotes dauer entry at the L1 decision stage (Golden and Riddle, 1984), but ASJ again changes its function in dauers, when it steers dauers to exit to post-dauer L4s during improved environments [Fig. 1.2A; (Bargmann and Horvitz, 1991; Cornils et al., 2011; Schackwitz et al., 1996)].

The nerve ring

As multicellular organisms evolved, the need to communicate between cells increased. Therefore, specialized cells called neurons have evolved. These neurons and their dendritic and axonal processes are capable of converting chemical signals into electrical signals and vice versa. The first and basic evidence of the nervous system begins with the cnidarians, *e.g.*, the jelly fish, which have a simple nerve net that spans the entire body of the animal (Bosch et al., 2017). In nematodes, the centralization of the nervous system transformed the nerve net into a nerve ring, whereas in flies, mice, monkeys and humans, this centralization led to brain development (Arendt et al., 2016; Burkhardt and Sprecher, 2017; Clark et al., 2019).

The nerve ring of *C. elegans* contains about 180 axons that pass through a ring-like structure, where they form *en passant* synapses with each other [Fig. 1.2A; (Albert and Riddle, 1983; Chen et al., 2006; Ward et al., 1975; Ware et al., 1975; White et al., 1986)]. Because the NR is situated centrally in the head of the worm, is surrounded by several ganglia, like the amphid neurons, and possesses a high number of chemical and electrical synapses, the NR can be considered a primitive brain (Arendt et al., 2016; Burkhardt and Sprecher, 2017; Clark et al., 2019). Yet, the NR is unlike the vertebrate brain as the NR only contains axons, which are from approximately 60% of the neurons in the worm nervous system. Nonetheless, the absence of dendrites in the NR bundle provides an excellent window to understand axonal communication between neurons in the animal brain during stressful and non-stressful conditions.

Although *C. elegans* lacks two basic senses, vision and audition, and thus considered to have an over-simplified nervous system, the general principles of neural communication in *C. elegans* is well conserved and can be compared to the human brain. Therefore, the *C. elegans* NR provides a basic anatomical structure that consists of many neural circuits that can be used to understand the concepts underlying animal consciousness, which can then be extrapolated across species.

Stress resets the senses

The dendrites of amphid neurons sense the environment and signal to the cell bodies, which process and further relay the signals to the NR axon bundle that subsequently transmits the information to the rest of the body (Ware et al., 1975; White et al., 1986). As the animal encounters and adapts to environmental stressors, the dauer nervous system undergoes remodeling compared to that of L3 or the adult (Albert and Riddle, 1983). For instance, the gustatory ASI neuronal dendrite is shortened and loses contact with the environment (Ward et al., 1975). In contrast, together with their glias, the olfactory AWC pair of neuronal dendrites expands and fuses together just below the

plugged mouth (Procko et al., 2011). Meanwhile, the gustatory ASJ neuron neither shortens nor expands its dendrite (Ward et al., 1975), despite being a key neuron that performs dual and paradoxical functions during the dauer program (Bargmann and Horvitz, 1991; Cornils et al., 2011; Schackwitz et al., 1996).

At first glance, the NR of dauers looks similar to that of non-dauers when a worm is transversely sectioned. However, reconstruction of the serial electron micrographs appears to show that the dauer NR has a greater volume than the NR of its developmental counterpart L3 (Ward et al., 1975; White et al., 1986). Under higher magnification of the electron micrographs, sections of individual dauer NR axons (Fig. 1.2B) show that they are broader with little or no space between adjacent axons, unlike non-dauer axons (Ward et al., 1975; White et al., 1986). However, it remains unclear if these differences arise from the angle of the sections (Fig. 1.2B) or from damage incurred during sample preparation for electron microscopy or whether these differences are also visible in the live dauer NR versus the non-dauer NR from all angles (Fig. 1.2 B-C).

As dauers are developmentally arrested counterparts of L3s, one might expect that the dauer nervous system will also be quiescent, but that is not the case. A magnified image of a dauer NR cross-section shows that the dauer NR is full of synaptic vesicles and gap junctions can be found in this link:

[(https://www.wormatlas.org/dauer/neuroanatomy/Images/dneurofig8leg.htm; (Albert and Riddle, 1983; Ward et al., 1975)]. Therefore, this image informs us that dauer NR retains the ability to communicate through synapses and gap junctions to endure and recover from stress when situations permit. Together the above data suggest that dauers do have an altered nervous system that is capable of functioning under adverse situations.

How does the amphid ganglia 'neural code' maintain physiological plasticity?

Since neurons are the means through which the environment influences physiology, the next question is how these neurons communicate to the rest of the body during adverse environments. How do they steer the animal's entire physiology into survival mode, *e.g.*, dauer arrest? How do dauers understand when they should exit to L4s? Environmental insults can stimulate neurons to release substances, such as neuropeptides, which will modulate synaptic strength and plasticity and achieve the optimal physiological response (Ailion et al., 1999).

What are neuropeptides?

Neuropeptides are peptides secreted by neurons from dense core vesicles (Li et al., 1999). The total number of neuropeptide genes in *C. elegans* are beyond one hundred, a feature similar to mammalian systems (Bargmann, 1998). These neuropeptides belong to three key classes: the FMRF-amide (Phe-Met-Arg-Phe-NH_2)-like peptides (FLPs), the insulin-like peptides (ILPs), and the neuropeptides that belong neither to the FLPs nor to the ILPs are termed neuropeptide-like peptides (NLPs) (Li et al., 1999; Li et al., 2003; Pierce et al., 2001). Of the three neuropeptide families, the ILP family has been established as a major regulator of the dauer program, since mutations in the ILP genes have led to altered dauer entry and exit rates (Cornils et al., 2011; Kimura et al., 1997; Li et al., 2003; Pierce et al., 2001).

ILPs and DAF-2/Insulin Receptor

At least some of the ILPs are ligands of the worm insulin receptor DAF-2 (Kimura et al., 1997; Li et al., 2003; Pierce et al., 2001), which is expressed in many different cells, such as neurons, intestinal cells, germ cells and epidermal cells [reviewed in (Kenyon, 2005)]. The neuronal DAF-2 receptor acts nonautonomously on non-neuronal cells to modulate physiology, where a decrease in DAF-2 activity increases dauer formation or

modulates dauer exit, similar to the phenotypes observed when certain combinations of amphid neurons have been ablated (Apfeld and Kenyon, 1998; Bargmann and Horvitz, 1991; Kenyon, 2005). Activation of the DAF-2 receptor leads to activation of the phosphoinositide-3 (PI-3) kinase, which produces phosphatidylinositol 3,4,5-trisphosphate (PIP_3) from phosphatidylinositol (4,5)-bisphosphate (PIP_2) (Mukhopadhyay et al., 2006; Murphy, 2013). PIP_3 recruits the serine/threonine kinases PDK-1, AKT-1, AKT-2 and SGK-1 to the plasma membrane, where PDK-1 phosphorylates and activates

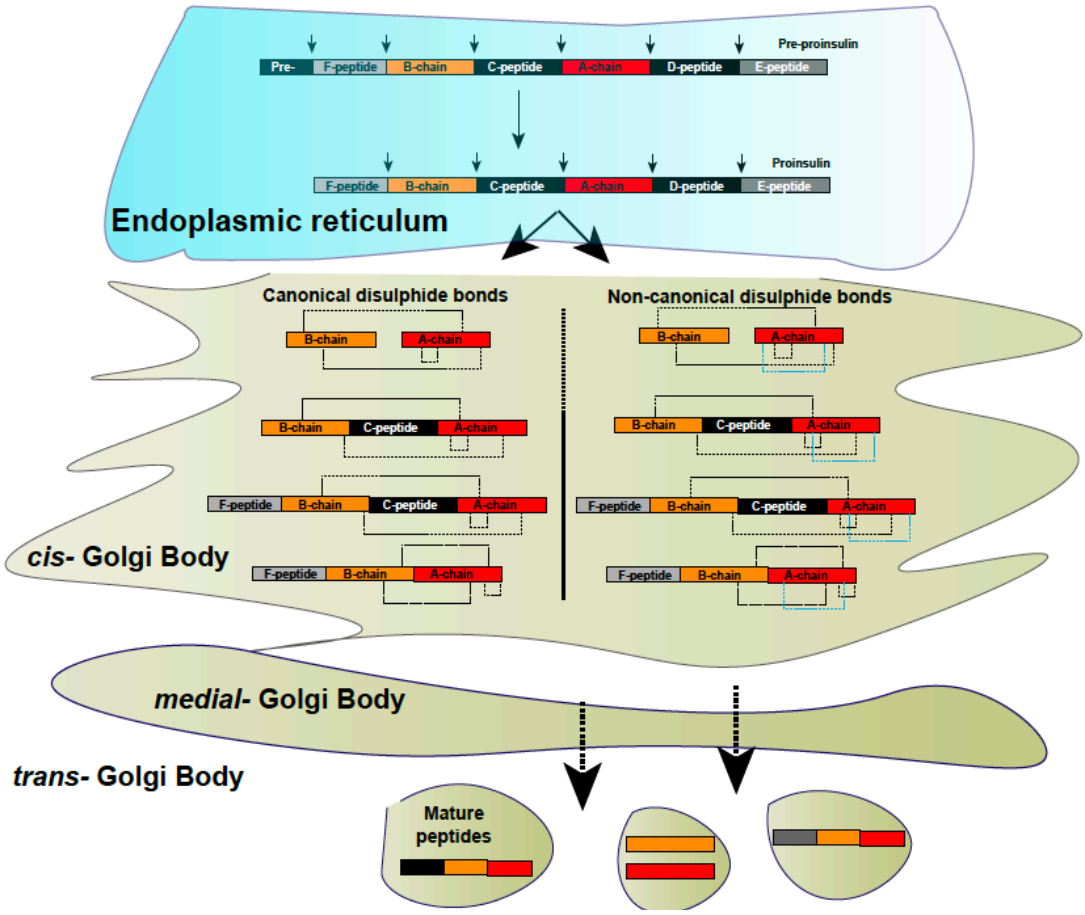

Fig. 1.3: Schematics of the insulin-like peptide processing machinery and the subcellular compartments that participate in processing the ILP peptides. ILPs are translated as pre-propeptides, which are converted to propeptides by the signal peptidase in the endoplasmic reticulum. Propeptides get processed further through proprotein convertases and carboxypeptidases, which occur in the Golgi bodies. Therefore, both endoplasmic reticulum and Golgi bodies are required to give rise to mature peptides. ILPs also form intramolecular and intermolecular disulfide bridges. These ILPs are packaged into dense core vesicles and are transported towards the peripheries of the neurons.

AKT-1, AKT-2 and SGK-1, which consequently phosphorylate DAF-16, a member of the forkhead (FOXO) transcription factor family (Mukhopadhyay et al., 2006; Murphy, 2013). Phosphorylated DAF-16 is sequestered in the cytosol, which would inhibit DAF-16-dependent gene expression (Mukhopadhyay et al., 2006). When ILP agonists are absent or act as antagonists of the DAF-2 receptor, AKT-1/AKT-2-dependent phosphorylation of DAF-16 does not occur, permitting DAF-16 nuclear translocation and the expression of a myriad of target genes (Mukhopadhyay et al., 2006; Murphy, 2013).

Like other neuropeptide families in mammals and *C. elegans*, ILPs are transcribed and translated as pre-proinsulins, which are cleaved by signal peptidases to form proinsulins in the endoplasmic reticulum [ER; Fig. 1.3; (Husson et al., 2006; Steiner, 1998)]. Due to (i) sequence similarities between *C. elegans* ILPs and the insulin, insulin-like growth factors (IGFs) and relaxins of humans and other animals and (ii) the conserved processing machineries, it is considered that the general principles of ILP processing remain fairly similar across species (Bedarkar et al., 1977; Brown et al., 1955; Kimura et al., 1997; Li et al., 2003; Pierce et al., 2001; Rinderknecht and Humbel, 1978). Thus, the 40 *C. elegans* ILPs are predicted to be further cleaved by proprotein convertases and carboxypeptidases and stabilized by a set of disulfide bonds to form the mature peptides [Fig. 1.3; (Jacob and Kaplan, 2003)]. Based on their cysteine residues, the different ILPs in the *C. elegans* genome are expected to undergo extensive processing to give rise to different peptides with different combinations of disulfide bridges (Duret et al., 1998; Fernandes de Abreu et al., 2014; Pierce et al., 2001; Rinderknecht and Humbel, 1978). However, some of the ILPs are proposed to resemble closely the known structures of human insulin, *i.e.*, they contain B and A peptides of variable lengths, which form intermolecular and intramolecular disulfide bridges [Fig. 1.3; (Pierce et al., 2001)]. The processing of the worm ILPs, which should begin in the ER, is believed to continue in the

Golgi bodies (referred to as Golgi hereafter) until they are packaged into dense core vesicles prior to secretion [Fig. 1.3; (Eskridge and Shields, 1983; Quinault et al., 2018; Xia et al., 2009)].

ILPs are proposed to act as modulators of neural DAF-2 signaling in the worm brain in response to stress (Cornils et al., 2011; Fernandes de Abreu et al., 2014). Similar to DAF-2, ILPs from different cells, which include the amphid neurons, modulate the entry into and exit from the dauer program (Ailion and Thomas, 2000; Chen et al., 2013; Cornils et al., 2011; Li et al., 2003; Pierce et al., 2001). Indeed, our laboratory has shown that a combination of ILPs regulate the switches between dauer and non-dauer programs, based on the individual and combined phenotypes of three ILP deletion mutants, *daf-28*, *ins-1*, and *ins-6* (Cornils et al., 2011). For instance, the ILP *daf-28* plays a major inhibitory role in dauer entry, but only weakly stimulates dauer exit (Chen et al., 2013; Cornils et al., 2011; Fernandes de Abreu et al., 2014). In contrast, the ILP *ins-6* has a minor inhibitory role in dauer entry, but a major stimulatory role in dauer exit (Cornils et al., 2011; Fernandes de Abreu et al., 2014), whereas *ins-1* ensures dauer arrest by promoting dauer entry and inhibiting dauer exit (Cornils et al., 2011).

Since the *C. elegans* ILPs do act combinatorially to regulate physiology (Cornils et al., 2011; Fernandes de Abreu et al., 2014), this prompts the next question on how they act together to regulate the choice between the dauer and non-dauer states.

The inter-ILP network

An ILP combinatorial code controls dauer entry and exit, where the subset of ILPs required to control dauer entry is different from the subset of ILPs that regulate dauer exit (Cornils et al., 2011; Fernandes de Abreu et al., 2014). Because the ILPs present in the same subset are not defined by a consensus sequence or by chromosomal clustering, quantitative reverse transcriptase PCR (qPCR) of all 40 ILPs in individual ILP deletion mutants were performed(Fernandes de Abreu et al., 2014). Analysis of the subsequent

data indicates that the 40 ILPs communicate among themselves through a network, known as the inter-ILP network [Fig. 1.4; (Fernandes de Abreu et al., 2014)]. Genetic analyses further suggest that this ILP network can be divided into subnetworks that regulate diverse processes, such as the dauer program, aversive olfactory learning, longevity or even thermotolerance (Chen et al., 2013; Cornils et al., 2011; Fernandes de Abreu et al., 2014). Therefore, distinct ILPs have distinct effects on specific processes and the ILP network provides the mechanism to implement the ILP combinatorial coding strategy to regulate these processes (Chen et al., 2013; Cornils et al., 2011; Fernandes de Abreu et al., 2014).

Interestingly, the ILP family exists as a large family not only in *C. elegans*, but also in many other animals (Bathgate et al., 2013). While *C. elegans* has 40 ILPs, *Drosophila* has 8, mammals have 10 and humans have 10 [including the relaxins; (Swanson and Riddle, 1981)]. This raises the possibility that the combinatorial ILP coding strategy implemented by an ILP network to coordinate diverse physiological processes is also conserved across species. Since this network organization is important for survival, the question then is how the network is regulated.

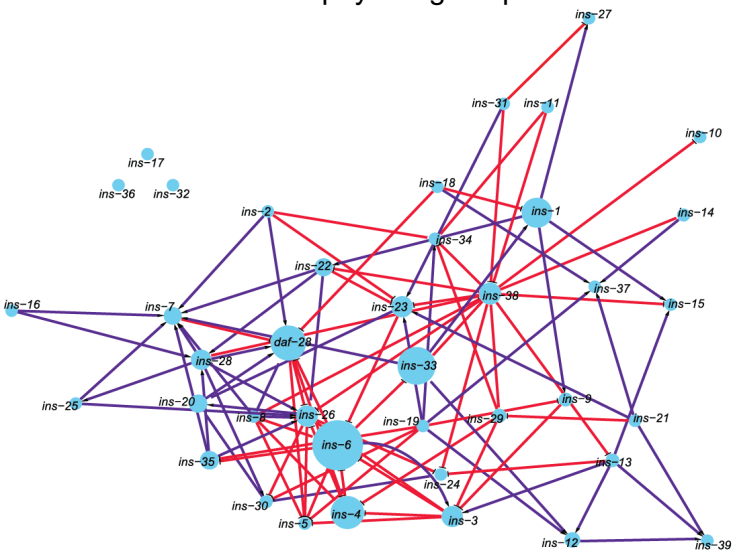

Fig. 1.4: An illustration of the inter-ILP network [modified from (Fernandes de Abreu et al., 2014)]. This is a free-edge network of ILP gene expression simulated on a spring-embedded model. Each node represents an ILP family member. The size of the node represents the number of connections each ILP makes with other individual ILPs, which means that those individual ILPs can regulate each other. Purple and red connections indicate stimulatory and inhibitory regulation between ILPs, respectively.

Scope of this thesis

Interestingly, the ILP *ins-6* forms a major relay node in this inter-ILP network (Fig. 1.4). *ins-6* expression is modulated by the expression of many other individual ILPs, while *ins-6* itself also affects other individual ILPs (Fernandes de Abreu et al., 2014). *ins-6* expression is tightly regulated in only two pairs of sensory neurons during the larval stages: ASI, a dauer entry-inhibiting neuron, and ASJ, a dauer entry-promoting and dauer exit-promoting neuron [Fig. 1.2; (Bargmann and Horvitz, 1991; Schackwitz et al., 1996)]. *ins-6* expression in ASI during the dauer entry decision stage, mid-L1, and to a minor extent in early L2 (Golden and Riddle, 1984) presumably functions to inhibit dauer entry, whereas *ins-6* from the dauer ASJ sensory neuron promotes exit (Cornils et al., 2011). These data indicate that the *ins-6* expression in these two neurons is important for the dauer program.

Because *ins-6* is a critical node in the inter-ILP network (Fig. 1.4) (Chen et al., 2013; Cornils et al., 2011; Fernandes de Abreu et al., 2014), **I hypothesized that identifying the *ins-6* regulators should also identify the regulators of the inter-ILP network.** Therefore, by conducting an unbiased and forward mutagenesis screen focused on altered *ins-6* expression, I should also isolate the regulators that will alter the dynamics of the entire inter-ILP network. I postulate that these *ins-6* regulators, and thus of the inter-ILP network, are the decisive factors that modulate physiology during adverse conditions, by bridging the mind of a worm to its body through the inter-ILP network.

CHAPTER 2 MATERIALS AND METHODS

Experimental model

Wild-type (N2) or mutant *C. elegans* hermaphrodites of different developmental stages were grown on *E. coli* OP50 at 20°C or 25°C, as specified, using standard protocols (see Chapter 3; Brenner, 1974). Wild-type and mutant dauer larvae were induced through starvation and overcrowding, with the exception of *daf-2* mutants, which formed constitutive dauers at 25°C (Gems et al., 1998). Wild-type and mutant post-dauer larvae were induced by transferring dauers to plates with abundant food, with the exception of *daf-2(e1368)* mutants, which exited after a few days at 25°C (Gems et al., 1998). The different mutants used in this thesis were also specified in the Chapters 3 to 6.

Fluorescence in situ hybridization

See the main and supplemental Materials and Methods sections of Chapter 3.

Forward genetic screen for ins-6 regulators

To isolate the regulators of *ins-6*, and thus, the inter-ILP network, we performed an unbiased screen. *drcSi68 ins-6p::mCherry*-expressing hermaphrodites were synchronized by picking ~1000 L1s within two hours. The L1s were then incubated at 20°C to let the L1s develop to the mid-L4 stage on the NGM plates (Brenner, 1974). After three washes with M9 buffer (86 mM NaCl, 42 mM $Na_2HPO_4 \cdot 7H_2O$, 22 mM KH_2PO_4) in 15 mL tubes, the worms were resuspended in 50 mM ethyl methanesulfonate (EMS) in M9 buffer for four hours. The EMS solution was later aspirated after the worms were pelleted at 700 g for three minutes (Brenner, 1974). We performed five fifteen-minute washes with M9 before plating the L4s. To perform an F2 non-clonal screen of dauers, we distributed 50 EMS-treated L4s on twenty-five 6-cm plates and transferred the subsequent fertile EMS-treated adults (P_0) after two days to fresh plates. After a day, we again transferred the EMS-treated P_0 adults to fresh plates to collect as many F1s as possible. The resulting

F1s produced enough F2 progeny to overcrowd the plates and increased the chances of finding F2 non-clonal dauers. After four days of noting the first F2 dauer on each plate, we screened the plates for dauers that exhibited aberrant *ins-6* expression. Through this method, we screened ~2700 dauers in a span of 48 hours and isolated 30 dauers that showed anomalous *ins-6* expression. We clonally amplified these 30 F2 mutant dauers and prioritized them based on lethality, sterility, penetrance and dauer-specific anomalous *ins-6* expression. Of the 30 mutants, only five viable strains had healthy brood sizes and dauer-specific aberrant *ins-6* expression.

Reverse genetic screen for ins-6 regulators

Because dauers have axonal *ins-6* mRNA, we performed a candidate-based search of molecular motors using the GO-Term tool of WormMine (powered by WormBase and Intermine) and AmiGO 1.8 (Consortium, 2004). The constraints used in both searches were “kinesin complex” or “dynein complex” in *C. elegans* (secondary constraint), while the third constraint “neural” further streamlined the search (Aerts et al., 2006; Consortium, 2004; Tiffin et al., 2005). The resulting list was manually curated for the availability of strains and simultaneously subjected to NCBI’s modified Basic Local Alignment Tool (BLAST): Constrained-based BLAST (COBALT), to find the species-specific changes in the nucleotide alignment; multiple-alignment tool, to find sequence similarity between multiple species; and smartBLAST, to find the similarity in protein structure through nucleotide alignment (Aerts et al., 2006). The alignments allowed us to prioritize the kinesins and the dyneins that were tested for axonal *ins-6* mRNA localization. Mutant availability and the evidence of severe phenotypes (such as lethality, sterility or defective locomotion) further tapered the list of prioritized candidates.

Whole genome sequencing (WGS)

To remove at least 98% of the background mutations that had no effect on the dauer-specific *ins-6* mis-expression, the *jx29* mutants were backcrossed to their parent

strain *drcSi68*, which was repeated for a total of six times (Zuryn et al., 2010). Isolated DNA from the cleaned *jx29* and *drcSi68* were sent for library preparation and Illumina Sequencing (to obtain a sequencing depth of 50-150) at the Michigan State University (Schneeberger, 2014; Zuryn et al., 2010). Using a locally installed GALAXY platform (FTP server), we compared the changes in the genome of N2 (wild type), *drcSi68* (the parent strain), and *jx29* [the EMS-mutagenized strain; (Doitsidou et al., 2016; Minevich et al., 2012)]. The first step of the pipeline was to clean the sequence reads by using the *FASTQ groomer* tool. Next, adapter sequences were removed from the paired-ends; and the *jx29* and *drcSi68* sequence reads were then sorted and indexed against the N2 reference genome, using the *BWA-mem* tool to generate SAM reads (Sequence Alignment/Map reads).

Because the generated dataset was large, we converted the SAM files into binary sAM (BAM reads). The variant calling of the BAM files were done in two steps: first, the aligned sequences were sorted based on inconsistencies/polymorphisms against the genomes of N2 and *drcSi68*; second, the inconsistent nucleotides were called “variant” (polymorphic). We filtered the variants or single-nucleotide polymorphisms (SNPs), using the *GATK suit/Picard tools*, and annotated the SNPs, using *SNPEff and snpSift*. We scored our variants based on the error rates for variant-calling by setting our quality score ≥ 30. This setting maintained a genome-wide probability of true variant calling by ≥ 97%. We also set the depth calling (DP) values to 30-50 to filter our variants. Depth calling is the number of times a base is called a variant in that position among the aligned reads. We used an upper limit (30-50) to restrict any variable number tandem repeats or false positives (Smith and Yun, 2017).

mRNA structure analyses

To predict the role of UTRs in the structure of *ins-6*, *daf-28* and *ins-1* mRNA, we used the Zuker’s mFold predictions provided by the Vienna RNA package (known as

RNAfold WebServer) to distinguish structural differences due to the lack of UTRs from the individual ILP mRNAs (Lee and Ambros, 2001; Zuker, 2003). To achieve accuracy, the minimum free energy (MFE) change and the partition function of base-pairing probabilities were determined at 20°C. Twenty different probabilities were analyzed to create one consensus RNA structure for each sequence analyzed.

Agarose pads and live-imaging of worms

To understand the NR morphology in dauers without any anesthetic agent, I used 10% low-melt agarose pads to increase the friction, because higher friction makes movement difficult and sluggish (Fang-Yen et al., 2009). The pads were kept at ~30°C (to maintain softness) and dried for 5 minutes to further increase the friction, before dauers were mounted on the pads and covered with a coverslip, while avoiding any bubble formation. The dauers slowed after ~20 minutes on the pad, which is when they were imaged. For all fluorescence-based live-imaging, I used 1% agarose pads to reduce the diffraction of fluorescent light through the agarose and increase accuracy. I also added either anesthetic agent, 9 mM sodium azide or 6 mM (–)-tetramisole hydrochloride (Sigma, Cat # L9756-5G) to the 1% agarose pads. Well-fed animals that were non-dauers were exposed to 3 mM (an effective dose for L1 and L2) or 5 mM (an effective dose for L3, L4 and adults) sodium azide. Otherwise, I used 3 mM (an effective dose for L1 and L2) or 5 mM (an effective dose for L3, L4, and adults) (–)-tetramisole hydrochloride. Depending on the experiment, the concentration of sodium azide or (-)-tetramisole hydrochloride were kept constant and specified.

Microscopy and imaging analyses and statistical analyses

See the main and supplemental Materials and Methods sections of Chapter 3.

CHAPTER 3 AXONAL TRANSPORT OF AN INSULIN-LIKE PEPTIDE MRNA PROMOTES STRESS RECOVERY IN C. ELEGANS

Abstract

Aberrations in insulin or insulin-like peptide (ILP) signaling in the brain causes many neurological diseases. Here we report that mRNAs of specific ILPs are surprisingly mobilized to the axons of *C. elegans* during stress. Transport of the ILP *ins-6* mRNA to axons facilitates recovery from stress, whereas loss of axonal mRNA delays recovery. In addition, the axonal traffic of *ins-6* mRNA is regulated by at least two opposing signals: one that depends on the insulin receptor DAF-2 and a kinesin-2 motor; and a second signal that is independent of DAF-2, but involves a kinesin-3 motor. While Golgi bodies that package nascent peptides, like ILPs, have not been previously found in *C. elegans* axons, we show that axons of stressed *C. elegans* have increased Golgi ready to package peptides for secretion. Thus, our findings present a mechanism that facilitates an animal's rapid recovery from stress through axonal ILP mRNA mobilization.

Keywords: axonal neuropeptide mRNA, axonal Golgi, insulin signalling, stress recovery

Significance statement

Stress transports mRNAs of specific insulin-like peptides (ILPs) to neuronal axons. This axonal mRNA transport is needed for rapid recovery from stress and beneficial for survival. Stress also increases axonal transport of Golgi bodies that can locally package newly synthesized peptides that will be secreted from the axons. Thus, we show how insulin signaling from a stressed nervous system improves recovery from stress.

Introduction

The inability to recover from stress predisposes us to many neurological dysfunctions, such as post-traumatic brain injuries and neurodegeneration [reviewed in (Blázquez et al., 2014; Esch et al., 2002; Frey, 2013; Zeng et al., 2016)]. Here we use the worm *C. elegans* to elucidate the mechanisms of stress adaptation and recovery, since

the worm can switch its developmental state in response to stress [reviewed in (Riddle and Albert, 1997)]. Like in humans [(Marcovecchio and Chiarelli, 2012); reviewed in (Blázquez et al., 2014; Frey, 2013; Zeng et al., 2016)], insulin-like peptides (ILPs) and their receptor enable worms to endure and recover from stress (Kimura et al., 1997; Riddle and Albert, 1997).

In *C. elegans*, environmental stressors, like food scarcity and high population density, cause the first larval (L1) stage of reproductive growth to form dauers, the stress-induced arrested alternative to the third-stage larva (L3) of the growth program (Golden and Riddle, 1984). Compared to L3, a dauer is more stress-resistant (Riddle and Albert, 1997). When dauers sense the return of favorable environments, they exit into the last larval (L4) stage and become a reproductive adult (Golden and Riddle, 1984; Riddle et al., 1981). These developmental switches are controlled by the combinatorial activities of specific ILPs from specific neurons (Bargmann and Horvitz, 1991; Cornils et al., 2011; Fernandes de Abreu et al., 2014; Li et al., 2003; Pierce et al., 2001; Schackwitz et al., 1996).

The *C. elegans* ILPs exist as a large family of peptides with 40 members (Li et al., 2003; Pierce et al., 2001), which are organized into a network where one ILP regulates the expression of other ILPs (Fernandes de Abreu et al., 2014). This inter-ILP network coordinates distinct subsets of ILPs that either regulate entry into or exit from dauer arrest (Cornils et al., 2011; Fernandes de Abreu et al., 2014). A major node of the network is the ILP *ins-6*, because *ins-6* expression is affected by the highest number of ILPs and *ins-6* in turn affects the expression of many other ILPs (Fernandes de Abreu et al., 2014). This is consistent with the highly pleiotropic phenotype of *ins-6*, which is also a major regulator of stress recovery (Chen et al., 2013; Cornils et al., 2011; Fernandes de Abreu et al., 2014).

ins-6 acts from ASJ sensory neurons to promote dauer exit (Cornils et al., 2011), a readout for stress recovery. Here we have surprisingly discovered that *ins-6* mRNA is transported to ASJ axons upon dauer arrest. Because we observe axonal *ins-6* mRNA only in dauers, we have investigated the significance and mechanism of axonal ILP mRNA transport in response to stress. We show that axonal mRNA transport is specific to the dauer exit-promoting ILPs, where axonal *ins-6* mRNA promotes rapid dauer recovery. This is further supported by our finding that dauers also have enhanced axonal mobilization of Golgi bodies that can locally package ILP mRNA products for prompt secretion from axonal compartments.

Insulin signaling is conserved between worms and humans [reviewed in (Alcedo and Zhang, 2013)]. Stress also influences insulin, insulin growth factor and ILP relaxin mRNAs that are expressed in the human brain [reviewed in (Blázquez et al., 2014; Fernandez and Torres-Aleman, 2012; Wilkinson et al., 2005)]. Thus, our study raises the possibility that stress-induced axonal transport of ILP mRNAs and Golgi bodies in worms is also present in humans to facilitate stress recovery.

Results

The insulin-like peptide *ins-6* mRNA is trafficked to dauer axons

The decision between reproductive growth and stress-induced dauer arrest is regulated by specific sensory neurons, many of which are in the amphids [Fig.S3.1A; (White et al., 1986)]. The amphid sensory neurons ASI and ADF act redundantly to inhibit dauer entry under non-stress environments (Bargmann and Horvitz, 1991), whereas the amphid sensory neuron ASJ has two opposing functions. ASJ promotes dauer entry in response to stress, but promotes dauer exit under improved environments (Bargmann and Horvitz, 1991; Schackwitz et al., 1996). These neurons send their axons to the nerve ring (NR) bundle (Fig. S3.1A), where axons synapse to each other (White et al., 1986).

Amphid neurons express ILPs that regulate the switches between reproductive growth and dauer arrest (Cornils et al., 2011; Fernandes de Abreu et al., 2014; Li et al., 2003; Pierce et al., 2001). These include the ILP *ins-6*, which inhibits dauer entry and facilitates exit from dauer after environments improve (Cornils et al., 2011; Fernandes de Abreu et al., 2014). We found through fluorescence *in situ* hybridization (FISH) that during the L1 dauer entry decision stage, endogenous *ins-6* mRNA was in the ASI neuronal soma, where it remained expressed in later stages (Fig. 3.1 A-E; Fig. S3.1 B-H). In a few second-stage larvae (L2s), *ins-6* also started to be expressed in the neuronal soma of ASJ (Fig. 3.1 B and E; Fig. S3.1H), where *ins-6* persisted in L3 and L4 (Fig. 3.1 C-E; Fig. S3.1 D-H).

In dauers induced by high population density and starvation, *ins-6* mRNA was lost in ASI, but found in the ASJ soma and intriguingly in the NR axon bundle (Fig. 3.1 F, F', G, G' and J; Fig. S3.2A). To confirm that the NR signal was specific to *ins-6* mRNA, we performed FISH on *ins-6* deletion mutant dauers and found that the *ins-6* NR signal was reduced to background in the mutants (Fig. 3.1 H, H' and J; Fig. S3.2A). The *ins-6* mRNA in the NR was transported from the ASJ soma, since dauers with genetically-ablated ASJ neurons also had background levels of *ins-6* mRNA in the NR (Fig. 3.1 I, I' and J; Fig. S3.2A). Moreover, *ins-6* mRNA was observed in the occasional unbroken ASJ axon (Fig. 3.1 K and L).

While the NR signal of *ins-6* mRNA was diffuse and broader than expected (Fig. 3.1 F, F', G and G'), this signal resembled the broad NR-spanning signal, after the FISH protocol, of a GFP protein (Fig. 3.1 M and N) that is expressed in only two pairs of axons (Li et al., 2003). We found that paraformaldehyde fixation and treatment with the hybridization buffer damaged the NR axons (Fig. 3.1N; Fig. S3.2 B and C), which caused the scattering of the GFP protein or the fluorescent-labeled mRNAs from the axonal sources to the neighboring axons of the NR bundle.

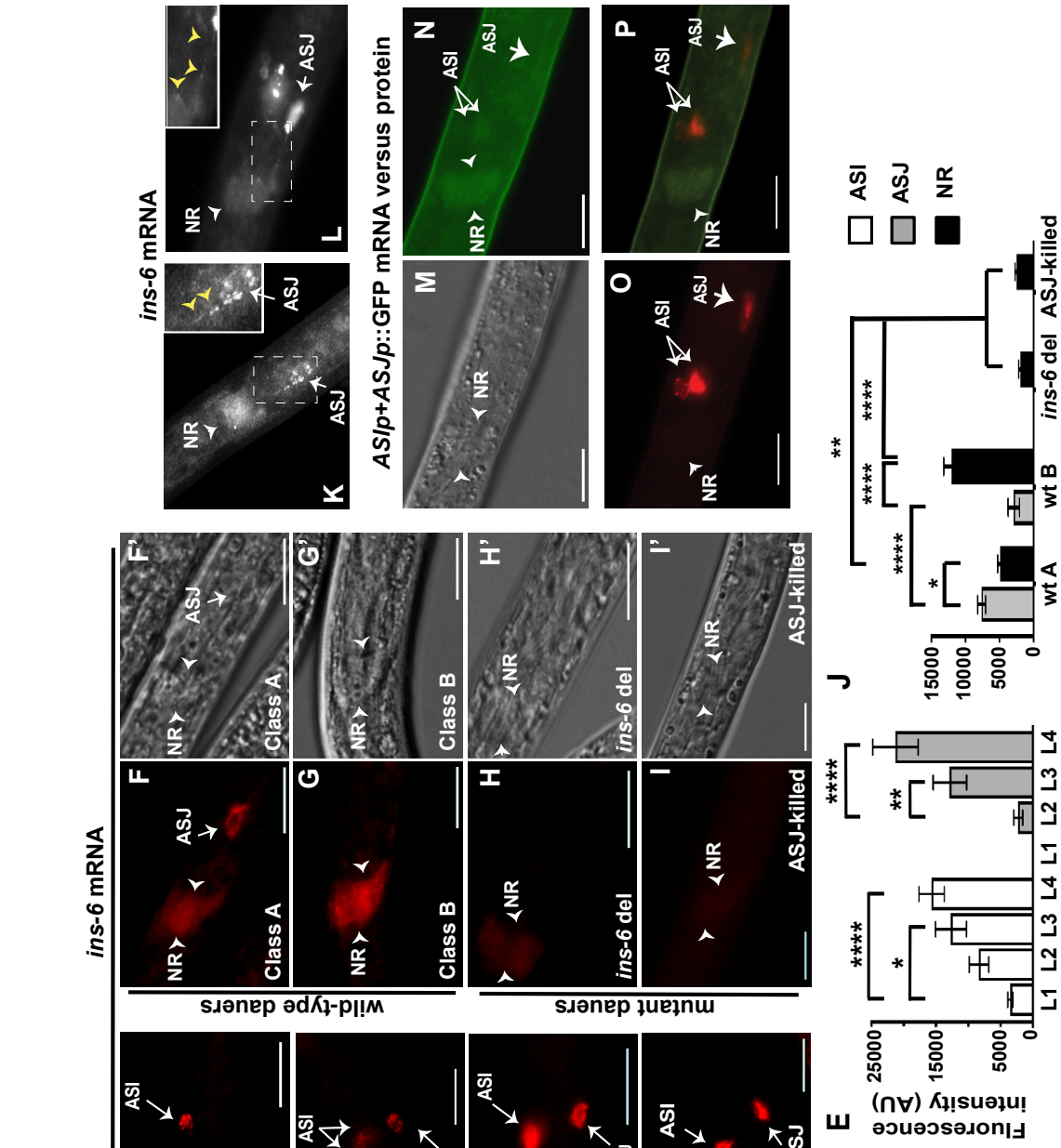
Chandra et al Fig 1
wild-type reproductive growth program
ins-6 mRNA
wild-type dauers
mutant dauers
ASJ-killed
ins-6 del
Class A
Class B
ASIp+ASJp::GFP mRNA versus protein
Fluorescence intensity (AU)
ASI
ASJ
NR
wt A
wt B
ins-6 del
L1 L2 L3 L4 L1 L2 L3 L4

Fig. 3.1. Dauers traffic *ins-6* mRNA to the nerve ring (NR) axon bundle from ASJ. (*A-D*) show *ins-6* mRNA in somas of ASI and/or ASJ of L1-L4 at 20°C. In this figure and later figures, anterior is to the left of each panel. Lateral views are shown, unless indicated. (*E*) Mean fluorescence (± SEM) of *ins-6* mRNA in ASI versus ASJ from 2 trials. (*F-I*) show *ins-6* mRNA in ASJ soma and/or NR of 5-day old dauers at 20°C; (*F'-I'*) are corresponding DIC images of *F-I*. (*F-G* and *F'-G'*) are two classes of wild-type (wt) dauers based on *ins-6* mRNA levels in axons and somas. *ins-6* mRNA is reduced to background in an *ins-6(tm2416)* deletion mutant (*H* and *H'*) and a dauer with ASJ-killed neurons (*I* and *I'*). (*J*) Mean fluorescence (± SEM) of *ins-6* mRNA in ASJ soma (grey bar) and NR (black bar) from 3 trials. (*K-L*) *ins-6* mRNA in wild-type (*K*, lateral view) and *ins-6*-overexpressing (*L*, ventrolateral view) 5-day old dauers at 20°C. Insets are magnified from dotted boxes in main panels. Yellow arrowheads in insets point to mRNA signal in ASJ axons. (*M-P*) A 5-day old dauer at 20°C that expresses GFP in two neuron pairs, ASI and ASJ: (*M*), corresponding DIC image of *N-P*; (*N*), NR-spanning GFP protein image after fixation and treatment with hybridization buffer; (*O*), *gfp* mRNA in ASI and ASJ somas; and (*P*), merged image of *gfp* mRNA from *O* (red) and protein from *N* (green). White arrowheads in *F-I*, *F'-I'* and *K-P* point to NR and/or its boundaries. Statistical significance in all figures are determined by two-way ANOVA and Bonferroni correction. *, $P < 0.05$; **, $P < 0.01$; ****, $P < 0.0001$; ns, not significant; AU, arbitrary units. Scale bar, 10 μm.

Chandra et al Fig S1

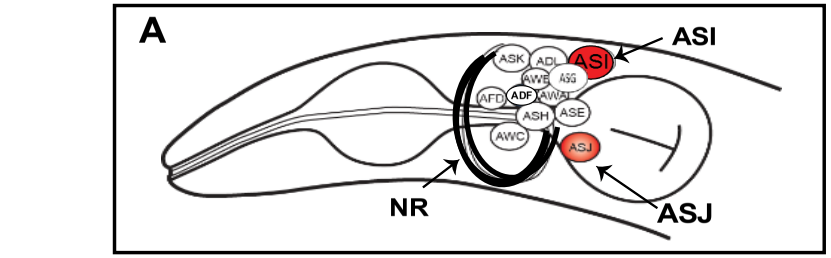

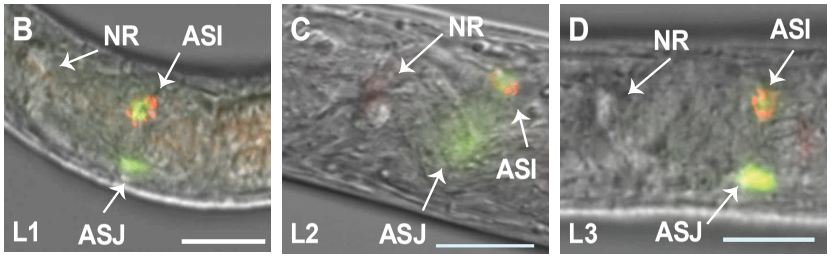

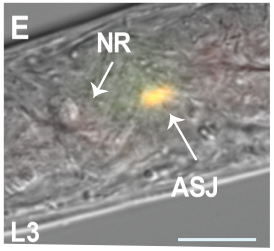

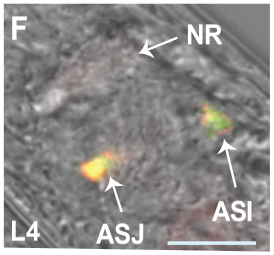

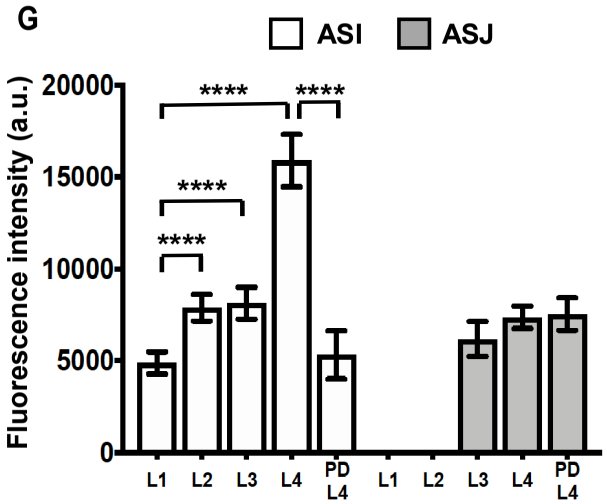

H

stage	# of animals with neuronal *ins-6* mRNA				mean total wt *ins-6* ± SEM	wild type	
	*daf-28p::*GFP		wild type			*P* vs L1	*P* vs L4
	ASI	ASJ	ASI	ASJ			
L1	23/23	0/23	24/24	0/24	3481 ± 399	-	< 0.0001
L2	33/33	0/33	21/21	2/21	10423 ± 2784	ns	< 0.0001
L3	32/32	24/24	23/23	23/23	25679 ± 4583	< 0.0001	0.03
L4	38/38	34/34	22/22	22/22	35166 ± 4121	< 0.0001	-
PD L4	8/14	14/14	-	-	-	-	-

Fig. S3.1. *ins-6* mRNA is expressed in the larval ASI and/or ASJ sensory neurons during reproductive growth. (*A*) Diagram of the 12 sensory neurons in the *C. elegans* amphid sensory organ (White et al., 1986). The ASI and ASJ sensory neurons are highlighted in red and NR indicates the nerve ring axon bundle. (*B-F*) An overlay of *ins-6* mRNA (red), GFP protein (green), and its respective DIC image in the same z-plane at 20^{o}C in L1 (*B*), L2 (*C*), L3 (*D-E*) and L4 (*F*). Yellow represents colocalization of *ins-6* mRNA and the GFP protein expressed specifically in ASI and ASJ [*daf-28p::gfp*; (Li et al., 2003)]. In this figure and later figures, the anterior of each animal is to the left of each panel. Lateral views are shown, unless otherwise indicated. Scale bar is 10 μm. (*G*) Mean fluorescence intensities (± SEM) of *ins-6* mRNA in ASI versus ASJ are shown from 2 trials for larval stages L1-L4 and post-dauer L4 (PDL4) in *daf-28p::gfp* animals (Li et al., 2003). The following indicates: a.u., arbitrary units; ****, $P < 0.0001$. (*H*) Distribution of larvae that express *ins-6* mRNA in ASI and/or ASJ in *daf-28p::gfp* or wild-type (wt) animals from 2 trials.

Chandra et al Fig S2

A **DAUERS**

strains	# of animals with neuronal *ins-6* mRNA			mean total *ins-6* ± SEM	*P* vs *ins-6*	*P* vs ASJ-killed
	ASI	ASJ	NR			
wt A	0/35	35/35	35/35	12427 ± 660	< 0.0001	< 0.0001
wt B	0/36	14/36	36/36	14851 ± 1452	< 0.0001	< 0.0001
ins-6 D	0/36	0/36	0/36	1841 ± 225	na	ns
ASJ-killed	0/36	0/36	0/36	2515 ± 251	ns	na

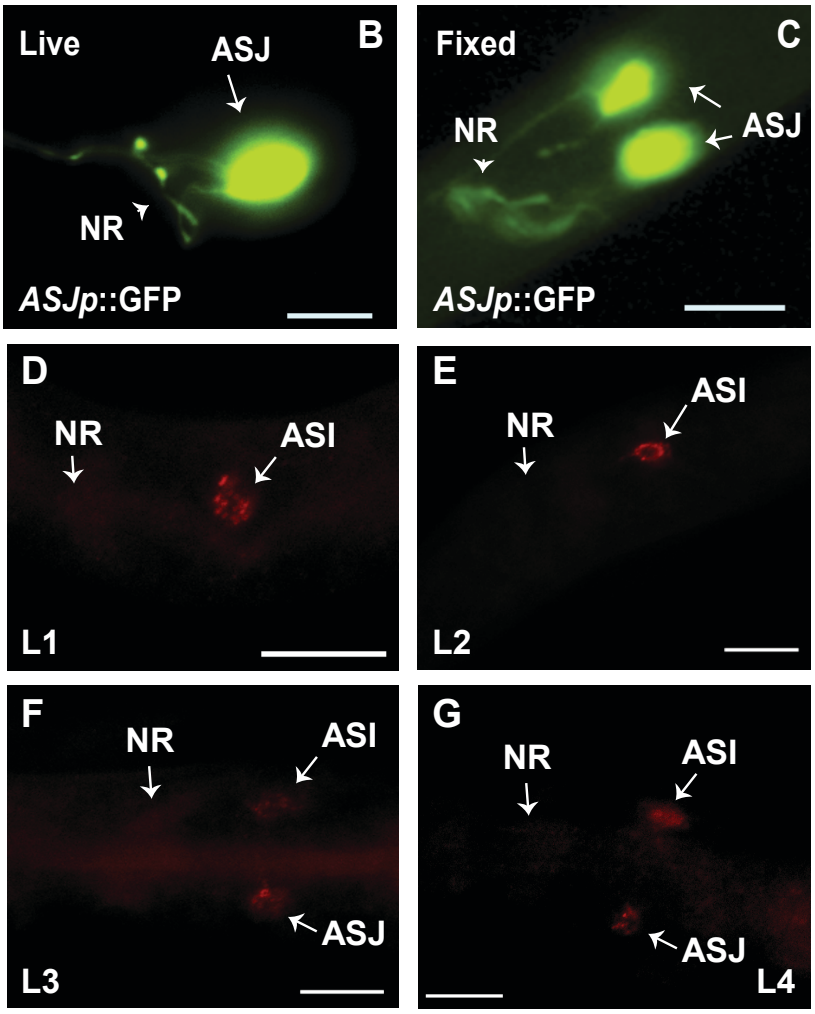

Fig. S3.2. *ins-6* mRNA is trafficked to the NR axon bundle in starvation-induced dauers, but not in response to starvation alone. (*A*) Distribution of wild-type (wt) or mutant dauers that express *ins-6* mRNA in ASI or ASJ soma or NR and mean total intensities (± SEM) of *ins-6* mRNA from 3 trials. (*B*) Image of a live, untreated 5-day old dauer that expresses GFP protein from the ASJ neuron pair. (*C*) Ventral view of a fixed and hybridization buffer-treated dauer that expresses GFP from the ASJ neuron pair, similar to *B*. Note the diffuse and broader GFP protein fluorescence in the NR in this panel compared to the NR fluorescence in *B*. (*D-G*) Representative fluorescent images of *ins-6* mRNA in starved wild-type L1 (*D*), L2 (*E*), L3 (*F*) and L4 (*G*) at 20°C. Animals were starved for about 5 days. Scale bar, 10 μm.

Wild-type dauers can be divided into two classes: class A dauers have higher *ins-6* mRNA in the soma, whereas class B dauers have higher *ins-6* in the axons (Fig. 3.1 F, G and J; Fig. S3.2A). This mRNA transport displayed specificity, since dauers that express GFP in ASJ and ASI neurons show no *gfp* mRNA in axons (Fig. 3.1 O and P; see also Fig. S3.4F). However, because starvation-induced dauers had *ins-6* mRNA in the NR, we tested if starvation alone was sufficient to traffic *ins-6* mRNA. While starvation reduced endogenous *ins-6* mRNA in ASI and ASJ neurons, no starved larvae had any *ins-6* mRNA in the NR (Fig. S3.2 D-G). Thus, the switch to dauer is needed to traffic *ins-6* mRNA to axons. Once dauers exit to the last larval stage [post-dauer (PD) L4s], *ins-6* mRNA was also lost in the NR, but found in the ASJ soma of all animals and in the ASI soma of some animals (Fig. S3.1 G and H). Together our data suggest that axonal *ins-6* mRNA transport occurs only under certain stressed conditions, such as dauers.

Dauer-exit promoting ILP mRNAs are in axons

Next, we asked whether other dauer-regulating ILP mRNAs are trafficked to the NR (Cornils et al., 2011; Fernandes de Abreu et al., 2014). Like *ins-6*, the ILP *daf-28* inhibits dauer entry and promotes dauer recovery (Cornils et al., 2011; Fernandes de Abreu et al., 2014; Kao et al., 2007; Li et al., 2003). Similar to *ins-6*, we found that *daf-28* mRNA was in wild-type dauer axons (Fig. 3.2 B and B') and absent in *daf-28* deletion mutant dauers (Fig. 3.2 C and C'). Wild-type dauers can again be divided into different classes based on *daf-28* mRNA subcellular localization. Class A dauers had more *daf-28* mRNA in ASI and ASJ neuronal somas (Fig. 3.2 A and A'); class B dauers had more *daf-28* mRNA in the NR (Fig. 3.2 B and B'). However, *daf-28* and *ins-6* mRNAs are trafficked to the dauer NR at different times (Fig. 3.2 D and E), which suggest different temporal requirements for the mRNAs.

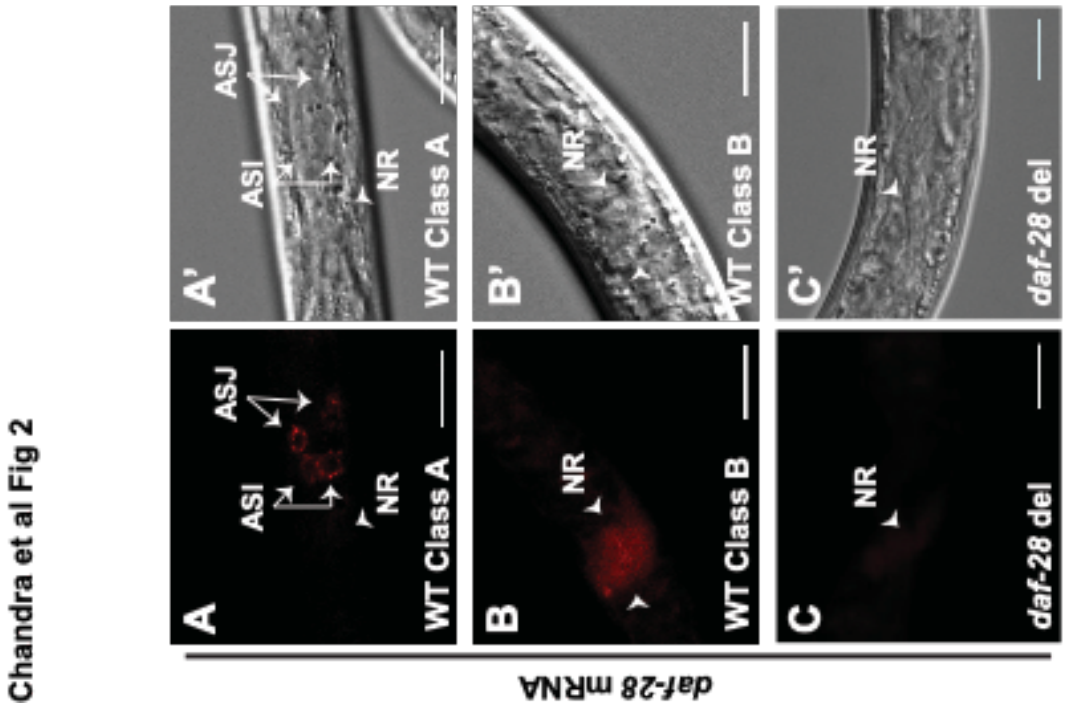

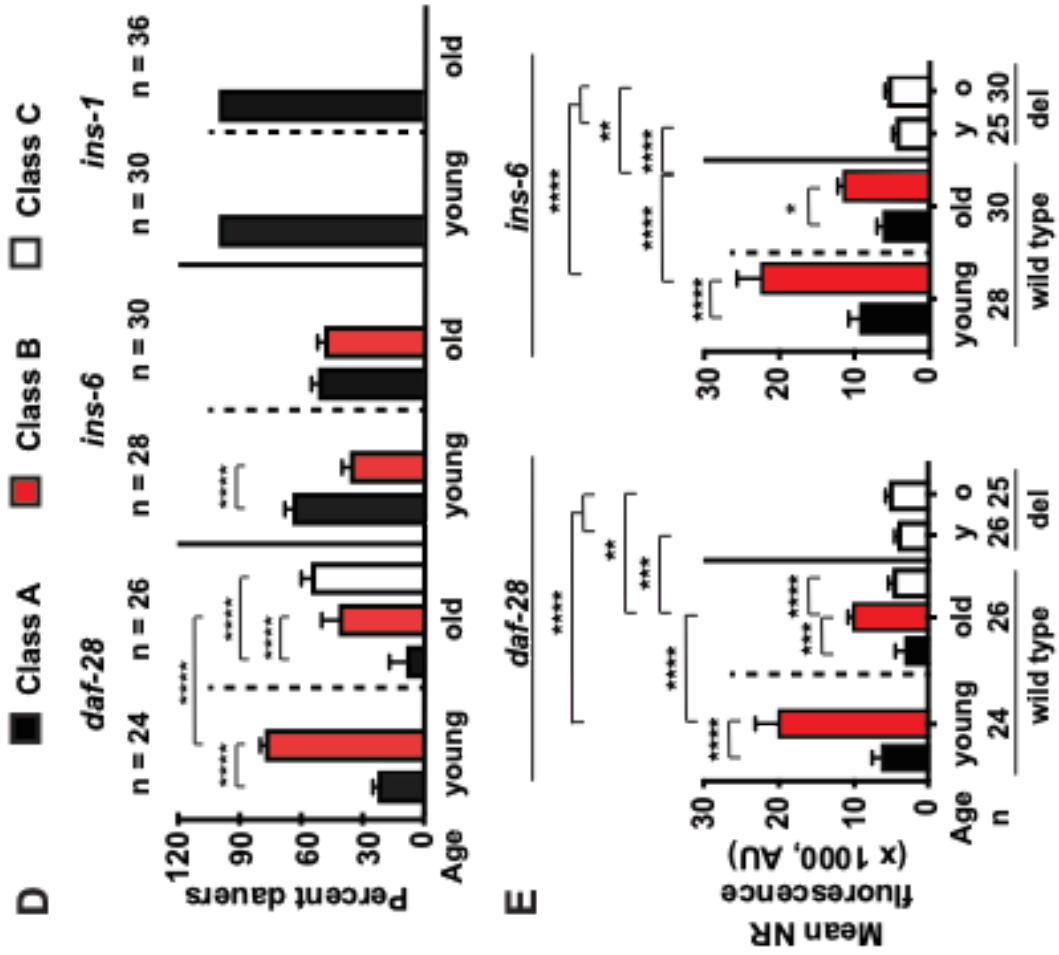

Chandra et al Fig 2

Fig. 3.2. Exit-promoting ILP mRNAs are trafficked to dauer axons. (*A*-*C*) *daf-28* mRNA in ASI and ASJ somas or NR. (*A'-C'*) Corresponding DIC images at 20°C of 2-day old wild-type (WT; *A*-*B*) or *daf-28(tm2308)* deletion mutant (*C*) dauers. Arrowheads in *A*-*C* and *A'-C'* point to NR and/or its boundaries. Scale bar, 10 µm. (*D*) Mean distribution (± SEM) of 3 classes of young (y; 2-day old) or old (o; 5-day old) WT dauers from at least 2 trials at 20°C, based on ILP mRNA levels in somas or NR. Class A dauers have more ILP mRNA in somas; class B, more ILP mRNA in NR; and class C, no expression in somas and NR. (*E*) Mean NR signals (± SEM) of *daf-28* or *ins-6* mRNA in WT (from *D*) or the corresponding ILP deletion mutant dauers, from at least 2 trials. AU, arbitrary units. *, $P < 0.05$; **, $P < 0.01$; ***, $P < 0.001$; ****, $P < 0.0001$.

Unlike the NR of young wild-type dauers, older dauer NR also had less *daf-28* or *ins-6* mRNA (Fig. 3.2E). In older wild-type animals, we observed a third class of dauers: the class C dauers that lack *daf-28* mRNA (Fig. 3.2 D and E), which indicates that some ILP mRNAs are progressively lost in older dauers. Yet, the longer perdurance of *ins-6* mRNA than *daf-28* mRNA in the dauer NR (Fig. 3.2E) highlights a more significant role for *ins-6* mRNA than *daf-28* in these axons. Since *ins-6* has a more important role than *daf-28* in dauer exit (Cornils et al., 2011), this suggests that axonal transport of *ins-6* and *daf-28* mRNAs must be to promote dauer exit.

In support of this hypothesis, the mRNA of an ILP that does not promote dauer exit was not in the NR [Fig. 3.2D; Fig. S3.3; (Cornils et al., 2011)]. The mRNA of ILP *ins-1*, which inhibits dauer exit (Cornils et al., 2011), was either in the somas of multiple neurons (Class A1; Fig. S3.3C) or in the soma of a single neuron in wild-type dauers (Class A2; Fig. S3.3D). While the number of neuronal somas that express *ins-1* decreased in older dauers (Fig. S3.3A), we did not see *ins-1* mRNA in any dauer NR (Fig. 3.2D; Fig S3.3 B-E). Due to the lack of non-exit promoting mRNAs in the NR, like *ins-1* and *gfp* (Fig. 3.1P; Figs. S3.3 and S3.4F), versus the presence of dauer-exit promoting *ins-6* and *daf-28* mRNAs in these axons, this suggests that dauer recovery depends on axonal transport of specific mRNAs.

Axonal *ins-6* mRNA transport depends on insulin signaling and specific kinesins

Next, we asked how axonal trafficking of *ins-6* mRNA is regulated, which would allow us to manipulate axonal *ins-6* mRNA levels and test our hypothesis above. The ILP receptor DAF-2 promotes dauer exit: at 25°C, the *daf-2(e1368)* mutation leads to transient dauer arrest, while the *daf-2(e1370)* mutation is a stronger allele that causes constitutive arrest (Gems et al., 1998). We analyzed the axonal *ins-6* mRNA levels of 3-day old dauers at 25°C, since wild type at this age and temperature showed a comparable distribution of class A and class B *ins-6*-expressing dauers as 5-day old wild type at 20°C (Fig. 3.3). Unlike wild type, we found that *daf-2* mutant dauers had much fewer class B dauers (Fig. 3.3A; Fig. S3.4A). The lack of exit in *daf-2(e1370)* dauers at 25°C (Gems et al., 1998) is likely due to loss of *ins-6* mRNA in some animals, because of the emergence of class C dauers that lost all *ins-6* expression (Fig. 3.3A). Thus, wild-type DAF-2 receptor stimulates *ins-6* mRNA transport to the NR to induce dauer recovery.

Chandra et al Fig S3

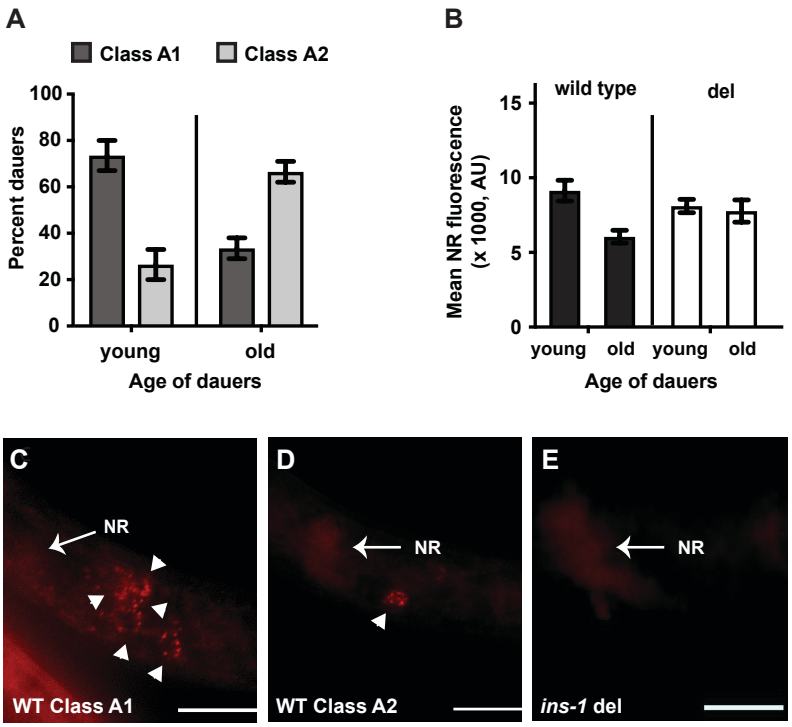

Fig. S3.3. The ILP *ins-1* mRNA is not trafficked to the dauer NR axon bundle. (*A*) The mean distribution (± SEM) of two classes of young (2-day old; n = 30) or old (5-day old; n = 36) wild-type dauers at 20°C, based on the number of neuronal somas that express *ins-1* mRNA. Class A1 dauers express *ins-1* mRNA in more neurons; class A2 dauers express *ins-1* mRNA in only one neuron. Values represent data from 4 trials. (*B*) The mean nerve ring (NR) signals (± SEM) of *ins-1* mRNA in wild-type (from panel A) or *ins-1(nr2091)* deletion mutant dauers. Number of *ins-1* deletion mutant dauers assayed for *ins-1* mRNA are 31 (young) and 29 (old) from 3 trials. AU, arbitrary units. (*C-E*) Fluorescent images of *ins-1* mRNA of old wild-type (*C-D*) and *ins-1* deletion mutant dauers at 20°C. Arrowheads indicate the neuronal somas that express *ins-1* mRNA in wild-type dauers. (*A-E*) *ins-1* mRNA is assayed using probes that are specific to sequences deleted in the *ins-1(nr2091)* mutant. The NR shows similar background signals in both wild-type and *ins-1* deletion mutant dauers. Scale bar, 10 μm.

Axonal transport requires kinesin motors that carry cargo along the microtubules of an axon [reviewed in (Scholey, 2013; Siddiqui, 2002)]. *C. elegans* has multiple neuronal kinesins (Scholey, 2013; Siddiqui, 2002). Two kinesins represent members of the kinesin-1 and kinesin-2 families that have been implicated in transporting mRNAs to different subcellular compartments in other animals (Kanai et al., 2004; Messitt et al., 2008). In *C. elegans*, *unc-116* is a kinesin-1 motor, *osm-3* is a kinesin-2 motor, and both kinesins are in ASJ (Sakamoto et al., 2005b; Scholey, 2013; Tabish et al., 1995). In *unc-116* or *osm-3*

loss-of-function mutants, class B *ins-6*-expressing dauers are lost (Fig. 3.3B; Fig. S3.4B), which indicates that wild-type *unc-116* and *osm-3* are needed to transport *ins-6* mRNA to dauer axons. The rescue of *osm-3* in ASJ alone, *jxEx194* and *jxEx195*, also rescued the class A and class B distributions of *ins-6*-expressing dauers, which shows that OSM-3 kinesin acts in ASJ to mobilize *ins-6* mRNA axonally (Fig. 3.3C; Fig. S3.4C).

Do neuronal kinesins absent in ASJ, like the *klp-6* kinesin-3 motor (Peden and Barr, 2005), have a similar effect on *ins-6* mRNA? Interestingly, a partial *klp-6* loss of function (Peden and Barr, 2005) enriched the class B *ins-6*-expressing dauers (Fig. 3.3B; Fig. S3.4B), which suggests that wild-type *klp-6* inhibits *ins-6* mRNA transport. Since KLP-6 is not in ASJ (Peden and Barr, 2005), this suggests that *klp-6*-dependent regulation of axonal *ins-6* mRNA involves a signal from *klp-6*-expressing cells. The *daf-2*-dependence of *ins-6* mRNA transport (Fig. 3.3A; Fig. S3.4A) suggests that the signal might be an ILP that binds DAF-2.

Yet, epistasis between *daf-2* and *klp-6* implies involvement of more than one signal (Fig. 3.3D; Fig. S3.4D). At 25°C and unlike wild-type or *daf-2* single mutant dauers, *klp-6* single mutants again had more class B *ins-6*-expressing

Chandra et al Fig 3

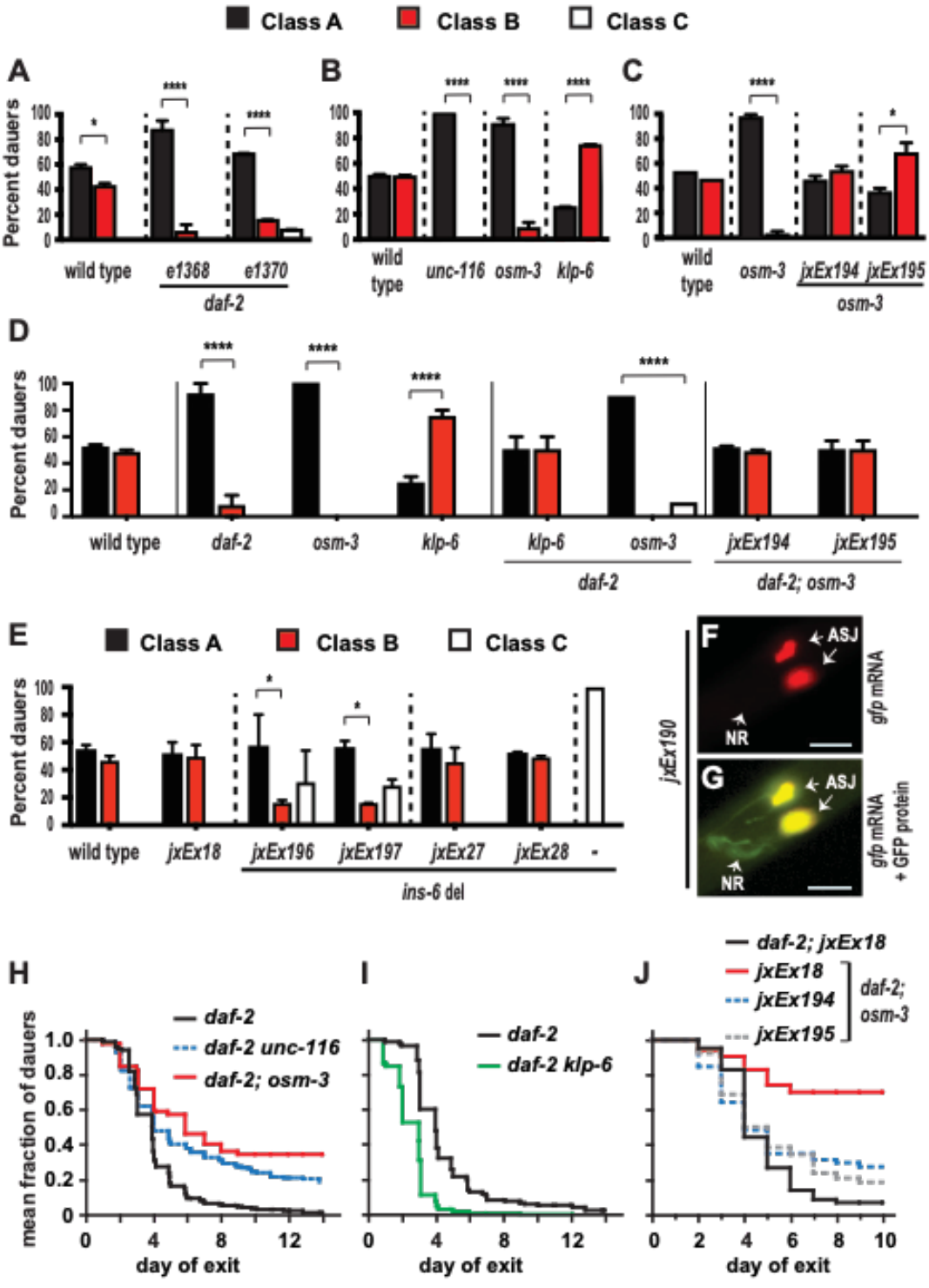

Fig. 3.3. Insulin signaling, specific kinesins and UTRs modulate axonal *ins-6* mRNA that facilitates dauer recovery. (*A*-*E*) Mean distribution (± SEM) of 3 classes of wild-type or mutant dauers. Class A dauers have more *ins-6* mRNA in ASJ soma; class B, more *ins-6* mRNA in NR; and class C, no *ins-6* expression in somas and NR. (*A*) Wild-type versus *daf-2* mutant 3-day old dauers at 25°C. (*B*) Wild-type versus kinesin [*unc-116(e2310)*, *osm-3(p802)*, and *klp-6(sy511*] mutant 5-day old dauers at 20°C. (*C*) ASJ-specific rescue of *osm-3* (*jxEx194* or *jxEx195*) in 5-day old dauers at 20°C. (*D*) *daf-2(e1368)* mutant 3-day old dauers at 25°C with or without the indicated kinesin mutations. (*E*) Wild-type or *ins-6* mutant 5-day old dauers that carry the indicated transgenes at 20°C: *jxEx18*, the *ofm-1::gfp* coinjection marker in all transgenic worms has no effect on dauer class distributions; *jxEx27* and *jxEx28* introduce the full *ins-6* genomic locus, while *jxEx196* or *jxEx197* introduce the UTR-less *ins-6* into *ins-6* deletion *tm2416*. Number of dauers assayed were 20-30 per strain. Statistical comparisons within each strain of animals are shown. See Fig. S4 for statistical comparisons across different strains. *, $P < 0.05$; ****, $P < 0.0001$. (*F*-*G*) *gfp* mRNA (red, *F*) and merged (*G*) mRNA (red) and protein (green) fluorescence at 20°C of GFP in a 5-day old dauer that expresses the *gfp-ins-6 UTR* mRNA hybrid in ASJ. Scale bar, 10 µm. (*H*-*J*) Dauer exit rates at 25°C of *daf-2(e1368)* mutants carrying the kinesin mutation *unc-116(e2310)*, *osm-3(p802)* or *klp-6(sy511)* or the *osm-3*-rescuing transgenes. Statistical comparisons between the dauer exit phenotypes of different animals are in Table S1.

Chandra et al Fig S4

A

	Strains	*P* vs wild type
	wild type n = 25	-
daf-2	*e1368* n = 25	< 0.001
daf-2	*e1370* n = 25	< 0.001

B

Strains	*P* vs wild type	*P* vs *klp-6*
wt n = 30	-	< 0.001
unc-116 n = 32	< 0.001	< 0.001
osm-3 n = 16	< 0.001	< 0.001
klp-6 n = 26	< 0.001	-

C

	Strains	*P* vs wild type	*P* vs *osm-3*
	wt n = 20	-	< 0.001
	osm-3 n = 25	< 0.001	-
osm-3	*jxEx194* n = 20	ns	< 0.001
osm-3	*jxEx195* n = 27	ns	< 0.05

D

Strains	wild type n = 20	*e1368* n = 25	*osm-3* n = 20	*klp-6* n = 25	*e1368 klp-6* n = 20	*e1368; osm-3* n= 38	*jxEx194* n = 27	*jxEx195* n = 28
							e1368; osm-3	
P vs wild type	-	< 0.0001	< 0.0001	< 0.01	ns	< 0.0001	ns	ns
P vs *e1368*	< 0.0001	-	ns	< 0.0001	< 0.05	ns	ns	ns
P vs *osm-3*	< 0.0001	ns	-	< 0.0001	< 0.0001	ns	< 0.001	< 0.001
P vs *e1368; osm-3*	< 0.0001	ns	ns	< 0.0001	< 0.0001	-	< 0.0001	< 0.0001

E

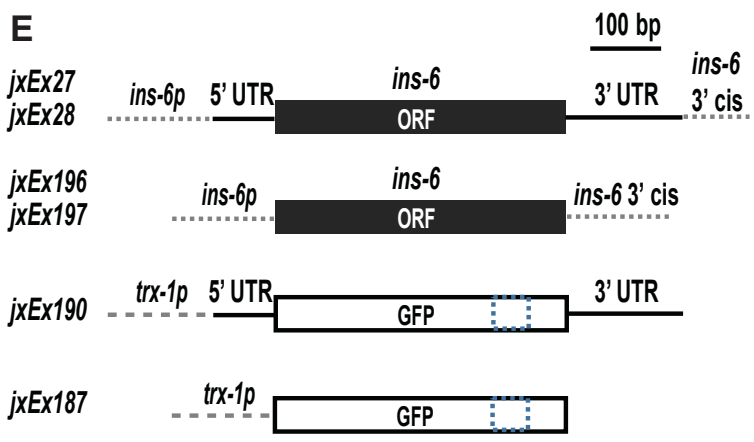

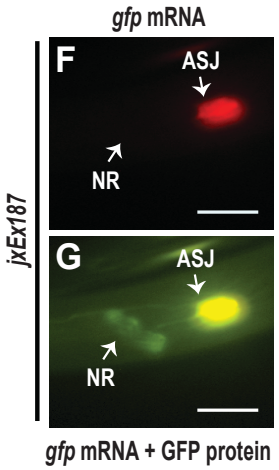

Fig. S3.4. Insulin signaling and specific kinesins regulate trafficking of *ins-6* mRNA to dauer axons. (*A-D*) Statistical comparisons across different strains from the corresponding panels in Fig. 3 *A-D*. Statistical analyses are determined by two-way ANOVA and Bonferroni correction. Values represent data from at least 2 trials. (*E*) Diagrams of transgenes used in studying the role of *ins-6* UTRs in axonal mRNA transport. *jxEx27* or *jxEx28* is an *ins-6* rescuing transgene with the full *ins-6* genomic locus (Cornils et al., 2011); *jxEx196* or *jxEx197*, the *ins-6* rescuing transgene lacking UTRs. *jxEx190* is a GFP cDNA flanked by the *ins-6* UTRs and specifically expressed in ASJ. *jxEx187* is an ASJ-expressed GFP construct that lacks the *ins-6* UTRs. The dotted box in GFP denotes its greater length than the *ins-6* ORF. The dotted lines of the *ins-6* or *trx-1* promoter or *ins-6* 3' *cis* regulatory region indicate that they are not drawn to scale. (*F-G*) *gfp* mRNA (red, *F*) and merged (*G*) mRNA (red) and protein (green) fluorescence at 20°C of GFP in a 5-day old dauer that carries *jxEx187* at 20°C. Yellow indicates colocalization of red and green fluorescence. Scale bar, 10 μm.

Table S1. Kinesins that modulate axonal *ins-6* mRNA levels also modulate dauer exit

Strain	No. of animals observed/total animals	No. of trials	*P* vs. *daf-2(e1368)*	*P* vs. *daf-2(e1368)*; *osm-3*; *jxEx18*
Kinesins that promote axonal *ins-6* mRNA				
daf-2(e1368)	481/604	5	-	na
daf-2(e1368) unc-116	329/483	3	< 0.0001	na
daf-2(e1368); *osm-3*	52/588	3	< 0.0001	na
Kinesin that inhibit axonal *ins-6* mRNA				
daf-2(e1368)	258/347	3	-	na
daf-2(e1368) klp-6	312/381	3	< 0.0001	na
ASJ-specific rescue of *osm-3* kinesin				
daf-2(e1368); *jxEx18*	193/229	2	na	< 0.0001
daf-2(e1368); *osm-3*; *jxEx18*	20/220	2	< 0.0001	-
daf-2(e1368); *osm-3*	10/114	2	< 0.0001	ns
daf-2(e1368); *osm-3*; *jxEx194*	64/135	2	ns	< 0.0001
daf-2(e1368); *osm-3*; *jxEx195*	82/163	2	ns	< 0.0001

Table S3.1. Statistical analyses are shown for the cumulative experiments in Fig.3 *H-J* of the dauer exit rates of *daf 2(e1368)* mutants in the presence or absence of specific kinesins at 25°C. The presence of the coinjection marker *ofm-1::gfp*, *jxEx18*, has little or no effect on dauer exit, according to the statistical comparison between *daf-2*; *osm-3*; *jxEx18* and *daf-2*; *osm-3.* Many of the *daf-2*; *osm-3* double mutants, with or without the coinjection marker, crawl off the plates during the assay. However, the ASJ-specific rescue of *osm-3* partly rescues this "crawl-off" phenotype. To determine the statistical significance of the differences between groups, the logrank test is used. The following indicate: na, not applicable; ns, not significant, since $P > 0.05$.

dauers (Fig. 3.3D; Fig. S3.4D). However, *daf-2 klp-6* double mutants showed the wild-type dauer distribution phenotype, which is an intermediate phenotype between those of *daf-2* and *klp-6* single mutants (Fig. 3.3D; Fig. S3.4D). This implicates a second signal that acts parallel to the DAF-2 ligand in the *klp-6*-dependent inhibition of axonal *ins-6* mRNA transport.

In contrast, kinesin OSM-3 likely functions downstream of DAF-2. As at 20°C, severe *osm-3* single mutants again lost class B *ins-6*-expressing dauers at 25°C, which resembled *daf-2* single mutants (Fig. 3.3D; Fig. S3.4D). Similar to stronger *daf-2(e1370)* single mutants (Fig. 3.3A; Fig. S3.4A), the *daf-2(e1368)*; *osm-3* double mutants produced class C dauers that had no *ins-6* expression (Fig. 3.3D; Fig. S3.4D). Because ASJ-specific rescue of *osm-3* in *daf-2(e1368)*; *osm-3* double mutants restored the wild-type class A and class B distributions of *ins-6*-expressing dauers (Fig. 3.3D; Fig. S3.4D), this suggests that OSM-3 activity in ASJ is downstream of DAF-2 to promote axonal *ins-6* mRNA transport in dauers.

The signals or motors might regulate axonal traffic of *ins-6* mRNA through its untranslated regions (UTRs; Fig. S3.4E), since UTRs can control the subcellular localization of other mRNAs (Bertrand et al., 1998; Gunkel et al., 1998; Thio et al., 2000). While the full *ins-6* genomic locus, *jxEx27* or *jxEx28* (Fig. S3.4E), rescued the *ins-6* deletion phenotype back to wild type (Fig. 3.3E), the UTR-less constructs, *jxEx196* or *jxEx197* (Fig. S3.4E), only partly rescued the *ins-6* mutant phenotype (Fig. 3.3E). The remaining class C dauers in the UTR-less worms (Fig. 3.3E) indicate that UTRs partly modulate *ins-6* mRNA levels. Since the UTR-less animals did exhibit class B dauers, but significantly fewer than the full-rescue *ins-6* lines (Fig. 3.3E), the UTRs are also only partly necessary for axonal *ins-6* mRNA. The absence in dauer axons of *gfp* mRNA (Figs. 3.1O and 3.3F; Fig S3.4F) that has or does not have the *ins-6* UTRs (Fig. S3.4E) further indicated that *ins-6* UTRs are insufficient for axonal mRNA transport.

Axonal *ins-6* mRNA modulates dauer recovery

Does dauer recovery depend on axonal *ins-6* mRNA levels? Since *daf-2(e1368)* mutant dauers exit after a few days (Gems et al., 1998), we tested how the presence or absence of the kinesins above modulate the dauer recovery of *daf-2(e1368)*. Mutations in kinesins *osm-3* and *unc-116* that failed to transport *ins-6* mRNA axonally (Fig. 3.3 B-D; Fig. S3.4 B-D) significantly delayed the exit of *daf-2(e1368)* dauers (Fig. 3.3H; Table S3.1). Yet, the ASJ-specific rescue of *osm-3*, which restored the high axonal *ins-6*-expressing class B dauers (Fig. 3.3C; Fig. S3.4C), rescued the delayed dauer exit of *daf-2*; *osm-3* double mutants back to the exit phenotype of *daf-2* single mutants (Fig. 3.3J; Table S3.1). These suggest that axonal *ins-6* mRNA expedites dauer recovery.

Reduced *klp-6* activity, which enriched the high axonal *ins-6*-expressing dauers (Fig. 3.3 B and D; Fig. S3.4 B and D), caused *daf-2(e1368)* mutant dauers to exit earlier to L4 (Fig. 3.3I; Table S3.1). Interestingly, the *daf-2*; *osm-3* double mutants that have wild-type *osm-3* in ASJ and the *daf-2 klp-6* double mutants showed similar distributions of class A and class B *ins-6*-expressing dauers (Fig. 3.3D; Fig. S3.4D), but different dauer exit phenotypes compared to *daf-2* single mutants (Fig. 3.3 I and J; Table S3.1). This implies that axonal *ins-6* mRNA is only one of the requirements needed for dauer exit. However, because restoring class B *ins-6*-expressing dauers to a population accelerated dauer exit [compare (i) *daf-2*; *osm-3* rescued worms to *daf-2*; *osm-3* non-rescued worms or (ii) *daf-2 klp-6* double mutants to *daf-2* single mutants], this highlights the role of axonal *ins-6* mRNA in dauer recovery.

Stress enhances Golgi mobilization to axons

Like other secreted proteins, ILP mRNAs have to be processed and packaged for secretion; but only the rough endoplasmic reticulum has been reported in wild-type *C. elegans* axons (Edwards et al., 2013). To determine if *C. elegans* axons also have Golgi that can package locally translated peptides, we used a pan-neuronally expressed YFP-

tagged Golgi marker, α-mannosidase II [*aman-2*; (Edwards et al., 2013; Sumakovic et al., 2009)]. *C. elegans* larvae, like L3 and dauer, have Golgi in neuronal somas, dendrites, and axons, which include the dorsal cord axons and NR, but not the commissures (Fig. 3.4; Fig. S3.5). Notably, dauers had more axonal Golgi (Fig. 3.4E; Fig. S3.5C), which suggests that stress increases Golgi mobilization to process newly synthesized axonal proteins.

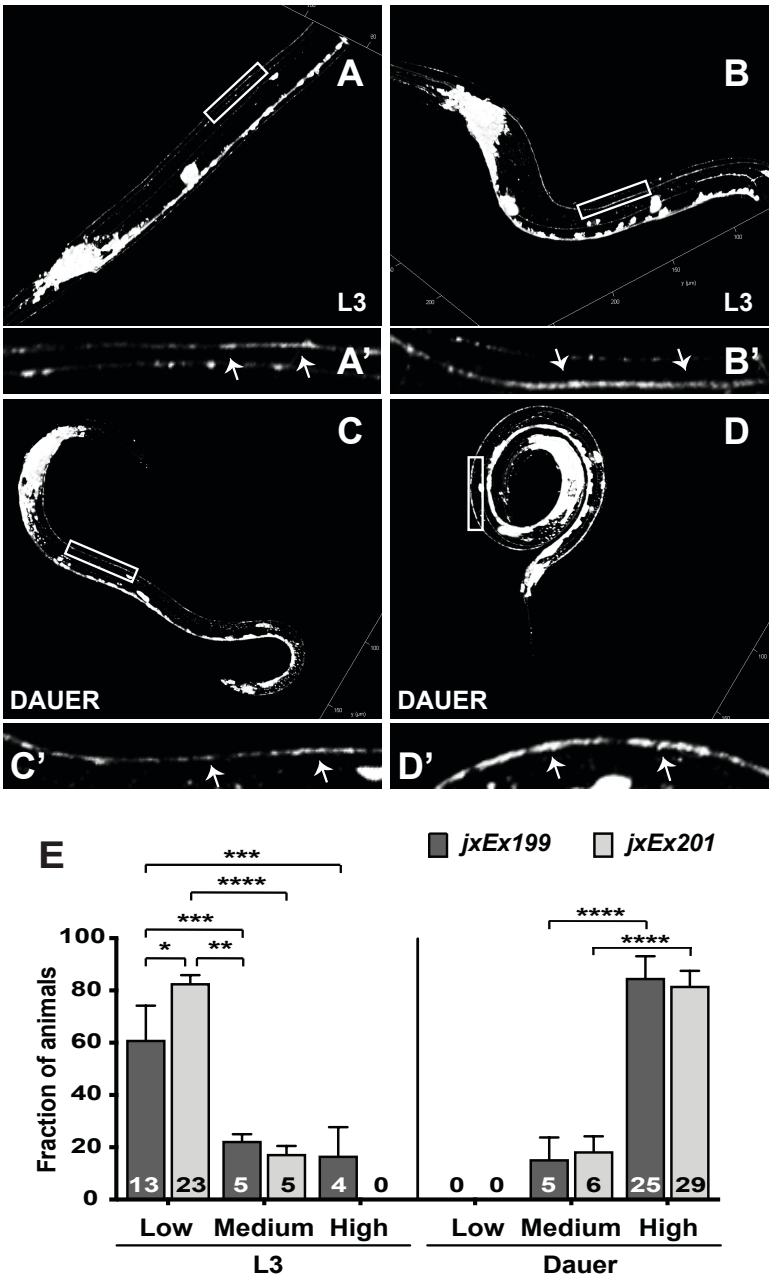

Fig. 3.4. Stress enhances Golgi mobilization to dorsal cord (DC) axons. (*A-D*) 3D-reconstruction of *jxEx199* larvae that express Golgi marker AMAN-2::YFP (Edwards et al., 2013; Sumakovic et al., 2009) at 20°C. (*A-B*) L3 with medium (*A*) or high (*B*) levels of Golgi in DC axons. (*A'-B'*) Magnification of a 50-μm section of L3 DC axons (arrows; boxes in *A* and *B*). (*C-D*) Dauers with medium (*C*) or high (*D*) levels of Golgi in DC axons. (*C'-D'*) Magnification of a 50-μm section of dauer DC axons (arrows; boxes in *C* and *D*). (E) Mean fractions (± SEM) of L3s and dauers with different levels of Golgi in DC axons of two independent lines from 3 trials.

Chandra et al Fig S5

A

jxEx199		Dauer		
	Golgi	**Low**	**Medium**	**High**
L3	**Low**	***P* < 0.001**	***P* < 0.01**	**ns**
	Medium	***P* < 0.001**	**ns**	***P* < 0.01**
	High	**ns**	**ns**	***P* < 0.0001**

jxEx201		Dauer		
	Golgi	**Low**	**Medium**	**High**
L3	**Low**	***P* < 0.0001**	***P* < 0.0001**	**ns**
	Medium	***P* < 0.001**	**ns**	***P* < 0.0001**
	High	**ns**	***P* < 0.001**	***P* < 0.0001**

B **Video of Golgi bodies in L3 axons and dendrites**

C **Video of Golgi bodies in dauer axons and dendrites**

Fig. S3.5. Axonal Golgi mobilization in *C. elegans* larvae. (*A*) Tables show the statistical comparisons between the Golgi levels in the dorsal cord axons of L3s and dauers in each line that express AMAN-2::YFP, *jxEx199* and *jxEx201* (from Fig. 4*E*). (*B*) A movie showing a non-stressed *jxEx199* L3 larva that also exhibits a significant amount of Golgi bodies in axons and dendrites at 20^{o}C. In this movie and the next movie, the anterior of each animal is to the left and the dorsal side is up. (*C*) A movie showing a *jxEx199* dauer with high amounts of Golgi bodies in axons and dendrites at 20^{o}C.

Discussion

Aberrant insulin signaling hampers stress recovery. Because insulin signaling ensures homeostasis (Blázquez et al., 2014; Fernandes de Abreu et al., 2014), ligands of the pathway undergo multiple levels of regulation to enable the pathway to function precisely (Fu et al., 2013). While the significance of ILP mRNA subcellular localization has not been considered, we show that certain stressors localize mRNAs of specific ILPs through distinct kinesin activities to *C. elegans* axons, which is accompanied by an increase in axonal Golgi mobilization. Importantly, our study suggests that these ILP mRNAs must be in axons and locally translated and packaged for prompt secretion to facilitate stress recovery. This illustrates a novel mechanism where ILP mRNAs maintain neuronal plasticity during stress and allow the prompt resetting of homeostasis after a major environmental fluctuation.

Yet, why do we see axonal ILP *ins-6* mRNA in dauers (Fig. 3.1 F, G and J-L; Fig. S3.2A), but not in starved non-dauers (Fig. S3.2 D-G)? This is likely because dauer is an adaptive response that the animal uses to survive a potentially protracted, harsh environmental change, as it awaits a better environment (Riddle and Albert, 1997). Accordingly, the dauer program should include a priming mechanism that promotes recovery, such as the axonal transport of an ILP mRNA whose peptide product promotes dauer exit. Because dauers have reduced global transcription (Dalley and Golomb, 1992; Wang and Kim, 2003), the local translation of a previously existing mRNA will lead to a faster response to improved environments. This is important, since a prolonged dauer state causes deficits in animals that eventually exit (Kim and Paik, 2008). Thus, it is not surprising that the mRNAs of ILPs that promote exit are the mRNAs that are localized to axons, whereas mRNAs of proteins that do not promote exit are not in axons [Figs. 3.1 and 3.2; Fig. S3.3; (Cornils et al., 2011)].

The longer perdurance of axonal *ins-6* mRNA than *daf-28* mRNA (Fig. 3.2 D and E) is consistent with the larger role of *ins-6* versus *daf-28* in promoting dauer recovery (Cornils et al., 2011). An increase in axonal *ins-6* mRNA in a dauer population enhances exit, whereas a decrease in axonal *ins-6* mRNA delays exit (Fig. 3.3 A-D and H-J; Fig. S3.4 A-D; Table S3.1). As an animal that recovers from dauer also shows no axonal *ins-6* mRNA (Fig. S3.1 G and H), this indicates that *ins-6* mRNA is not needed in axons in post-recovery, further highlighting the significance of axonal ILP mRNA in stressed animals. While axonal *ins-6* mRNA is only one of the requirements for dauer exit, the importance of axonal *ins-6* mRNA in dauer recovery is evident in the enhanced exit of dauers (Fig. 3.3 I and J; Table S3.1) to which axonal *ins-6* mRNA is restored (Fig. 3.3 C and D; Fig. S3.4 C and D). The regulation of axonal *ins-6* mRNA transport by two opposing signals—a *daf-2*-dependent versus a *daf-2*-independent, but *klp-6*-dependent signal (Fig. 3.3D; Fig. S3.4D)—also emphasizes that *ins-6* mRNA must be in axons only when needed, *e.g.*, when an animal prepares for recovery.

The *C. elegans* insulin receptor DAF-2 stimulates dauer exit (Gems et al., 1998), at least by regulating *ins-6* mRNA fate (Fig. 3.3 A and D; Fig. S3.4 A and D). This positive feedback in insulin signaling allows the rapid responses necessary in switching from one state to another (Kaplan et al., 2019), such as exit from dauer to post-dauer state. Our data imply that DAF-2 signaling activates OSM-3 kinesin in ASJ to promote *ins-6* mRNA traffic to axons (Fig. 3.3 A-D; Fig S3.4 A-D), which facilitates dauer exit (Fig. 3.3 H-J; Table S3.1). Animals with the weak loss-of-function *daf-2*(*e1368)* and the strong *osm-3* loss of function also show the more severe phenotype of the strong *daf-2* loss-of-function mutant *e1370*, where some dauers have no *ins-6* expression in both soma and axon (Fig. 3.3 A and D). This suggests that DAF-2 and OSM-3 have two roles: to promote axonal *ins-6* mRNA transport and to maintain *ins-6* mRNA. While this is similar to the function of *ins-6* UTRs, which are partly required for *ins-6* mRNA transport and steady-state levels (Fig.

3.3E), it remains unknown if OSM-3 is the kinesin that mobilizes *ins-6* mRNA via the *ins-6* UTRs in response to DAF-2 signaling.

The axonally transported mRNAs are presumably locally translated to expedite protein processing near the synapse [reviewed in (Holt and Schuman, 2013; Jansen, 2001)], but an ILP peptide also has to be packaged from Golgi before secretion. The rough endoplasmic reticulum is in axons of *C. elegans* and other animals [(Edwards et al., 2013); reviewed in (Spaulding and Burgess, 2017)], but axonal Golgi is rarely reported in other species (Morest, 1971; Wigglesworth, 1960; Willis et al., 2011) and has not been found in adult *C. elegans* (Edwards et al., 2013). Interestingly, as in *Drosophila* larval axons (Cao et al., 2014), we find Golgi in axons of L3 and at much higher levels in axons of dauers (Fig. 3.4; Fig. S3.5), which suggests that stress increases axonal Golgi mobilization.

Why then should *C. elegans* larvae have axonal Golgi? Axonal translation is important in axon migration and synaptogenesis (Holt and Schuman, 2013). In *C. elegans*, synaptogenesis along the axonal length and axon outgrowth occur in larvae [(Gujar et al., 2017; Lipton et al., 2018; Shen and Bargmann, 2003; White et al., 1978; White et al., 1986; Zhao and Nonet, 2000); reviewed in (Chisholm et al., 2016)], which might require axonal Golgi to package the necessary proteins (Colón-Ramos et al., 2007; Shen and Bargmann, 2003). Dauer axons are also remodeled (Schroeder et al., 2013) and lead to synaptogenesis. Since dauers have reduced global transcription (Dalley and Golomb, 1992; Wang and Kim, 2003), mRNAs involved in stress recovery and axon remodeling are likely axonally trafficked. The packaging of locally translated membrane or secreted proteins that promote axon outgrowths, synaptogenesis, and stress adaptation and recovery will require axonal Golgi. Ultimately, our study suggests a mechanism that promotes plasticity during stress and allows for optimal recovery from stress, a mechanism that might be conserved across metazoans.

Materials and methods

Experimental model. Wild-type (N2) or mutant *C. elegans* hermaphrodites were grown on *E. coli* OP50 at 20°C or 25°C, as indicated, using standard protocols (Brenner, 1974; Cornils et al., 2011). Dauers were induced naturally through overcrowding and starvation (Golden and Riddle, 1984), except for *daf-2* mutants that routinely form dauers in the presence of abundant food at 25ºC (Gems et al., 1998). Dauer exit assays were performed according to Cornils et al. (Cornils et al., 2011).

Worm mutants were backcrossed at least four times to our lab N2 strain before any analysis was performed, including the ASJ-ablated animals that have the *trx-1p::ICE* transgene (Cornils et al., 2011) integrated into their genome (gift of Miriam Goodman). Generation of transgenic animals used standard protocols (see Supporting Information).

Fluorescence *in situ* hybridization (FISH). ILP or GFP mRNAs were visualized by FISH. Worms were washed with sterile water and fixed for 45 min with 4% paraformaldehyde at ~22°C (Stewart et al., 2007). After 3 five-min washes with phosphate-buffered saline (PBS), fixed worms were placed on a nutator and treated with 70% ethanol for 5 hrs to overnight at 4°C (Tautz and Pfeifle, 1989). Hybridization with the appropriate probe set (1:500 dilution) in hybridization buffer (15% deionized formamide, 10% dextran sulfate, 1 mg/ml *E. coli* tRNA, 4 mM vanadyl ribonuleoside complex and 0.2 mg/ml RNase-free BSA) was performed for 16 hrs in the dark at 30°C, followed by multiple 2- or 3-hr washes in 10% formamide in 2X SSC buffer for a period of 36 hrs (Raj and Tyagi, 2010). The lower formamide concentration in the washes ensured signal retention during washes. After the last wash, worms were kept at 4°C for 3 hours in 2X SSC buffer before treatment with Prolong Diamond Antifade (ThermoFisher; cat # P36961; refractive index, 1.47) for at least 24 hrs at 4°C.

Probes (18-mer to 22-mer oligomers) were labeled with CAL-Fluor 610 at the 3' end and generated through the Stellaris RNA-FISH Probe Designer 2.0, (highest specificity: non-specificity masking level 5) from LGC Biosearch Technologies (Petaluma, CA). See Supporting Information for probe sets, FISH signal analyses, confocal laser scanning microscopy and statistical analyses.

Acknowledgements

We thank S. Mitani, *Caenorhabditis* Genetics Center (NIH P40 OD010440), S. Eimer, A. Fire, M. Goodman, P. Sengupta for reagents used in the study; R. Lillich and R. Patten (Mager Scientific Inc, Dexter, MI) and D. DeSantis and L. Mayernik (WSU-MICR Facility) for advice on fluorescence microscopy and the confocal scanning system; Alcedo lab members, M. Friedrich, D. Njus, and S. Todi for discussions. This work was supported by the Thomas C. Rumble University Graduate Fellowship to R. C. and by Wayne State University and NIH (R01 GM108962) to J. A.

Chandra et al: Axonal transport of an insulin-like peptide mRNA promotes stress recovery in *C. elegans*

Supporting information

Supplementary materials and methods

Transgene constructions

To generate an ASJ-specific rescue of *osm-3*, we drove the expression of a GFP-tagged *osm-3* cDNA from an ASJ-specific promoter [pQZ93; (Cornils et al., 2011)]. We replaced the *srh-114* promoter of OSM-3::GFP in the pAGB060 plasmid (gift from Piali Sengupta) with the ASJ-specific *trx-1* promoter (Cornils et al., 2011; Miranda-Vizuete et al., 2006). To generate the UTR-less *ins-6* transgene (pQZ97), we deleted the 72-bp 5' UTR and 110 bp from the 3' UTR of the full *ins-6* rescuing construct pQZ11 (Cornils et al., 2011). The polyA signal was kept at the 3' UTR of pQZ97. To create the ASJ-specific GFP-expressing lines with the *ins-6* 5' and 3' UTRs (pQZ91), we fused the 72-bp *ins-6* 5' UTR to the 5' end of the GFP cDNA in pQZ34, which used the *trx-1* promoter to drive GFP expression (Fig. S4*E*) from the vector backbone of pPD95.77 (gift from Andrew Fire). We also inserted the 124-bp *ins-6* 3' UTR to the 3' end of the GFP cDNA in pQZ34 (Fig. S4*E*).

Transgenic worms

To create the ASJ-specific *osm-3* rescue lines, we injected 25 ng/μl of pQZ93 with 25 ng/μl of the coinjection marker *ofm-1::gfp* into *osm-3(p802)* mutants. The two resulting independent lines, *jxEx194* and *jxEx195*, were also crossed to *daf-2(e1368*) to generate the *daf-2; osm-3* double mutants, in which *osm-3* was rescued in the ASJ neurons. To determine the effects of the *ins-6* UTRs on the *ins-6* mRNA subcellular localization, we created the lines *jxEx196* and *jxEx197* by injecting 2 ng/μl of pQZ97 with 25 ng/μl of the coinjection marker *ofm-1::gfp* into *ins-6(tm2416)* mutants. These were compared to the full *ins-6* rescuing lines *jxEx27* and *jxEx28*, which were injected with 2 ng/μl of pQZ11 and

25 ng/μl of the coinjection marker *ofm-1::gfp* into the *ins-6(tm2416)* mutants (Cornils et al., 2011). The coinjection marker *ofm-1::gfp* (25 ng/μl) has little or no effect on *ins-6* mRNA subcellular localization (Fig. 3*E*) or dauer exit [Table S1; (Fernandes de Abreu et al., 2014)].

To test the sufficiency of the *ins-6* UTRs in trafficking *ins-6* mRNA to the axons, we injected 50 ng/μl of pQZ91 into the wild-type background, generating the extrachromosomal line *jxEx190*. This was compared to the extrachromosomal line *jxEx187*, which has been injected with 50 ng/μl of pQZ34 into the wild-type background and lacks the *ins-6* 3' UTRs.

To confirm that dauer axons have Golgi bodies that can package newly synthesized INS-6 peptides, we injected 5 ng/μl of the pan-neuronal *rab-3p::aman-2::yfp* plasmid (gift of Stefan Eimer) with 25 ng/μl of the coinjection marker *ofm-1::gfp* into wild-type worms, generating the two lines *jxEx199* and *jxEx201*.

Lists of probe sets used in FISH

Gene name	Probe sequences (5' –> 3')
ins-6	tagtaaagacagagttcat, gtgcgcacaaaacgaagat, attgacggaaacttgcagc, cagacattgaaggaccgaa, gttgcatgcttgctgattc, tgtgttgaagttcacggag, ggtgagctgattccatcat, gaacacgtcttgctcgtgg, cacgagtttctcctggtgc, agatgagttttcttccgca, cacagacagccatgactaa, tcttgtgggttgcaaagat, tcagtcgcaatgtcctttc, agaacactgatttccgcag, agcagatcttatgtagtca, aggtaaaaattcatggaca, cagagactgatatcggagt, acgagattcaaaaaaacga, atttgatgagacacgggtg, tacaagccactgggatgac
daf-28	gcgatgagcttgcagttc, gagaggacgagtacggca, tccgagatgagccgagac, tcggccttgaagttggcg, gactgcacggcttagtgg, acggccacacctggaaca, acgaggcgacgaccacag, gacactccacacatacgg, gtggttcacaggcgtctc, gcgatgtcaattccttct, ataggtgcagcattgtgt, gtatatactcggcagtgc, aacgtgggcaacaggcag, cgggcgggaagacgtgaa, aagtgcagatgcgagcgg, tagaggaagagcgggggg
ins-1 nr2091-deletion specific sequences	gccaaagaagaacgagggt, cgagaggagaaggatcgcg, gatgcgtctgaaggcgtcg, cgtgatccacatagtcgaa, gctaaaagggttgttgtga, cacagctgattccggcata, gtttgaaagcggttaatcc,

	cataggattggtcggcgga, aaagatcgcgagttgttgg, cgcttttgttggtggtgaa, acattctgtcgcaattccg, gcaaatgaacatcgcttct, gcagcagaatgttttgaga, gttatcaattatcgtcctg, cacgagacccgatgatgag, ccgcgcagtctaataatgc, tattgacctgatcagaggc
gfp	actcatttcctcttcttgaaaa, gacctcaacagggttaagaaca, ttaatctaccactacaattacc, tgtttaaaagacagtcacctct, gtatgccttttgaatgggaatt, ataaacgtgatgacctttgat, ccggttgtgaacagtgatgaaa, caataccacaagttacgaagag, ctatgggtctagtatactttgc, actgaaaaagttctcacggtac, cttccaatacatgtcctttctt, ataaaaagtttctactgccctt gttctgtgcaacgacttcagtt, aacttccactatgggaacaatt, cttagctcaattttccataact, aatttcttctacctttgtaaga, ctgtgtttaaccttatgttgat, agtgtgttacatatgtagtacc, gtttgttttcttaccttagttt, taatctgtgttgtaacttctac, cgcaagttgatcgtctggtaat, ttgttttatgaggttaaccgct, cgggacaggaaaatggtctgtt, taatggacaggtgtgttagacg

Image analyses of hybridized worms

Within a week of hybridization and Antifade-treatment, worms were mounted on 1% agarose pads and imaged on a Nikon Eclipse Ti-E or Ni-U microscope (Nikon Instruments Inc, Tokyo, Japan). Images were captured with a CoolSNAP MYO or ES2 CCD camera (Photometrics, Arizona, USA). Fluorescence intensities were quantified through a built-in fluorescence quantification algorithm (NIS-Elements/Annotations and Measurements/Mean Average Fluorescence Intensity, Nikon Instruments Inc), after a region-of-interest (ROI) background subtraction. Exposure time was kept constant at 900 ms without any neutral-density filter for all fluorescence imaging studies. All FISH images were taken at 400X magnification using the Nikon 40X N2 oil objective.

Confocal laser scanning microscopy and live-image analyses of Golgi-marked worms *image acquisition.* For live imaging of AMAN-2::YFP, well-fed L3 worms were mounted on 1% agarose pads with 5 mM sodium azide (Sigma-Aldrich, CAS No. 26628-22-8), whereas dauers were mounted on pads with 9 mM sodium azide (Simpkin and Coles, 1981). All confocal images were taken at 400X magnification within 30-40 min of mounting the worms. All confocal images and movies were acquired through a Leica

laser-scanning confocal system (SP8), using a diode laser of 488 nm at 5% power (with a selected gated band-width of 500-560 nm, according to the Dye-Assistant plug-in of the LAS-X software). To achieve maximum sensitivity, emitted signals are detected through a photomultiplier tube at 500 nm. To obtain high signal-to-noise ratio from specimens, high-definition (1024 X 1024 dpi) images were scanned at a speed of 400 Hz/sec, with a line averaging of 4. To achieve true confocality with minimum photo-bleaching, the pinhole aperture was set to 1 airy unit of the 40X oil objective with a smart-gain value of 630.

To classify animals according to the amount of Golgi present in their dorsal cord axons, we used a particle analyzer provided by FIJI (Schindelin et al., 2012). Animals with low axonal Golgi have less than 20 particles in a 50-μm section of the dorsal cord; animals with a medium amount of axonal Golgi have 21-40 particles in a 50-μm section of the dorsal cord; and animals with high axonal Golgi have greater than 40 particles in a 50-μm section of the dorsal cord.

Movie acquisition and 3D reconstruction. Using the protocol described above for image acquisition, each animal was scanned from bottom to top at 0.27-μm intervals to produce a stack of images, which were then bound together at three frames per second to produce a movie. To generate a 3D reconstructed image of an entire L3 or dauer larva from a 16-bit movie, we used the Leica 3D reconstruction program (LAS-X software; threshold = 20-120), which eliminated noise and puncta clusters (Sibarita, 2005). We used a volume-rendering method at 100% opacity during the 3D-reconstruction of each animal (Pawley, 2006).

Statistical analyses. All statistical analyses were performed using GraphPad Prism 7.0, except for dauer exit analyses. Wild-type *ins-6* hybridization signals were analyzed using 2-way ANOVA and Bonferroni correction with 95% confidence interval. Chi-square test was also performed to compare the differences between the classes of

dauer populations across wild-type and mutant animals. For dauer exit, which were analyzed in JMP 6 from SAS, Kaplan-Maier probabilities were calculated and the *P*-value estimates were based on logrank comparisons.

CHAPTER 4 TRANSCRIPTIONAL REGULATORS OF THE INTER-ILP NETWORK: A FORWARD GENETIC APPROACH

Introduction

As mentioned in an earlier chapter, the ability of an animal to survive stress largely depends on insulin-like peptide (ILP) signaling. Across species, ILPs are not only conserved, but also exist as a large family of peptides. For example, humans have 10 ILPs, *D. melanogaster* have 8, and *C. elegans* have 40 different ILPs (Bathgate et al., 2013; Bathgate et al., 2002). However, why would animals need large ILP families? In collaboration with the ILP consortium, our lab performed a comprehensive analysis of all available *C. elegans* ILP deletion mutants to categorize ILPs based on function and gene expression (Cornils et al., 2011; Fernandes de Abreu et al., 2014). By focusing on how ILPs regulate the switches between a stress-induced dauer arrest program and the non-stressed reproductive growth program, different, but partly overlapping subsets of ILPs were found to modulate dauer entry versus exit (Fernandes de Abreu et al., 2014). These data suggest that ILPs apply a combinatorial coding strategy to control the dauer program.

Yet, it remained unknown how the function-based subset-specificity of ILPs are formed and how one subset of ILPs communicate with other ILP subsets. While chromosomal gene clusters and sequence homologies failed to identify the criteria that determine subset classification, quantitative PCR of the different ILP mRNAs in different ILP deletion mutants showed that ILPs regulate each other's transcript levels (Fernandes de Abreu et al., 2014). Therefore, ILPs turned out to be organized into an inter-ILP network, which can be further subdivided into subnetworks (Fernandes de Abreu et al., 2014). Thus, the network allows an ILP to communicate with other ILPs through gene expression changes. More importantly, the inter-ILP network provides the mechanism for the implementation of the ILP combinatorial coding strategy in carefully controlling these switches in developmental programs.

The importance of the ILP network in *C. elegans* survival necessitates a tight regulation to ensure optimal physiology, but the regulators of the inter-ILP network that modulate physiology remain to be discovered. Interestingly, the relay of information within the ILP network has a large impact on *ins-6* expression, making *ins-6* a busy node within the network, and therefore, one of the most pleotropic ILPs (Fernandes de Abreu et al., 2014). Since *ins-6* is an important node (Cornils et al., 2011; Fernandes de Abreu et al., 2014), identifying the *ins-6* regulators should also identify the regulators of this network, which will ultimately shed light into how ILP combinatorial coding is regulated.

Apart from its subcellular localization, we found that *ins-6* expression also changes between two neurons in response to the presence or absence of dauer cues [(Cornils et al., 2011); Chapter 3]. During reproductive growth, endogenous *ins-6* is expressed in ASI and/or ASJ neurons depending on the developmental stage (Chapter 3). During dauer arrest, *ins-6* expression is lost in ASI, leaving ASJ as the only source of *ins-6* mRNA (Chapter 3). The regulators that cause this change in *ins-6* expression in dauers are not known. Given the fact that *ins-6* is a major node in the network and that *ins-6* plays an important role in stress recovery (Cornils et al., 2011; Fernandes de Abreu et al., 2014), the regulators of dauer-dependent *ins-6* expression should inform how the network regulates physiological switches in response to stress. Therefore, we performed a forward and unbiased F2 screen to isolate the regulators of the dauer-specific *ins-6* expression.

Results and Discussion

Identification of an ins-6 transcriptional reporter for an EMS screen

Identifying the regulators of *ins-6* expression first required the identification of an *ins-6* transcriptional reporter that closely resembles the endogenous cell-specific expression pattern of *ins-6*. We found that the transcriptional fluorescence reporter *drcSi68* [(Queelim Ch'ng, Diana Fernandes de Abreu, and Antonio Caballero, generous gift and personal communication); Fig. 4.1] best reflects the endogenous *ins-6* expression

(Fig. 3.1 A-J; Fig. S3.1). *drcSi68* contains a single-copy insertion of the *mCherry* cassette (Fig. 4.1A) at 0.77 centiMorgan (cM) to the right of the center of the second chromosome at an intergenic position. The *mCherry* is flanked by the *cis* regulatory elements of *ins-6* at the 5' and 3' ends and faithfully represents the endogenous *ins-6* expression pattern at different developmental stages (Fig. 4.1B). In *drcSi68* animals, *ins-6p::mCherry* begins to be expressed in ASI of L1s (Fig. 4.1B). Under favorable conditions and like endogenous *ins-6* (Fig. S3.1H), a few *drcSi68* L2 animals expresses *ins-6p::mCherry,* while all *drcSi68* L3s, L4s and adults express the *ins-6* reporter in both ASI and ASJ (Fig. 4.1B). Again, like endogenous *ins-6* (Fig 3.1J; Fig. S3.2A), 5-day old *drcSi68* dauers lost the *ins-6* reporter expression in ASI, but kept its expression in the ASJ neurons (Figs. 4.1 B-C). Thus, we chose to mutagenize *drcSi68* in a screen that will identify mutant regulators of *ins-6* expression in dauers.

Forward genetic screen to identify ins-6 transcriptional regulators

Ethyl methanesulfonate (EMS) is a mutagenic compound ($C_3H_8SO_3$), whose ethyl group alkylates nucleotides through a mixed SN_1/SN_2 mechanism and has the highest affinity for guanines. The interaction of EMS with guanine gives rise to O^6-ethylguanine, which during replication is recognized as adenine by the DNA polymerase, which then introduces thymine instead of cytosine (Sega, 1984). Therefore, EMS randomly causes base substitution from G/C to A/T in a genome. We used this principle to produce recessive and/or null alleles of genes that regulate dauer-specific *ins-6* expression.

C. elegans hermaphrodites produce sperm until the mid-L4 stage and switch to oogenesis at late L4 (Browning and Strome, 1996; Hubbard and Greenstein, 2005; Kimble and White, 1981). In adults, the oogonia are pushed from the gonad arm into the spermatheca, where the sperm then fertilize the eggs (Cheng et al., 2009; Kimble and White, 1981; Parry et al., 2009). The mid-to-late L4 hermaphrodites exposed to EMS should incorporate nucleotide substitutions in their oogonia, since the replication

machinery is still active in these cells (Hubbard and Greenstein, 2005). Because recessive mutations incorporated into the F1 progeny will not be phenotypically visible in a heterozygous genotype, we performed an F2 screen [Fig. 4.2; (Jorgensen and Mango, 2002)]. To identify the regulators that affected the loss of ASI-specific and maintenance of ASJ-specific *ins-6* expression in dauers, we screened about 2700 F2s that became dauers (Fig. 4.2). To isolate mutants of the inter-ILP network regulators through induction of *ins-6* mis-expression in dauers, we used the following selection criteria:

(i) dauers that expressed *ins-6* in both ASI and ASJ neurons (class I mutant);

(ii) dauers that had reduced or no *ins-6* expression in ASJ (class II mutant); and

(iii) dauers with ectopic *ins-6* expression in multiple neuronal/non-neuronal cells (class III mutant; Fig. 4.2).

Characterization of the jx mutations

Following these selection criteria, we isolated about 30 mutants for clonal amplification (Fig. 4.2). The mutants that were sterile, lethal or displayed aberrant *ins-6* expression in non-dauer stages were eliminated. This secondary screen provided five different *jx* mutations distributed across the different selection criteria (Fig. 4.3A). The mutant phenotypes showed more than 90% penetrance in the dauer populations.

Because these regulators affect the dauer-specific *ins-6p::mCherry* expression and *ins-6* modulates entry into and exit from the dauer program (Chen et al., 2013; Cornils et al., 2011; Fernandes de Abreu et al., 2014), we measured the dauer entry and exit phenotypes of the five *jx* mutations. The *jx24* mutation increased dauer formation compared to all other strains tested (Fig. 4.3B). Because *jx24*, a class II mutant (Fig. 4.3A), did not show aberrant expression during the L1 stage, which is the dauer-entry decision stage, this suggests that *jx24* may affect other genes and/or ILPs that regulate dauer entry (Fig. 4.3 A-B). In addition, *jx24* had a delayed dauer exit phenotype, which is consistent with its low *ins-6p::mCherry* expression in ASJ (Fig. 4.3C) since *ins-6* from ASJ expedites

exit from dauers (Cornils et al., 2011). However, *jx22*, another class II mutant that showed decreased *ins-6p::mCherry* in ASJ, did not delay dauer exit, which indicates that the *jx22* mutation affects a gene that can bypass decreased *ins-6* expression to promote dauer exit (Fig. 4.3C).

Interestingly, the class I mutant *jx29,* showed continued *ins-6p::mCherry* expression in ASI, but had no significant effect on dauer entry (Fig. 4.3B). On the other hand, *jx29* showed normal *ins-6* expression in the dauer ASJ neuron, but showed a delayed dauer exit phenotype (Fig. 4.3C). This indicates that the *jx29* mutation may affect other factors, such as other ILPs that act downstream and/or parallel to *ins-6* in regulating dauer entry and exit. Thus, because *jx29* animals had dauer program phenotypes that might affect multiple ILPs that modulate dauer physiology, we focused on the identification of *jx29* to dissect the mechanism(s) that underlie the regulation of the inter-ILP network.

Mapping and identification of jx29 mutation

The mutants that belonged to the same class, such as the class I mutants *jx22* and *jx24*, or the class II mutants *jx27* and *jx29*, did not exhibit similar dauer entry or exit phenotypes, which make them less likely to be different alleles of the same gene. Therefore, we performed an EMS-based SNP mapping of the *jx29* mutation (Fig. 4.3) over a complementation-based chromosomal mapping.

The background mutations present in the strains may have confounded the dauer entry and exit phenotypes. Therefore, to reduce the EMS-induced mutations that are of no interest, we backcrossed the *jx29* mutant hermaphrodite to its male parent strain *drcSi68*. The resulting homozygote F2 hermaphrodites were selected based on *ins-6* misexpression in dauers. As the F1 dauers did not exhibit any *ins-6* misexpression in ASI, the causal mutation is likely recessive. The recombinant *jx29* F2 hermaphrodites were again backcrossed to its male parent *drcSi68* five times to eliminate 98% of the background mutations. During outcrossing, we observed that *jx29* F2 dauers are both

males and hermaphrodites in equal numbers upon dauer exit. Therefore, as males have only one X chromosome, and *jx29* mutation is recessive in nature, *jx29* mutation cannot reside on the X chromosome. After outcrossing *jx29* six times to its parent strain, we isolated the outcrossed genomic DNA for whole-genome sequencing (WGS; Michigan State University's Sequencing Facility).

We analyzed the genomes of N2 (wild-type reference), *drcSi68* (parent strain) and *jx29* (test strain) by following the standard protocols that use GALAXY and its already existing toolshed [website server (https://usegalaxy.org)]. Our workflow of the automated pipeline that identified the candidate mutations is described in Fig. 4.4. Since the *jx29* mutation is recessive and EMS induces random GC to AT transitions in the genome, we filtered our variants using the logic that the SNPs/variants must be homozygous. Next, depending on the SNP clusters, depth of coverage and quality of reads, we sifted through these SNPs for GC to AT transitions (Fig. 4.4). We chose only those genes that had at least 100X coverage and is a homozygous variant, which meant that 100 different Illumina sequence reads confirmed that the SNP at a given position (with map-ID from the reference genome) is in the *jx29* genome (Fig. 4.4). Through this approach, we identified seven candidate genes that might harbor the *jx29* mutation (Fig. 4.4).

The bioinformatic analyses confirmed our observation that the *jx29* mutation must be an autosomal recessive mutation, since none of the seven candidates were present on the X chromosome. However, because the mutation present in *jx29* is the causal mutation for *ins-6* misexpression, the SNP must be different from both the wild-type genome and the genome of its parent *drcSi68* (Figs. 4.1 and 4.4). Therefore, I predict that the candidate SNPs in *spe-15*, *clec-2* and *Y25C1A.7* are less likely to induce *ins-6* misexpression in dauers. While the SNPs in these three genes are absent in the *drcSi68* genome*,* they are present in the wild-type genome (Fig. 4.4) and wild-type dauers do not show any *ins-6* misexpression (Figs. 3.1 F-J, 4.1 and Fig. S3.2A). Therefore, these three SNPs are silent

SNPs present that do not cause any change in the *ins-6* expression and/or dauer paradigm.

The remaining four candidate SNPs that might cause *ins-6* misexpression were *egg-4, che-7, unc-62* and *F53G2.2* (Fig. 4.4). For further rescue experiments, we prioritized the four candidates according to their roles in physiology, reproducibility of the SNP peaks through two different bioinformatic analyses, expression patterns and SNP clustering. The bioinformatic analyses revealed that the SNP in *F53G2.2* (-12.80 cM) was tightly linked to the SNPs in *clec-2* (-8.97 cM) and *Y25C1A.7* (-8.5 cM) on chromosome II. These SNPs were difficult to recombine away during backcrossing and were therefore found as a cluster. This is typical of a genome generated by an EMS-based density map, where the causal mutation is tightly linked to other SNPs. This SNP cluster thereby marked the boundary of an affected genomic region, where the frequency of recombination events would be reduced within that region. Within this chromosome II cluster, the previously uncharacterized F53G2.2, which is a predicted scaffold-like protein, was a strong candidate for inducing *ins-6* misexpression in dauers. However, because (i) the *jx29* mutation is recessive and is expected to inactivate or downregulate the gene product and (ii) dauers have very low expression of F53G2.2, the priority for further phenotypic rescue experiments of this SNP was lowered.

A second candidate is *unc-62*, which encodes a predicted homologue of the human MEIS2 (Meis homeobox 2) protein and is expressed in dauers [modENCODE and Wormbase (Van Auken et al., 2002; Van Nostrand et al., 2013)]. *unc-62* is predicted to have DNA binding activity, which makes UNC-62 a prime candidate to bind to the *cis* regulatory elements of *ins-6* and affect *ins-6* expression (Van Nostrand et al., 2013). Yet, the *cis* regulatory sequences of *ins-6* lack any MEIS 2-like binding elements, which makes *unc-62* a less likely regulator of *ins-6*, unless *unc-62* indirectly affects *ins-6* through another gene.

The third candidate, the pseudotyrosine phosphatase gene *egg-4*, acts in combination with *egg-5* to promote oocyte maturation in *C. elegans* (Cheng et al., 2009; Parry et al., 2009). The *egg-4* gene product has a serine to arginine substitution in its first exon within the *jx29* genome (Fig. 4.4). DAF-2, an ILP receptor, promotes oogenesis through the RAS-ERK pathway (Cheng et al., 2009; Parry et al., 2009). Therefore, it is highly possible that *egg-4* is also an ILP regulator, whose missense mutation impairs its phosphatase domain and hinders the proper function of the ILP pathway. However, while *egg-4* is abundantly expressed in L4s and in the developing embryos, it is not expressed during the dauer entry decision stage or in dauers (Cheng et al., 2009; Parry et al., 2009), which decreases the likelihood that *egg-4* regulates *ins-6* in dauers.

The final and potentially the most important candidate is *che-7*, which encodes a gap-junction protein that mediates sensory responses to environmental cues (Bargmann et al., 1993; Bhattacharya et al., 2019; Mori and Ohshima, 1997). Unlike wild-type animals, mutants of *che-7,* also known as *inx-4 (innexin-4)*, fail to return to their cultivation temperature when placed in a higher, dauer-inducing temperature (Mori and Ohshima, 1997). *che-7* is also abundantly expressed in L1s, L2s and dauers, but reduced in L3s, L4s and adults, which suggests that *che-7* expression is specific to certain developmental stages (Bhattacharya et al., 2019). A recent study additionally showed that *che-7/inx-4* has a dauer-specific expression and function in controlling dauer-specific behavioral responses (Bhattacharya et al., 2019). Moreover, from two different bioinformatic analyses using two different sets of sequencing coverage (10x versus 100x), only the SNPs in *che-7* and *egg-4* were consistently isolated (Fig. 4.4). This suggests two things. First, our bioinformatic pipeline produces reproducible data and we can fine-tune our variant-calling based on the depth of sequencing coverage of the different genomic regions. Second, the SNPs in *che-7* and *egg-4* are clearly present in the *jx29* genome. Therefore, it is highly possible that CHE-7 and EGG-4 both regulate *ins-6* expression in a stage-specific way,

which is suggested by the mutually exclusive expression pattern of *che-7* and *egg-4* (Bhattacharya et al., 2019; Cheng et al., 2009). Currently, we are performing gene-specific rescue experiments to identify the causal mutation for *jx29*.

The dauer-specific expression of *che-7* and the role of *che-7* in promoting dauer-specific neuro-electrical activity in an insulin signaling-dependent manner make the SNP in *che-7* a strong candidate for the *jx29* mutation (Bhattacharya et al., 2019). It is possible that *che-7* affects the electrical activity of the ASI neuron to regulate *ins-6* expression in this neuron, where lower ASI electrical activity induces *ins-6* expression. In the future, it will be interesting to note if *che-7* also affects the subcellular localization of *ins-6* mRNA in response to altered electrical activity. In such a scenario, this will imply that electrical flow between adjacent neurons can localize ILP mRNAs to the necessary subcellular compartments.

A

B

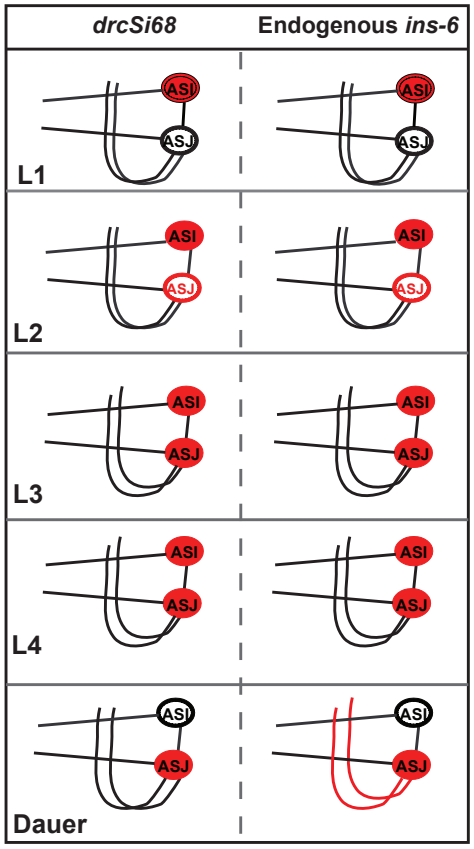

C

	drcSi68		Endogenous *ins-6*	
Stage	ASI	ASJ	ASI	ASJ
L1	60	00	58	00
L2	30	02	39	02
L3	44	44	41	40
L4	64	64	36	38
Dauer	00	94	00	100

No *ins-6* expression

Few animals do not express *ins-6*

All animals express *ins-6*

Fig. 4.1: Comparison of endogenous *ins-6* expression with transcriptional reporter *drcSi68*. (A) A schematic diagram of the inserted transgene in *drcSi68*. In *C. elegans*, 0.77 cM near the center of the second chromosome is a *Mos1* transposon site, the insertion site of the *mCherry* cassette whose expression is driven by the 5' and 3' *cis* regulatory elements of *ins-6*. Within the shown cassette, II is an intergenic region in the second chromosome; *Mos* denotes the *Mos1* transposon site; *ins-6p* is the 1.65-kb sequence upstream of the *ins-6* translation start site; and *ins-6 cis* represents the 7.5-kb sequence downstream of the *ins-6* translation stop site. Therefore, *mCherry* expression in this strain is also regulated by the *ins-6* 5' UTR and 3' UTR. (B) Qualitative comparisons between the *mCherry* expression of *drcSi68* and endogenous *ins-6*. Like endogenous *ins-6*, *drcSi68* shows that favorable conditions promote *ins-6p::mCherry* expression in ASI neurons throughout development, whereas *ins-6p::mCherry* is expressed in the ASJ neurons during L2 (2/39, see panel C) to adulthood. In dauers, *ins-6p::mCherry* is lost in ASI, while the ASJ neurons are the only neurons that continue to express *ins-6p::mCherry*. (C) Pooled number of animals assayed for *ins-6* FISH and the transcriptional mCherry reporter (performed simultaneously) from five different trials. None of the dauers showed *ins-6* in ASI.

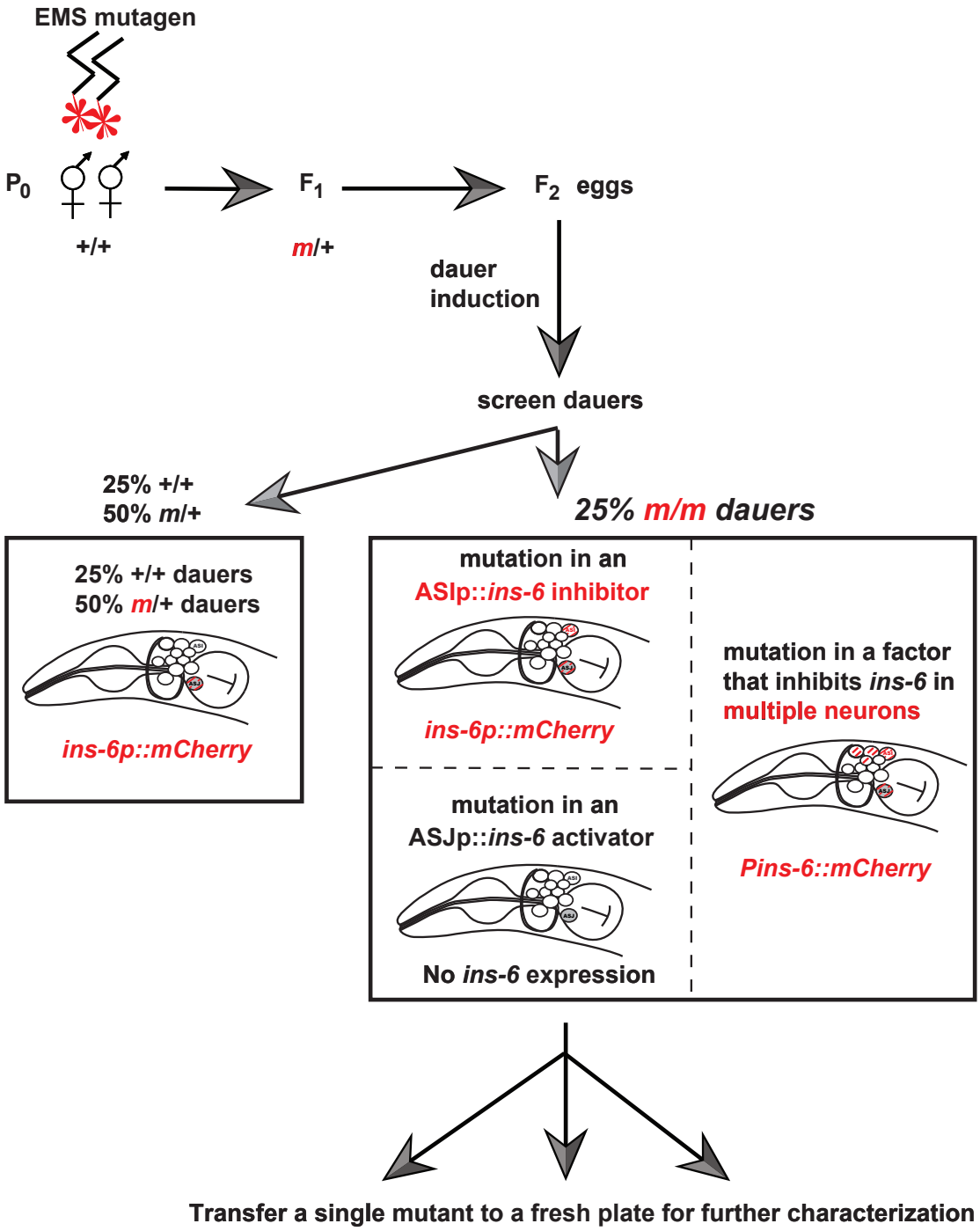

Fig. 4.2: A schematic diagram of the EMS screen that used the *drcSi68* parent strain. 'm' indicates the presence of a mutation and '+' indicates wild type. L4 hermaphrodites were treated with EMS for four hours and then allowed to recover and produce F_1. These F_1 grew to produce F_2 progeny, which were grown under dauer-inducing conditions. Four days after noting the first dauer in each plate, we screened about 2700 dauers in 48 hours based on three selection criteria shown in the box on the right. We selected about 30 mutant dauers having anomalous *ins-6p::mCherry* expression, which were then clonally amplified for a secondary screen and preliminary analyses.

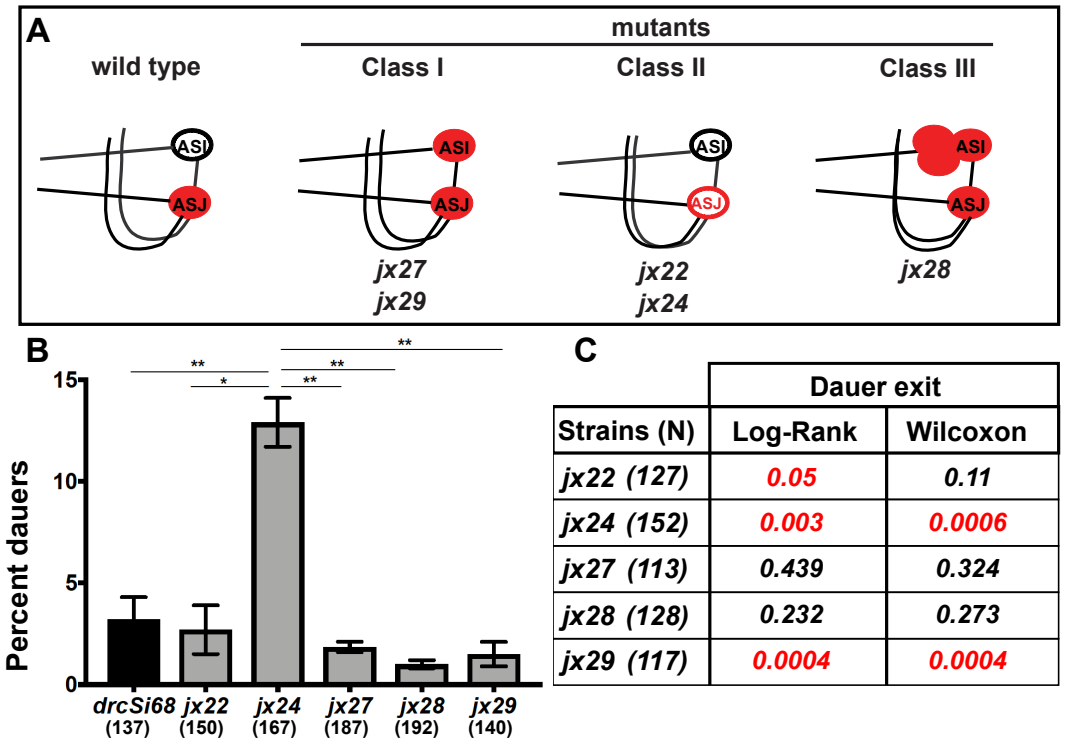

	Dauer exit	
Strains (N)	Log-Rank	Wilcoxon
jx22 (127)	*0.05*	*0.11*
jx24 (152)	*0.003*	*0.0006*
jx27 (113)	*0.439*	*0.324*
jx28 (128)	*0.232*	*0.273*
jx29 (117)	*0.0004*	*0.0004*

Fig. 4.3: EMS mutations that alter *ins-6p::mCherry* expression in five-day old **dauers.** (A) Unlike wild-type dauers, which only express *ins-6p::mCherry* (closed red circle) in ASJ neurons, class I mutant dauers express *ins-6p::mCherry* in both ASI and ASJ neurons. In contrast, class II dauers have no *ins-6p::mCherry* in ASI (open black circle) and low or no *ins-6p::mCherry* in ASJ (open red circle), while class III dauers have ectopic *ins-6p::mCherry* in multiple neurons. Mutants are defined by their *jx* names. (B) Dauer entry assay of the EMS mutants. Eggs were laid for 4 hours at 25^0C, then were shifted to 27^0C, a temperature known to induce dauer formation. Dauers were scored after 48 hours. *jx24* exhibited a higher percentage of dauers at 27^0C, compared to the parent strain, *drcSi68*, and other mutants. * indicates $p < 0.05$ and ** indicates $p < 0.01$, according to one-way ANOVA, with Bonferroni's correction. (C) The dauer exit assay results. The worms were grown at 20^0C and were allowed to form dauers. These dauers were then picked and transferred to a plate with food, which would promote dauer exit. The p values of the comparisons between the dauer exit rates of the mutants versus the parent strain at 20^0C are shown. *jx22*, *jx24,* and *jx29* showed delayed dauer exit phenotypes, which are significantly different from the parent strain, *drcSi68*.

Raw WGS reads

Quality of FASTQ reads and summary of sequencing ← ↓ Filtered reads using *FASTQ groomer*

BWA-mem aligned *jx29* with wild-type and *drcSi68*

Depth of coverage and duplicate trimming ← ↓ *PICARD* and *GATK* processed alignment

Filtered for GC > AT variants

snpSift filtered homozygous mutations ↓ *SNPEff* subtracted background mutations

List of genes with affected SNPs

Gene	wild type	*drcSi68*	*jx29*	Genotype	Region
egg-4	*0/0*	*0/0*	*1/1*	C/C > A/A Ser > Arg	Exon
che-7	*0/0*	*0/0*	*1/1*	C/C > T/T silent	intron
unc-62	*0/0*	*0/0*	*1/1*	C/C > T/T silent	intron
F53G2.2	*0/0*	*0/0*	*1/1*	C/C > A/A silent	intron
spe-15	*0/0*	*1/1*	*0/0*	A/A>C/C>A/A silent	intron
clec-2	*0/0*	*1/1*	*0/0*	A/A>G/G>A/A silent	intron
Y25C1A.7	*0/0*	*1/1*	*0/0*	T/T>G/G>T/T silent	intron

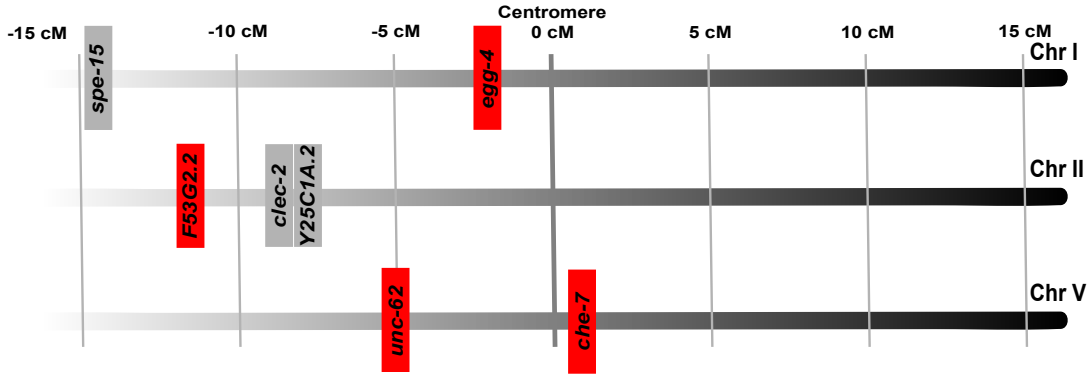

Fig. 4.4: Summary of the workflow used to identify the candidates. The raw WGS reads were uploaded to the local GALAXY server, using the guidelines given by www.usegalaxy.org. Using the FASTQ groomer tool from the GALAXY toolshed, we sifted through the good quality sequences, which informed us about the quality of the sequencing. About 99.2% of the reads were readable and of good quality. We then aligned the wild-type genome, which was imported from the UCSC genome browser, with the groomed *drcSi68* and *jx29* sequences, using BWA-mem. The files were further processed by SAM tool from the toolshed, which converts the Sequence-Aligned Maps (SAMs) into binary SAMs (BAMs), which provides "0" versus "1" annotations for the different nucleotides. This BAM file was then re-read for reorganization using Picard tools. With the help of the GATK suite, the file was primed for homozygous variant selection. Once the variant calling was done, the SNPs were subjected to background subtraction from the wild-type and *drcSi68* sequences, using the SNPEff tool. Since *jx29* is an autosomal recessive mutation, we used snpSift to further qualify the variants based on homozygosity. This further narrowed the list and the common genes obtained from SNPEff and snpSift were annotated, which are shown above in a tabular form with its genotype and the affected gene region. The first four genes (in white rows) are our best candidates for further rescue experiments and characterization. The genes listed in gray are homozygous mutations compared to the parent strain *drcSi68*, but are present in the wild-type genome, and are thus less likely to be the causal mutation of *ins-6* misexpression.

A genomic map of the listed candidates is shown in the lower panel. The red mutations are our best candidates and the gray mutations are likely background variants that do not affect *ins-6* misexpression. The SNP cluster in the second chromosome suggests that the tightly linked F53G2.2 might be a good candidate. Because the *C. elegans* chromosomes are holocentric, a five-cM genetic distance between *unc-62* and *che-7* in the fifth chromosome is another example of SNP clustering, which also makes at least one of them a strong candidate in inducing *ins-6* misexpression. *egg-4* is an isolated SNP in the first chromosome, which reduces its possibility for being the causal mutation, although its missense mutation in its first exon makes it an attractive candidate for further characterization.

CHAPTER 5 CANDIDATE REGULATORS OF THE ILP *INS-6*: A REVERSE GENETIC APPROACH

Introduction

The *C. elegans* inter-ILP network shows that ILPs positively or negatively regulate the transcription of other ILPs (Chen et al., 2013; Cornils et al., 2011; Fernandes de Abreu et al., 2014). However, this network organization has not necessarily depicted potential feedback regulatory loops (Fernandes de Abreu et al., 2014). In rats and canines, insulin added to islets of Langerhans and perfused pancreas inhibits pre-proinsulin synthesis, which indicates a negative-feedback loop of insulin synthesis (Iversen and Miles, 1971; Malaisse et al., 1967). In humans, intravenous insulin delivery reduces the levels of ILPs that contain the C peptide in both obese and lean groups, albeit the relative decrease in ILPs in the obese group was lower than the observed decrease in the lean group (Elahi et al., 1982). This shows that the negative feedback loop in insulin signaling in obese people is a weaker response that decreases the insulin sensitivity of these people and predisposes them to diabetes. This observation also emphasizes that feedback regulation in the ILP signaling system is important for survival and that the *C. elegans* ILPs also have self-regulatory loops that modulate the inter-ILP network for optimal survival. Moreover, the *C. elegans* ILP feedback systems will likely stretch beyond one individual ILP to multiple ILPs. Thus, the worm ILPs themselves are prime candidate regulators of the inter-ILP network. In this chapter, I have further explored how ILPs misexpress or mislocalize *ins-6* mRNA and have found that *ins-6* does regulate its own expression.

The third chapter of this thesis has extensively detailed the axonal localization of *ins-6* mRNA in dauers, which establishes the role of kinesins *unc-116*, *osm-3* and *klp-6* in *ins-6* mRNA transport. However, the entire mechanism of ILP mRNA transport is far from understood, especially when one considers that an individual cell can express an array of molecular motors that can traffic specific RNA/protein cargoes to different subcellular

compartments (Hirokawa et al., 2009). Because I found that *daf-28* mRNA also localizes to dauer axons (Chapter 3), there is the possibility that the motors that transport *daf-28* mRNA may or may not be similar to the motors that localize *ins-6* mRNA. To identify the motors in the *C. elegans* genome, specifically the kinesins or dyneins that might participate in *ins-6* and *daf-28* mRNA mobilization, we performed a gene-ontology based search of kinesin-like or dynein-like genes in the *C. elegans* genome. Here I report two additional kinesin mutants that affect *ins-6* mRNA fate. Furthermore, in this chapter I identify potential signals that might regulate the activities of the different motors in mRNA mobilization—JNK-dependent and synaptic transmission-dependent signals. Thus, this chapter offers a glimpse of the different possibilities in *ins-6* mRNA regulation.

Results and Discussion

ILPs regulate ins-6 localization and expression

Multiple ILPs can collectively affect *ins-6* expression and modulate the inter-ILP network response to stress. To test this hypothesis, I imaged endogenous *ins-6* mRNA in two different *daf-28* mutants (Fig. 5.1A). I found that while a *daf-28(sa191)* gain-of-function mutant inhibited *ins-6* mRNA transport, a deletion specific to *daf-28*, *tm2308*, did not affect *ins-6* mRNA localization (Fig. 5.1A). The gene product of *daf-28(sa191)* has been proposed to sequester the enzyme that processes multiple ILPs that include *daf-28* [Fig. 5.1B; (Li et al., 2003)]. A defect in *ins-6* mRNA transport in *sa191* mutants suggests that impaired processing of an ILP, but not DAF-28 (Fig. 5.1A), failed to localize *ins-6* mRNA to the axons. This is consistent with my earlier finding that the insulin receptor DAF-2 promotes *ins-6* mRNA transport to the axons (Fig. 3.3 A and D; Fig. S3.4 A and D). At present, the specific ILP(s) that promote *ins-6* mRNA mobilization remain to be identified.

The *sa191* gene product has also been proposed to impair the processing of the INS-6 peptide (Li et al., 2003), which led me to test if *ins-6* can regulate its own expression. I imaged and quantified the *drcSi68 ins-6p::mCherry* transcriptional reporter (Fig. 4.1A) in the *ins-6(tm2416)* deletion mutant background (Fig. 5.1C). I found that the absence of a

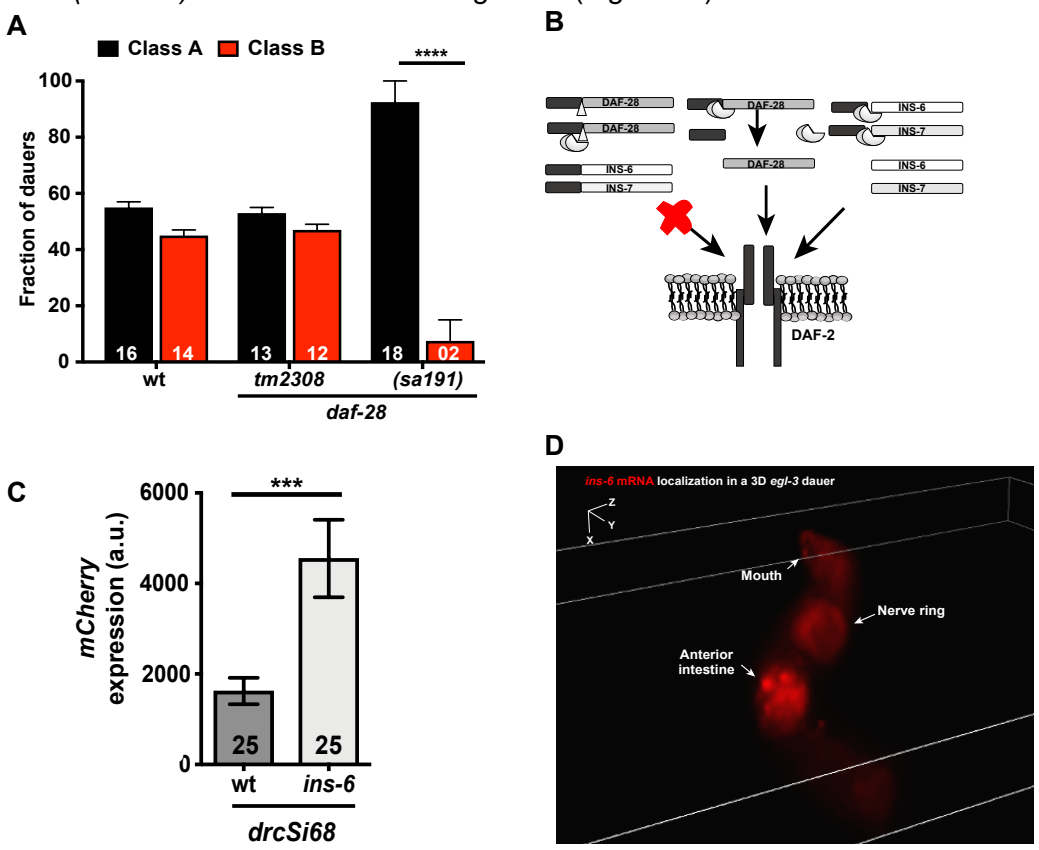

Fig. 5.1: ILPs regulate *ins-6* localization and expression. (A) Two alleles of *daf-28*, *tm2308* and *sa191*, have different effects on axonal *ins-6* mRNA. Wild-type dauers show equal distribution of class A and class B dauers, when they are 5-day old at 20°C. The number of animals observed for each condition is shown in each bar. (B) The predicted mechanism of peptide processing in the *sa191* mutation, which affects other ILPs (Li et al., 2003). A missense mutation, arginine to cysteine, near the N-terminal region of DAF-28 is believed to hamper a peptidase processing site. As this peptidase recognizes the same motif in DAF-28 and other ILPs, the *sa191* mutation is predicted to sequester the peptidase, which makes it unavailable to cleave and activate other ILPs. This increases the pool of unprocessed ILPs, which cannot activate DAF-2. (C) Quantification of *mCherry* expression in 25 wild-type animals and 25 *ins-6* mutants in the *drcSi68* background show *ins-6* can inhibit its own transcription. When *ins-6* mRNA is absent, the *cis* regulatory regions of *ins-6* in *drcSi68* become more active and produce higher amounts of *mCherry*. (D) In dauers that carry a mutation in an ILP pro-protein convertase, *egl-3, ins-6* mRNA is mislocalized at the anterior intestine, in a cluster of yet unidentified cells. While 3D-reconstruction of an *egl-3* mutant dauer show *ins-6* mRNA in the nerve ring, none of the neural cell bodies in the head region (toward the top of the panel) showed any *ins-6* expression.

functional INS-6 peptide increased *ins-6* transcription (Fig. 5.1C), which suggests that INS-6 negatively regulates its own mRNA expression. Therefore, a regulator of a major node of the inter-ILP network is *ins-6* itself.

In support of an *ins-6* negative feedback loop, I next tested if *ins-6* mRNA is also affected by EGL-3, which has been shown to limit INS-6 peptide levels (Hung et al., 2014). EGL-3 is the only known homolog of the proprotein convertase 2 [PC-2; (Thacker and Rose, 2000)] that cleaves a number of proproteins, including INS-6 at the R^{51}/R^{52} position, to form bio-active peptides (Hung et al., 2014). As expected, *ins-6* mRNA expression is affected in *egl-3* mutant dauers (Fig. 5.1D). In this mutant dauers, I observed that (i) none of the amphid somas express *ins-6*, (ii) the nerve ring (NR) axon bundle shows faint *ins-6* mRNA signals, and (iii) *ins-6* mRNA is now found in the anterior part of the intestine (Fig. 5.1D). These data suggest that EGL-3 is also a regulator of the inter-ILP network by processing different ILPs, including INS-6, to maintain the levels and cell-specific expression of *ins-6* mRNA. Since EGL-3 will likely process other neuropeptides, such as FRMF-like peptides (FLPs) or NLP neuropeptides (Kass et al., 2001), the possibility of other neuropeptides controlling the ILP network remains wide open.

Kinesins control both ins-6 localization and expression

Chapter 3 identified kinesins that are required for *ins-6* mRNA transport. These kinesins were selected from a gene-ontology based search for potential *C. elegans* kinesins and dyneins that can be tested as *ins-6* regulators (Fig. 5.2). We tested kinesins from each class that is depicted in Fig. 5.2 for defects in *ins-6* mRNA transport. In addition to the kinesins *unc-116*, *osm-3*, and *klp-6* that were shown in chapter 3 (Fig. 3.3 B-D; Fig. S3.4 B-D), two additional kinesins, *klp-4* and *unc-104*, affected *ins-6* expression (Fig. 5.3 A-B). While *klp-4* mutant dauers appeared to have the same distribution as wild-type dauers in terms of *ins-6* mRNA enrichment in somas versus axons (Fig. 5.3A), *klp-4* mutant dauers had variable effects on total *ins-6* mRNA levels (Figs. 5.3B and 5.4A). The

klp-4 mutation*, ok3537*, can increase *ins-6* mRNA levels in ASJ in a fraction of the dauer population (Figs. 5.3B and 5.4A). Although class A *klp-4* mutant dauers accumulated more *ins-6* mRNA in the soma, they still had more *ins-6* mRNA in the NR compared to the NRs of wild-type class A and class B dauers (Fig. 5.3B). In contrast, the class B *klp-4* mutant dauers showed similar *ins-6* mRNA levels in the NR compared to the NR of wild-type class B dauers (Fig. 5.3B). It is unclear if the higher axonal *ins-6* mRNA in the class A *klp-4* mutant dauers is due to bulk flow of increased *ins-6* mRNA in the ASJ soma (Fig. 5.3B). This is because *osm-3* mutant dauers had high levels of total *ins-6* mRNA in ASJ (Fig. 5.4A), but no enrichment in axonal *ins-6* mRNA (Fig. 3.3 B-D; Fig. S3.4 B-D). Together, this is consistent with the idea that axonal mobilization of *ins-6* mRNA must be regulated, where *klp-4* has two roles in regulating *ins-6* mRNA—one during mobilization and another during transcription or message stability. Likewise, *osm-3* and *klp-6* may have roles in both processes, because mutations in both kinesins affect *ins-6* mRNA subcellular localization (Fig. 3.3 B-D; Fig. S3.4 B-D) and total *ins-6* mRNA levels in dauers (Fig. 5.4A).

Interestingly, unlike the above kinesin mutants, *unc-104(e1265)* mutant dauers exhibited a completely altered *ins-6* transcriptional pattern rather than localization, where *unc-104* dauers lost most of their *ins-6* expression (Figs. 5.3 A-B and 5.4A). Because all four kinesin mutations affected *ins-6* expression in dauers, I also tested if they affect *ins-6* expression in well-fed or non-stressful conditions (Figs. 5.4B and 5.5). While *osm-3* and *klp-6* mutants had less of an effect on non-dauer *ins-6* mRNA (Fig. 5.4B), I found that *klp-4* and *unc-104* had a stronger effect on *ins-6* mRNA in the ASI and/or ASJ cell bodies during well-fed conditions (Fig. 5.5). The *klp-4* mutation increased *ins-6* mRNA in ASI at all stages and in ASJ in a stage-specific manner, whereas the *unc-104* mutation decreased *ins-6* mRNA in ASI at all stages, except for L1, and in ASJ at all stages (Fig. 5.5).

A

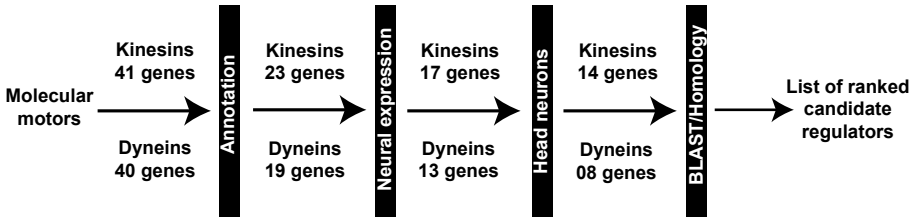

B

Kinesins	*C. remanei*	*C. briggsae*	*C. brenneri*	*D. melanogaster*	*D. rerio*	*M. musculus*	*H. sapiens*
klc-2	93%	92%	92%	67%	64%	65%	62%
osm-3	93%	94%	91%	45%	54%	60%	61%
klp-20	87%	91%	91%	50%	54%	55%	55%
unc-116	97%	98%	96%	59%	60%	59%	52%
ZC262.7	88%	93%	86%	58%	51%	59%	52%
klp-11	NA	62%	NA	NA	50%	54%	55%
unc-104	91%	93%	93%	52%	49%	49%	49%
klp-7	79%	79%	80%	60%	47%	46%	48%
klp-4	100%	99%	100%	47%	46%	43%	45%
klp-6	94%	95%	91%	15%	37%	37%	39%
klp-16	56%	54%	54%	36%	38%	36%	37%
klp-12	94%	89%	80%	55%	48%	36%	36%
klp-13	87%	89%	82%	51%	37%	36%	36%
vab-8	93%	91%	91%	NA	30%	30%	32%

Dyneins	*C. remanei*	*C. briggsae*	*C. brenneri*	*D. melanogaster*	*D. rerio*	*M. musculus*	*H. sapiens*
dlc-1	NA	NA	NA	93%	96%	96%	92%
dhc-1	94%	94%	92%	56%	56%	56%	56%
dyla-1	92%	92%	92%	0	44%	0	44%
che-3	91%	87%	87%	30%	44%	42%	41%
dli-1	90%	88%	88%	30%	31%	31%	31%
dylt-2	81%	81%	80%	32%	33%	36%	25%
dylt-3	66%	NA	NA	NA	35%	NA	NA
xbx-1	90%	89%	86%	28%	38%	34%	31%

Fig. 5.2: Candidates for *ins-6* mRNA transport. (A) The flowchart for the candidate genes to be tested. Using Intermine and Gene Ontology (GO) annotations, we sorted 41 kinesins and 40 dyneins in 23 kinesins and 19 dyneins, respectively. Based on head-neuron specific expression, we found that 14 kinesins and 8 dyneins were of interest. When we performed BLAST analyses, we could prioritize the kinesins and the dyneins based on the sequence similarity of the nucleotides. (B) The list of prioritized kinesins and dyneins. The sequence similarity is denoted for a fraction of the *Caenorhabditis* species, another invertebrate (*Drosophila melanogaster*), fish (*Danio rerio*) and mammals (mouse and humans). The white rows show the kinesins and dyneins that are present in all the species tested and have similarity in sequences across species. The light-gray rows are those kinesins and dyneins that have sequence similarity of 40-50% across species, except for *klp-11* (which lacks a similar gene in *Caenorhabditis sp*.) and *dyla-1* (which is lacking in flies and mice). The dark-gray rows list those motor proteins that have sequence similarity below 40% between different animals and are sometimes absent in other species. For example, *vab-8* is absent in *Drosophila,* while a similar gene to *dylt-3* is only present in *D. rerio*.

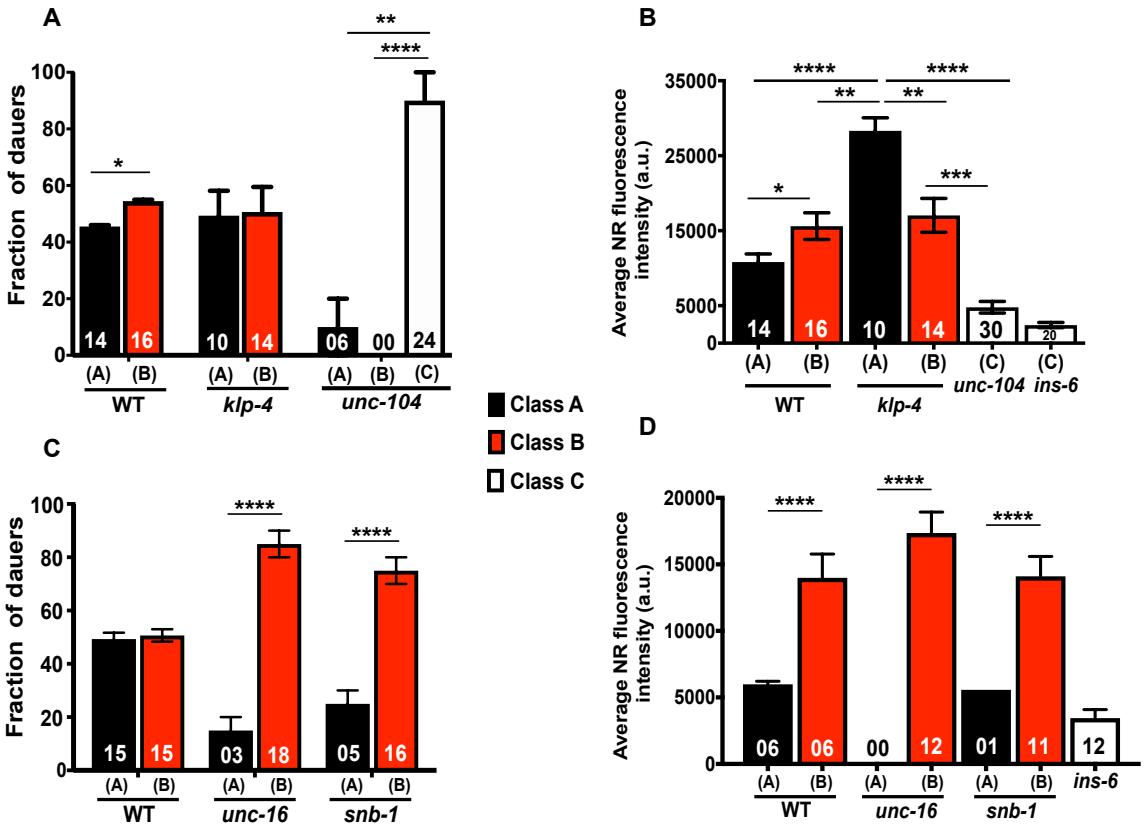

Fig. 5.3: Kinesin III family, UNC-16 adapter and synaptobrevin regulate *ins-6* levels in the NR. (A) The distribution of class A and class B dauers in *klp-4* mutants is similar to the wild-type distribution of dauers, while the *unc-104* mutant dauers show little to no *ins-6* expression and are largely classified as class C dauers. (B) The average NR fluorescence intensity of class A and class B dauers are shown in wild type (WT) and mutants of the kinesin III family, *klp-4* and *unc-104*. Because the NR of *unc-104* mutants show a fluorescence intensity similar to those of *ins-6* deletion mutants, they are classified as class C dauers. Axonal *ins-6* mRNA was higher in the class B population of wild-type dauers. While *klp-4* class A mutants had higher *ins-6* mRNA in the soma than in their NR, they also had higher *ins-6* mRNA in the NR compared to the NR of wild-type class A dauers. (C) The fraction of *unc-16* or *snb-1* mutant dauers that accumulate *ins-6* mRNA in the NR is higher than in wild type. This indicates that wild-type *unc-16*, which is a kinesin adapter and axonal gatekeeper, and *snb-1*, which regulates neurotransmission, prevent *ins-6* mRNA transport. (D) The average *ins-6* mRNA in the NR of wild-type, *unc-16* and *snb-1* mutant dauers.

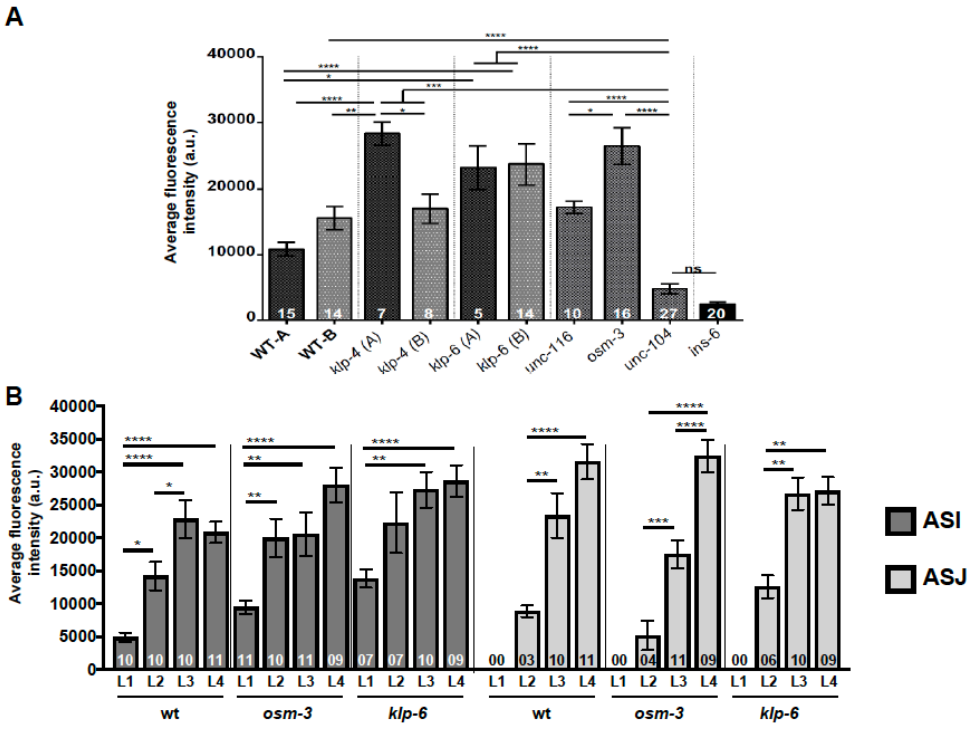

Fig. 5.4: *ins-6* mRNA levels in stressful and non-stressful conditions. (A) The total *ins-6* mRNA levels in wild-type and kinesin mutant dauers. (B) During reproductive development, *osm-3* and *klp-6* animals show similar patterns of dynamic *ins-6* expression in both ASI and ASJ neurons, which indicate that *osm-3* and *klp-6* do not greatly change *ins-6* expression in these larval stages. The number of animals assayed are shown in the bars.

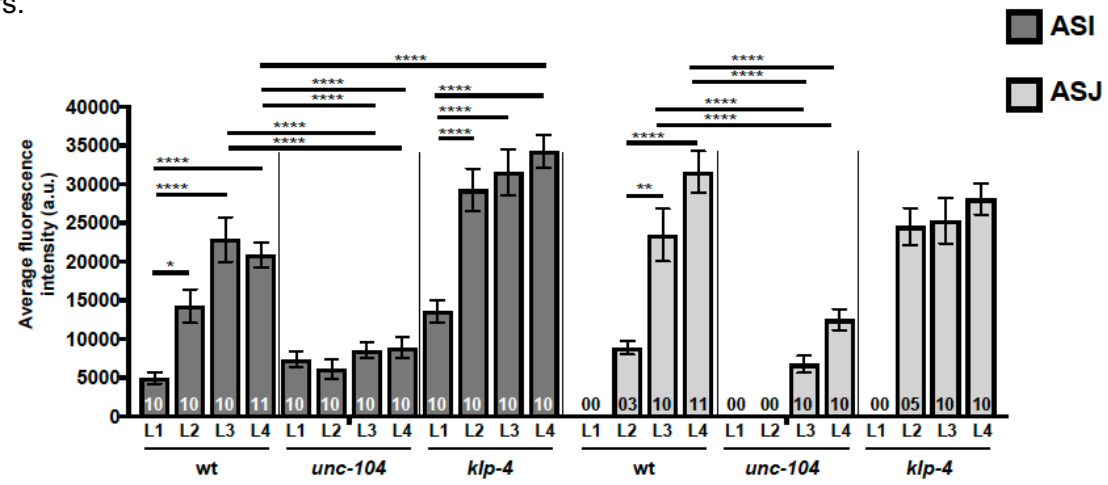

Fig. 5.5: *ins-6* mRNA levels during non-stressful conditions in *unc-104* and *klp-4* mutants. The number of animals assayed are shown in the bars. During development, *unc-104* and *klp-4* mutants regulate *ins-6* expression in well-fed conditions. In ASI neurons, *unc-104* mutants have significantly lower *ins-6* expression in L3s and L4s, while *klp-4* mutants have significantly higher *ins-6* expression in L4s. The *unc-104* ASJ neurons do not show *ins-6* expression until the animals are in L3 and have low *ins-6* expression in L3s and L4s. *ins-6* expression in the ASJ neurons of *klp-4* animals were like wild type, except for the L2s.

Together my data above suggest that kinesins might also participate in the regulation of *ins-6* mRNA steady-state levels (Fig. 5.1C) and the ILP network. Since kinesins are molecular motors in the cell, it will be interesting to uncover how kinesins, such as *klp-4* and *unc-104*, regulate *ins-6* transcription and/or stability, including the specific cargoes that these kinesins carry to regulate the inter-ILP network.

The JNK-dependent kinesin adapter UNC-16 inhibits axonal ins-6 mRNA transport

To ensure efficient cargo delivery, kinesins and dyneins bind to adapters, like UNC-16, which recognize the motors and/or their cargoes, and direct cargo delivery to the proper subcellular compartments (Byrd et al., 2001; Hirokawa et al., 2009). For example, *unc-104* kinesin mutants mislocalize the synaptobrevin SNB-1 in an *unc-16*-dependent manner (Byrd et al., 2001). Similarly, delivery of the *ins-6* and *daf-28* transcripts to the nerve ring may require the UNC-16 adapter to bind the kinesins and guide their movement away from the cell bodies. UNC-116, the *C. elegans* homolog of the kinesin-1 motor KIF5A, promotes *ins-6* mRNA transport to the dauer axons (Fig. 3.3B; Fig. S3.4B). In support of the above hypothesis, UNC-116 and its partner KLC-2, as well as UNC-104, the worm kinesin-3 motor KIF1A, have been shown to bind UNC-16, which is also known as Sunday Driver or the JNK-Interacting Protein (JIP) (Brown et al., 2009; Byrd et al., 2001; Sakamoto et al., 2005a).

The kinesin adapter UNC-16 is a direct target of the c-Jun N-terminal Kinase (JNK) pathway, which includes the kinases JNK-1, JKK-1, and SEK-1 (Byrd et al., 2001). Interestingly, like UNC-16, mutations in JNK-1 and JKK-1 mislocalize synaptobrevin-marked vesicles in the axons of motor neurons (Brown et al., 2009; Byrd et al., 2001; Sakamoto et al., 2005a). The JNK signaling pathway has been shown to be a stress sensor and interacts with insulin signaling by phosphorylating and activating the insulin pathway effector, the DAF-16/FOXO transcription factor (Oh et al., 2005). Because UNC-

16 is a kinesin adapter (Byrd et al., 2001) that responds to stress sensors that modulate insulin signaling (Oh et al., 2005), I next tested if UNC-16 influenced axonal *ins-6* mRNA transport. *unc-16* mutants exhibited increased axonal *ins-6* mRNA (Fig. 5.3 C-D), which is also consistent with the function of UNC-16 as an axonal gatekeeper that prevents the flow of organelles and vesicles into the axons (Edwards et al., 2015). Future experiments will be needed to determine whether wild-type UNC-16 inhibits axonal *ins-6* mRNA transport in response to the JNK pathway and/or insulin signaling.

Synaptic transmission also modulates ins-6 mRNA localization

A decrease in *unc-16* activity increased transport of both *ins-6* mRNA (Fig. 5.3 C-D) and synaptobrevin-marked vesicles to the axons (Byrd et al., 2001), which raises the possibility that synaptobrevin itself will also affect *ins-6* mRNA. The synaptobrevin SNB-1 is a synaptic vesicle-associated membrane protein that is required for vesicle exocytosis and neurotransmission (Nonet et al., 1998). I found that a mutation that decreased SNB-1 activity increased *ins-6* mRNA levels in the NR and the number of animals that showed *ins-6* mRNA in the NR (Fig. 5.3 C-D), which suggests that low or altered neurotransmission promotes axonal mRNA transport. This presents an intriguing model that remains to be tested: stress decreases or alters the activities of both UNC-16 and SNB-1 to traffic *ins-6* mRNA to dauer axons, where the mRNA is poised to respond to the removal of stress cues.

OSM-3 may directly transport ins-6 mRNA to specific subcellular compartments

The transport of *ins-6* mRNA to the axons begs the identity or identities of the kinesins that directly traffic the mRNA to the axons. OSM-3, a *C. elegans* kinesin II motor that acts in the same neuron to promote *ins-6* mRNA transport (Fig. 3.3 B-D; Fig. S3.4 B-D), is an excellent candidate. While there is no direct proof that OSM-3 physically associates with *ins-6* mRNA in a protein-mRNA complex, I found that a GFP-tagged OSM-3 (OSM-

3::GFP) co-localized with *ins-6* mRNA in dauers (Fig. 5.6). The ASJ neurons of *osm-3(p802)* mutant dauers that had been rescued with OSM-3::GFP (Fig. 3.3C) showed co-localization of *ins-6* mRNA and GFP in the cell bodies. All rescued dauers (Fig. 3.3C) also showed co-localization of both mRNA and protein signals in the NR. In addition, I observed the same co-localizations in the ASJ soma and NR axon bundle of *daf-2(e1368)*; *osm-3(p802)* double mutants that were again rescued with OSM-3::GFP in the ASJ neuron (Fig. 3.3D). Intriguingly, however, about a quarter of the rescued double mutants also showed GFP-marked dendritic arbors in the ASJ neurons (Fig. 5.6), which suggests that stress can induce branching in the ASJ dendrites. In addition, these OSM-3::GFP-marked dendritic regions co-localized with *ins-6* mRNA (Fig. 5.6), although the significance of the *ins-6* mRNA in the dendritic arbors or the proximal parts of the dendrites remain to be determined. Because the ASJ cell body and arbors (Fig. 5.6 D-F) showed co-localization of OSM-3::GFP and *ins-6* mRNA in a precise manner, this is consistent with OSM-3 directly trafficking *ins-6* mRNA to the proper subcellular compartment.

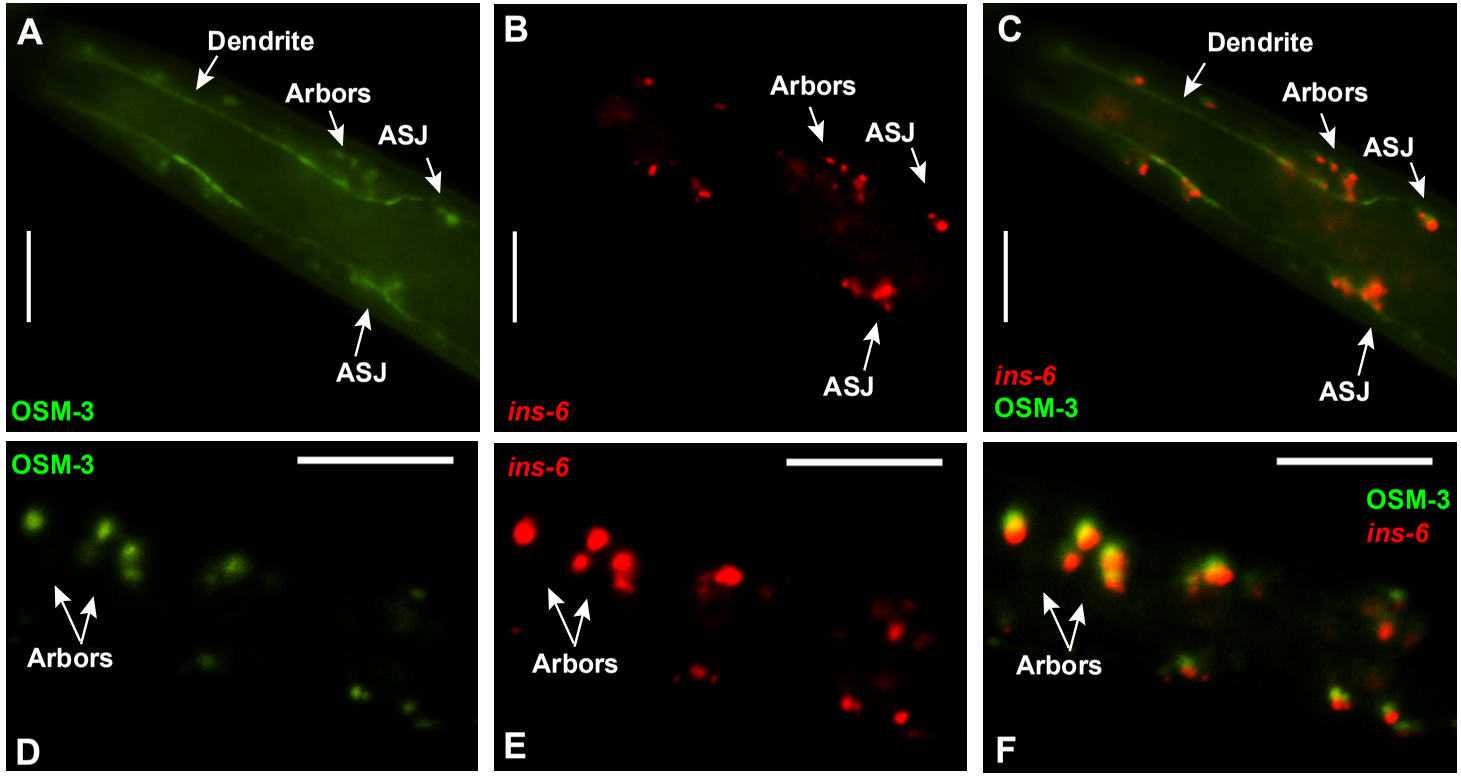

Fig. 5.6: OSM-3 potentially transports *ins-6* mRNA to the dendritic arbors of ASJ in dauers. (A) OSM-3::GFP in the dendrites and cell bodies of both ASJ neurons. In a quarter of rescued *daf-2(e1368)*; *osm-3* double mutant dauers (n = 5 of 20 total dauers), the ASJ dendrites arborize. (B) Endogenous *ins-6* transcripts are present in the dendritic arbors and cell bodies of the dauer ASJ neurons. (C) Co-localization of OSM-3::GFP and *ins-6* transcript in the dendritic arbors and cell bodies of ASJ suggests that OSM-3::GFP directly transports *ins-6* mRNA towards ASJ processes. (D) Higher magnification of individual OSM-3::GFP clusters in the dendritic arbors and cell bodies. (E) *ins-6* mRNA is also found in magnified dendritic arbors and cell bodies. (F) Co-localization of *ins-6* mRNA and OSM-3::GFP in the dendritic arbors and cell bodies suggest that OSM-3::GFP can directly bind and transport *ins-6* mRNA to specific subcellular compartments. The orientation of *ins-6* mRNA with respect to the OSM-3 protein in each cluster suggest that the binding and transport of the kinesin-mRNA complex involves a specific organization, which might include additional factors. ASJ denotes cell bodies of ASJ; arbors denote dendritic arbors; and dendrites denote arborless tracts. Scale bar, 10 μm.

The potential role of mRNA structure and stability in axonal transport

The untranslated regions (UTRs) of mRNAs provide stability to the mRNA, play a role in transport to various parts of the cell and interact with proteins that aid in translation. Therefore, I dissected the role of *ins-6* UTRs in mRNA transport. Although I found that the *ins-6* UTRs are insufficient to traffic mRNA to the axons (Fig. 3.3 F-G), the *ins-6* UTRs do play a role in mRNA stability, since a lack of the UTRs caused a reduction in *ins-6* mRNA levels (Fig. 3.3E). My finding that a second dauer exit-promoting ILP mRNA, *daf-28*, is transported to the NR (Fig. 3.2) next led me to dissect the role of UTRs in maintaining the predicted structural integrity of the ILP mRNAs that are present or absent in the axons. mRNA structures are important for the mRNA-protein interactions that are crucial during the transport, stabilization and translation of the mRNAs (Mignone et al., 2002). By using Zuker's mFold algorithms provided by the Vienna RNA package (http://rna.tbi.univie.ac.at), I systematically predicted twenty different structures for the ILPs *daf-28*, *ins-6*, and *ins-1*, in the presence or absence of their respective UTRs. The figures, Figs. 5.7 to 5.10, show the most likely structures (1st probability, > 98%) that are predicted by Zuker's mFold for each set of ILP mRNAs that are full length (Fig. 5.7), lack all UTRs (Fig. 5.8), lack only the 5' UTRs (Fig. 5.9), or lack only the 3' UTRs (Fig. 5.10). These predictions have the highest thermodynamic stability at 20°C (Fig. 5.11), the temperature at which the worms were largely grown in the studies described in this thesis, unless otherwise specified.

The full-length *ins-6* mRNA (Fig. 5.7) is predicted to form a bubble, where the 5' UTR and 3' UTR meet each other. This trend is similar in all three ILPs tested so far. However, the dauer exit-promoting ILPs *daf-28* and *ins-6* also form stem-loop structures that presumably provide anchor-points for proteins to bind the mRNAs. *ins-6* mRNA has a primary three-pronged stem, which additionally contains two-or three-pronged stems. The presence of multi-pronged stem-loops in both dauer exit-stimulating ILP mRNAs, *ins-*

6 and *daf-28*, and the absence of such stems in the dauer exit-inhibiting *ins-1* mRNA (Fig. 5.7) raise the possibility that the multi-pronged stems play an important role in *ins-6* and *daf-28* function.

When the UTRs are removed from its ILP RNA sequence, *ins-1* adopted a centroid structure unlike the full-length *ins-1* mRNA (Figs. 5.7 and 5.8). However, when the UTRs were deleted from the dauer exit-promoting ILP mRNAs, *ins-6* and *daf-28,* they became more tubular with fewer stem-loops or they form a stunted loop at the end of the tubule, as predicted for *daf-28* mRNA (Fig. 5.8). Therefore, unlike *ins-1* mRNA, loss of UTRs in the *ins-6* and *daf-28* mRNAs predicts tubular structures that might be less likely to interact with proteins compared to the predicted structures of their full-length transcripts (Figs. 5.7 and 5.8).

Since the *ins-6* and *daf-28* UTR-less RNA constructs predict altered RNA structures, I next tested if elimination of either 5' or 3' UTRs also made any differences in the predicted structures of the ILP mRNAs (Figs. 5.9 and 5.10). While loss of the 5' UTR had little effect on the predicted *ins-1* mRNA structure, loss of either UTRs did alter the mRNA structures of both *ins-6* and *daf-28* and deletion of the 3' UTR again promoted the centroid structure of *ins-1* mRNA (Figs. 5.9 and 5.10). Together the predictions support the importance of the UTRs in the ILP mRNA structures. Although more experiments will be needed to understand the specific roles of the multi-pronged stem loops in *ins-6* or *daf-28* mRNA function, one cannot deny that the UTRs of *ins-6* and *daf-28* provide thermodynamic stability to the mRNAs (Fig. 5.11). Indeed, the UTR-less constructs of *ins-6* decreased its mRNA levels, as well as its transport to the axons (Fig. 3.3E).

I also analyzed the Gibb's free energy change of each of these predicted structures and found that UTR-less mRNAs are less stable than full-length ILP mRNAs or mRNAs that have lost one of the UTRs (Fig. 5.11). Another way to interpret these bioinformatic predictions is to assume that the full-length RNA structure with its given

thermodynamic properties provides the best chance under physiological conditions. I have shown by genomic rescue experiments (Fig. 3.3E) that full-length *ins-6* is fully functional

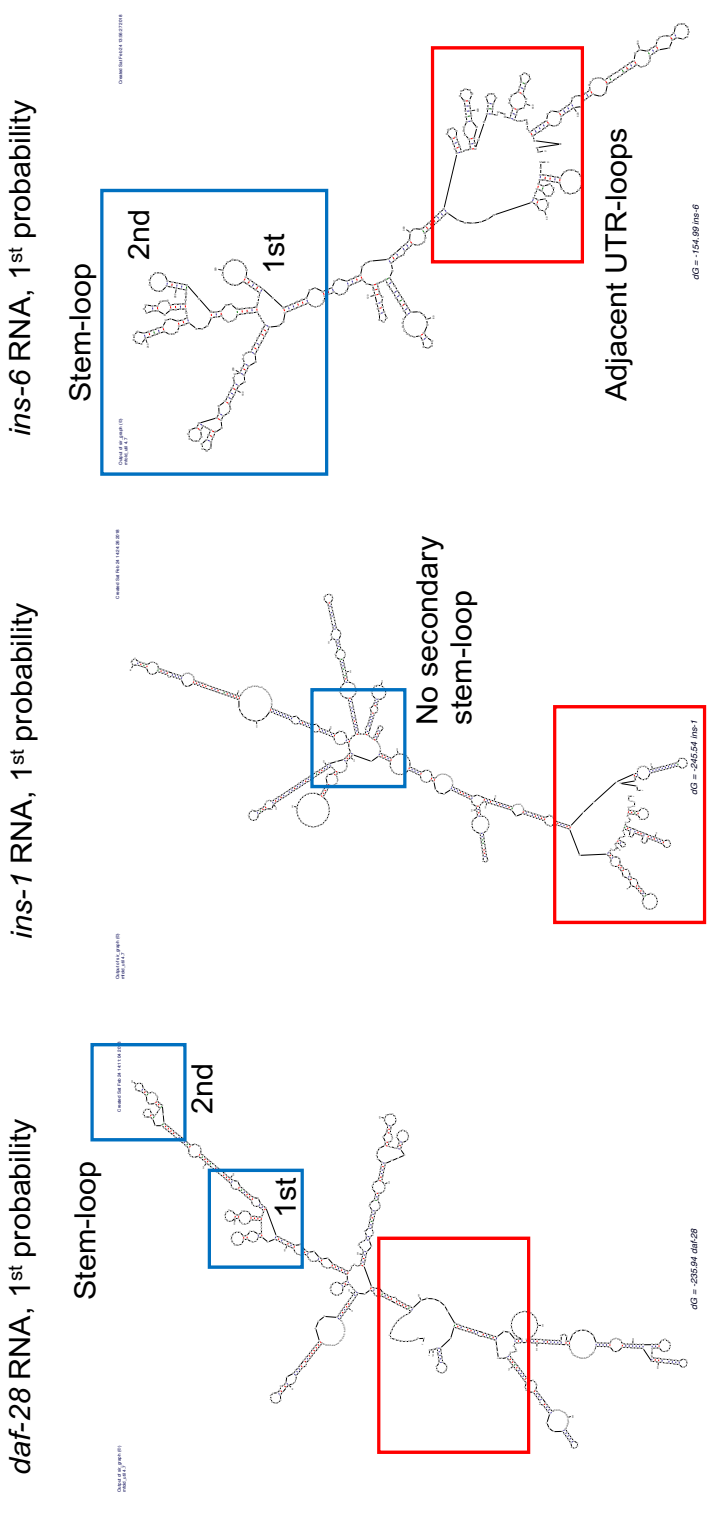

Fig. 5.7: Predicted structures of full-length ILP mRNAs: *daf-28, ins-1* and *ins-6*. The first probability of 20 probabilities are shown. The red boxes indicate the loops between the start (5' UTR) and the end (3' UTR) of each mRNA. The 5' to 3' direction of the mRNA is shown in the clockwise direction. The UTRs of each ILP fold onto each other to maintain thermodynamically stable mRNA structure in the cytosol. The blue boxes indicate the stem-loop structures that each ILP mRNA forms. *daf-28* and *ins-6* form secondary multi-pronged loops, but *ins-1* does not form any secondary, multi-pronged loops.

and localizes to the axons like wild type, indicating that the resulting full-length *ins-6* mRNA structure should bind to the correct set of proteins. Therefore, searching for the absence and presence of secondary loops within a given range of free energy change must indicate how the UTRs change RNA structure and affect stability and its potential protein interactions. By this logic, when we combine the structural results with the given free energy change, we observe that losing the 5' UTR alters the stem-loop structures of *ins-6* mRNA without much change in its free energy (Figs. 5.7, 5.9, and 5.11). However, it is possible that losing the 5' UTR may actually cause the mRNA to bind to different proteins or the mRNA may function in a way that is yet unknown. If so, then any UTR-interacting proteins are also candidate regulators of the inter-ILP network. In other words, because a UTR-less *ins-6* mRNA structure does affect *ins-6* expression, any gene that affects *ins-6* RNA structure are fair candidates for regulators of *ins-6* and the inter-ILP network.

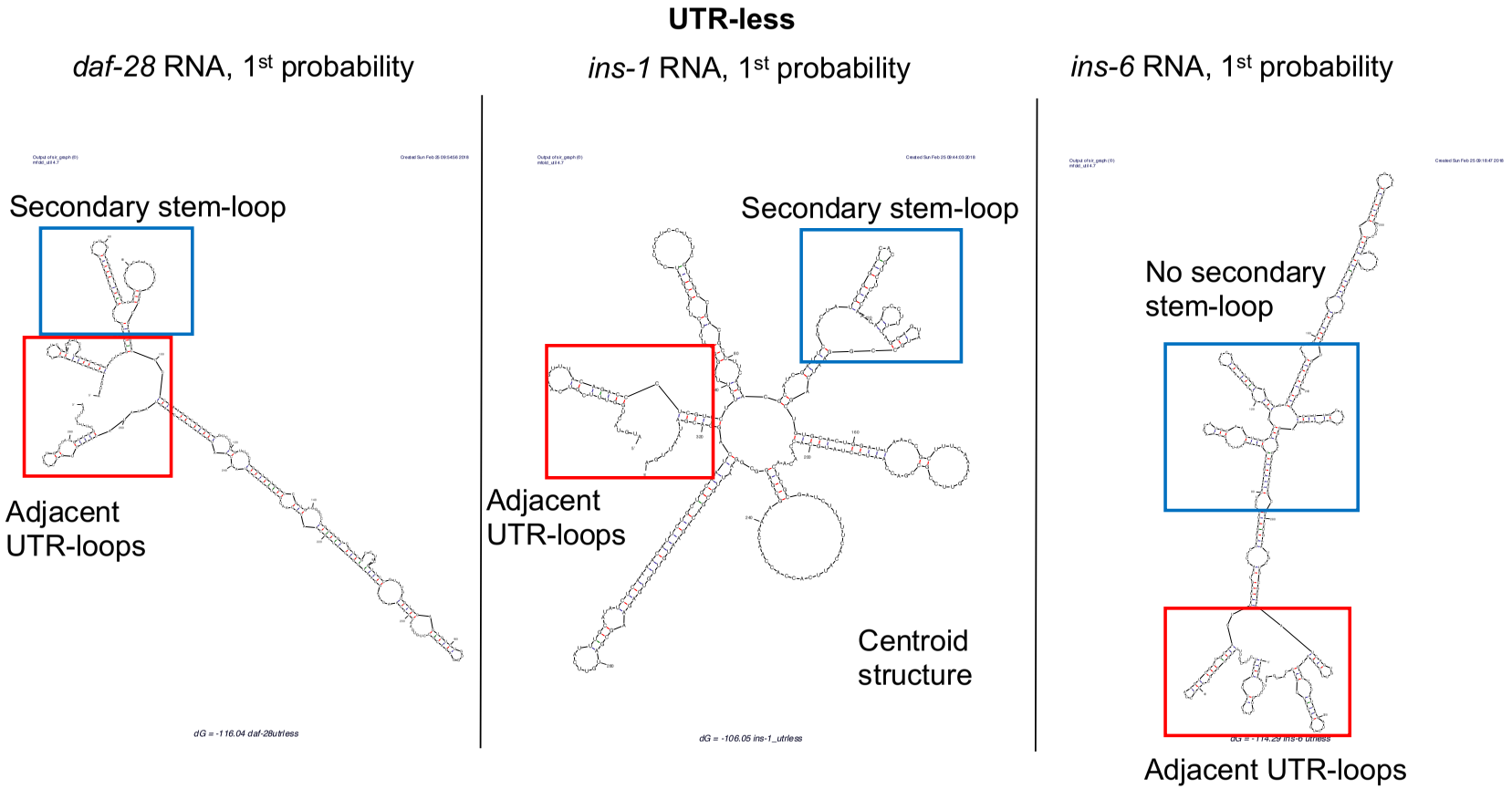

Fig. 5.8: Predicted structures of ILP mRNAs that lack UTR structures: *daf-28, ins-1* and *ins-6.* The first probability of 20 probabilities are shown. The red boxes indicate the loop between the start and the end of each mRNA. The 5' to 3' direction of the mRNA is shown in the clockwise direction. The blue boxes indicate the stem-loop structures that each ILP mRNA forms. Without the UTRs, *ins-1* forms secondary multi-pronged stem-loops and has a more centroid structure, which is much more stable than its own full-length mRNA.

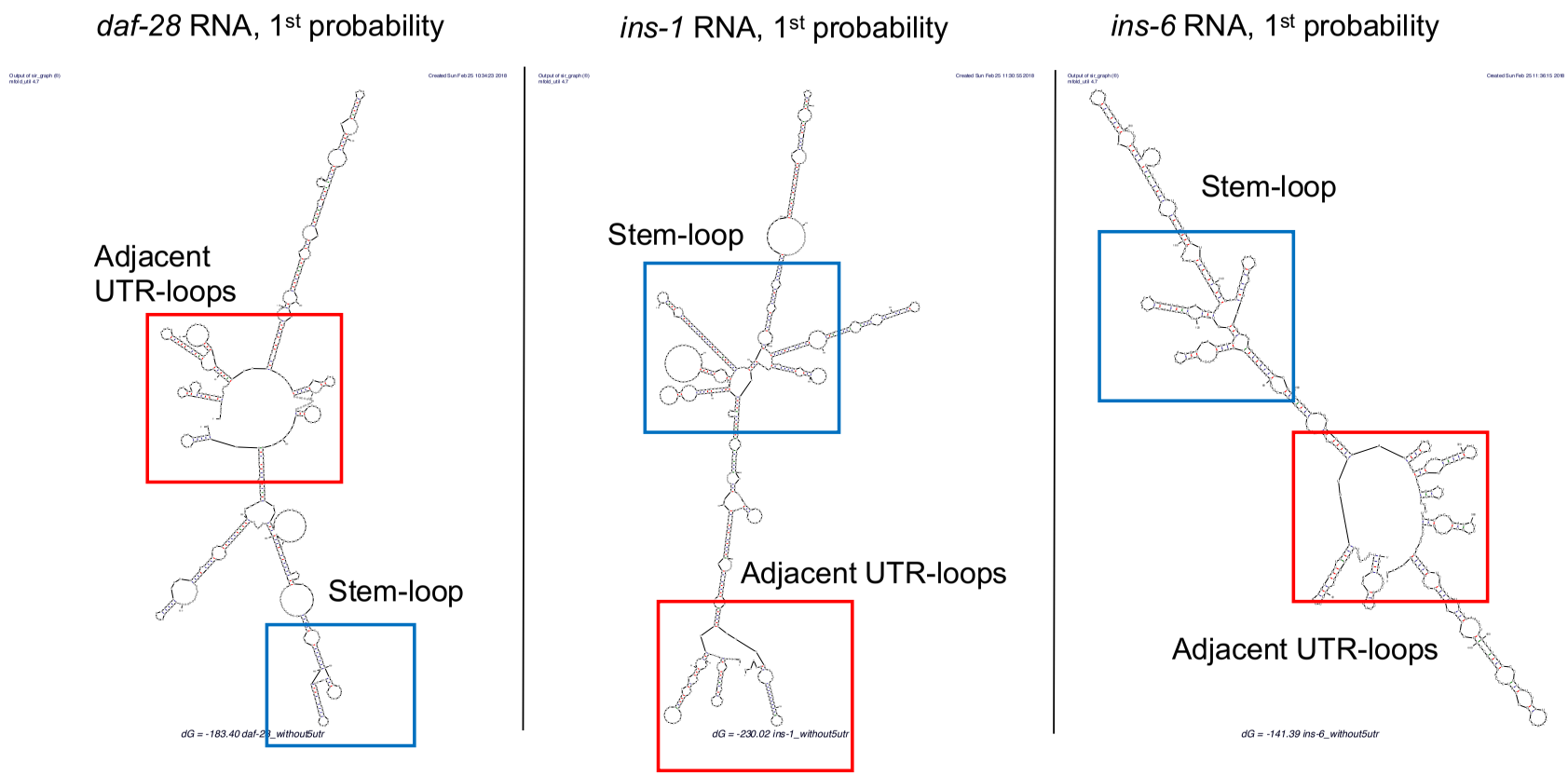

Fig. 5.9: Predicted structures of ILP mRNAs that lack 5' UTRs: *daf-28, ins-1* and *ins-6.* The first probability of 20 probabilities are shown. The red boxes indicate the loop between the start and the end of each mRNA. The 5' to 3' direction of the mRNA is shown in the clockwise direction. The UTRs of each ILP fold onto the translated regions and maintain thermodynamically stable mRNA structures in the cytosol. The blue boxes indicate the stem-loop structures that each ILP mRNA forms.

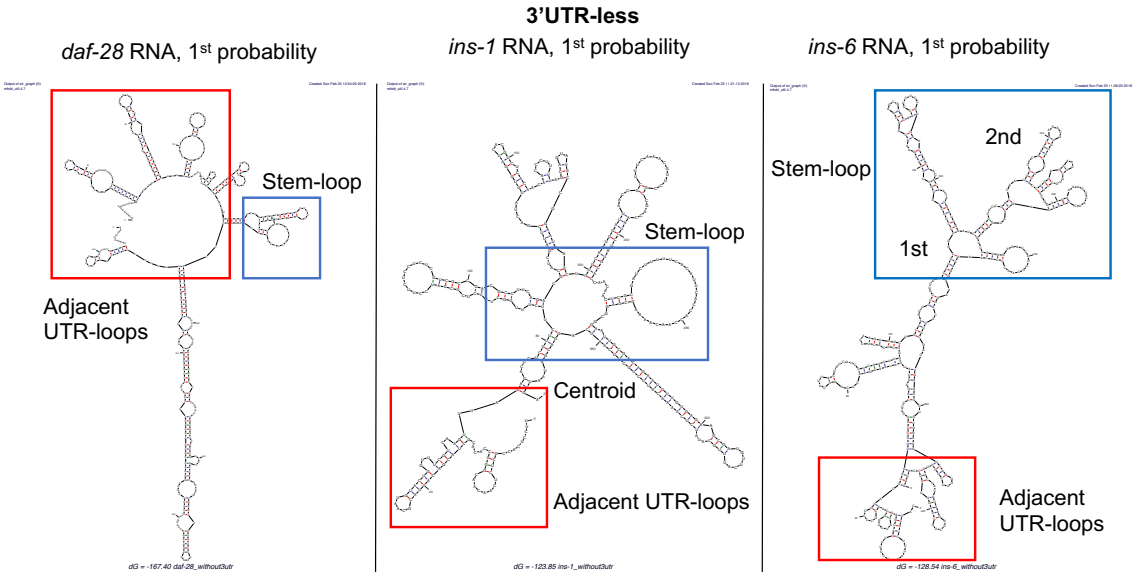

Fig. 5.10: Predicted structures of ILP mRNAs that lack 3' UTRs: *daf-28, ins-1* and *ins-6.* The first probability of 20 probabilities are shown. The red boxes indicate the loop between the start and the end of each mRNA. The 5' to 3' direction of the mRNA is shown in the clockwise direction. The blue boxes indicate the secondary stem-loop structures that each ILP mRNA forms.

Internal energy and stability of RNA structure

ΔG kCal/Mol	Full length	5' UTR-less	3' UTR-less	UTR-less
daf-28	-235.94	-183.40	-167.40	-116.04
ins-1	-245.54	-230.02	-123.45	-106.05
ins-6	-154.99	-141.39	-128.54	-114.29

Fig. 5.11: Predicted free energy change of ILP mRNA structures: *daf-28, ins-1* and *ins-6.*

CHAPTER 6 STRESS-INDUCED PLASTICITY IN THE *C. ELEGANS* NERVE RING

Introduction

Students before an exam, soldiers on duty, and stock-market traders in a fluctuating market may seemingly have nothing in common, except for the tenet that each of them are responding to stress, albeit differently. Stressful experiences provoke certain specific physiological and psychological changes in humans that allow them to endure stress, as described by the outstanding neuroscientist Hans Seyle, beginning with his theories on the general adaptation to stress (Selye, 1950, 1993). About 70 years later, we now know that such general adaptation to stress leads to structural changes in the brain, observed in humans, as well as in several other experimental models (McEwen and Morrison, 2013). Despite extensive stress-induced studies in several animals, many questions still remain. For example, how does our brain exit from stress and does the imprint of the stressed brain carry over to the post-stressed brain, anatomically and functionally? This is important because failure to exit from stress leads to post-traumatic stress disorders, anxiety, depression and several other forms of illnesses (Breslau, 2002; Flory and Yehuda, 2015).

For humans, fear is a form of stress (Cordero et al., 2003; Shin and Liberzon, 2010). Since it is difficult to perform fear conditioning in humans, fear-induced Pavlovian conditioning in many different animal models, from rodents to primates, have been used to understand the basis of stress conditioning (Cordero et al., 2003; Wojnarowicz et al., 2017). In rats, fear-induced chronic stress causes dendritic shrinkage; and as soon as the animals are rested, the dendrites regenerate and expand, which demonstrates the structural plasticity of the brain in response to stress (Bloss et al., 2010). In addition, the prefrontal cortex, orbitofrontal cortex, limbic system and amygdala undergo anatomical changes during stress, but much remain unknown about how each of these brain regions

is reorganized upon recovery from stress (Bloss et al., 2010; Cordero et al., 2003; Shin and Liberzon, 2010).

These anatomical changes have functional consequences (Bloss et al., 2010). Stress-induced loss of dendritic spines in the prefrontal cortex is associated with decreased working memory: the degree of memory impairment directly correlates with dendritic spine loss (Bloss et al., 2010). Therefore, structural plasticity in the brain allows the rats to adapt to stress, which might also be accompanied by a decrease in working memory. Like rats, humans exhibit stress-related functional plasticity, based on functional magnetic resonance imaging (fMRI) of analogous brain regions in stressed versus non-stressed humans (Liberzon and Sripada, 2007). Although we lack studies that directly link the structural changes in the human brain with the structures that optimize stress responses, it is not surprising that similar plasticity exists in the human brain.

In an enriched environment that stimulates neural activity, humans, primates, rodents, birds, fish and other animals, also exhibit neural plasticity, which is reflected by structural and functional alterations (Ball et al., 2019; Hannan, 2014; Mandolesi et al., 2017). Insulin-like growth factor 1 (IGF-1) is hypothesized to change pre-natal and post-natal brain development including experience-dependent plasticity, neurogenesis and synaptogenesis (Costales and Kolevzon, 2016). IGF-1 also promotes neural plasticity in adults exposed to enriched environments. When IGF-1 is administered exogenously into aging adult visual cortices that have reduced plasticity, IGF-1 restores cortical neural responses to visual inputs in these adults (Maya-Vetencourt et al., 2012). This suggests that changes in any kind of environmental cues can change the brain circuitry with functional consequences. Therefore, I asked if the environment will also change circuit morphology in *C. elegans*, especially because dauer is an adaptive response to harsh environmental changes. I specifically addressed whether dauers have a structurally altered nerve ring (NR) structure, which contains many of the synapses within the animal's

nervous system. The advantages that *C. elegans* offers as a model organism, *e.g.*, easy culturing conditions and a mapped nervous system that allows live imaging, should facilitate studies that aim to understand the mechanisms governing structural and functional circuit plasticity in the nervous system.

A very recent study suggests that dauers undergo extensive electrical remodeling of the neurons in the NR region through *che-7* (Bhattacharya et al., 2019), a candidate gene from our EMS screen for transcriptional regulators of *ins-6* (Fig. 4.4; Chapter 4 Results and Discussion). However, the global effect of stress on the entire NR morphology remains unknown. Here I report that the *C. elegans* nervous system, especially the NR, which serves as the primitive brain of the worm, undergoes stress-dependent structural alterations, according to differential interference contrast (DIC) microscopy. I also find that these structural changes in the NR are plastic: the NR of dauers that exit into post-dauer L4s resembles the NR of animals that never entered the dauer program. However, as the molecular mechanisms of these structural alterations are only beginning to be understood (Bhattacharya et al., 2019), it is difficult to assess if and how the *C. elegans* post-dauer NR differs from the NR of worms that were never exposed to stress. In the future, it will be interesting to discover if the mechanisms that alter the *C. elegans* NR structure in response to stress will also be conserved in the brains of higher animals, such as flies, fish, rodents and humans.

Results

Stress-induced broadening of the nerve ring axon bundle

During evolution, the animals that branched off early from the evolutionary tree, such as cnidarians, corals, and sea anemones, have a diffused nerve net throughout their bodies in place of the central and peripheral nervous systems found in higher animals (Arendt et al., 2016; Burkhardt and Sprecher, 2017; Clark et al., 2019). As animals evolved, the nervous system became more centralized: in nematodes, like *C. elegans*, the

nerve net developed into a nerve ring; in flies and chordates, the nerve net evolved into the brain (Arendt et al., 2016). Although the origin of a bilaterally symmetric and centrally located nervous system has been debated (Arendt et al., 2016; Burkhardt and Sprecher, 2017), *C. elegans* already exhibits a simple bilateral nervous system with a centrally located neuropil, similar to the human central nervous system. This centrally located

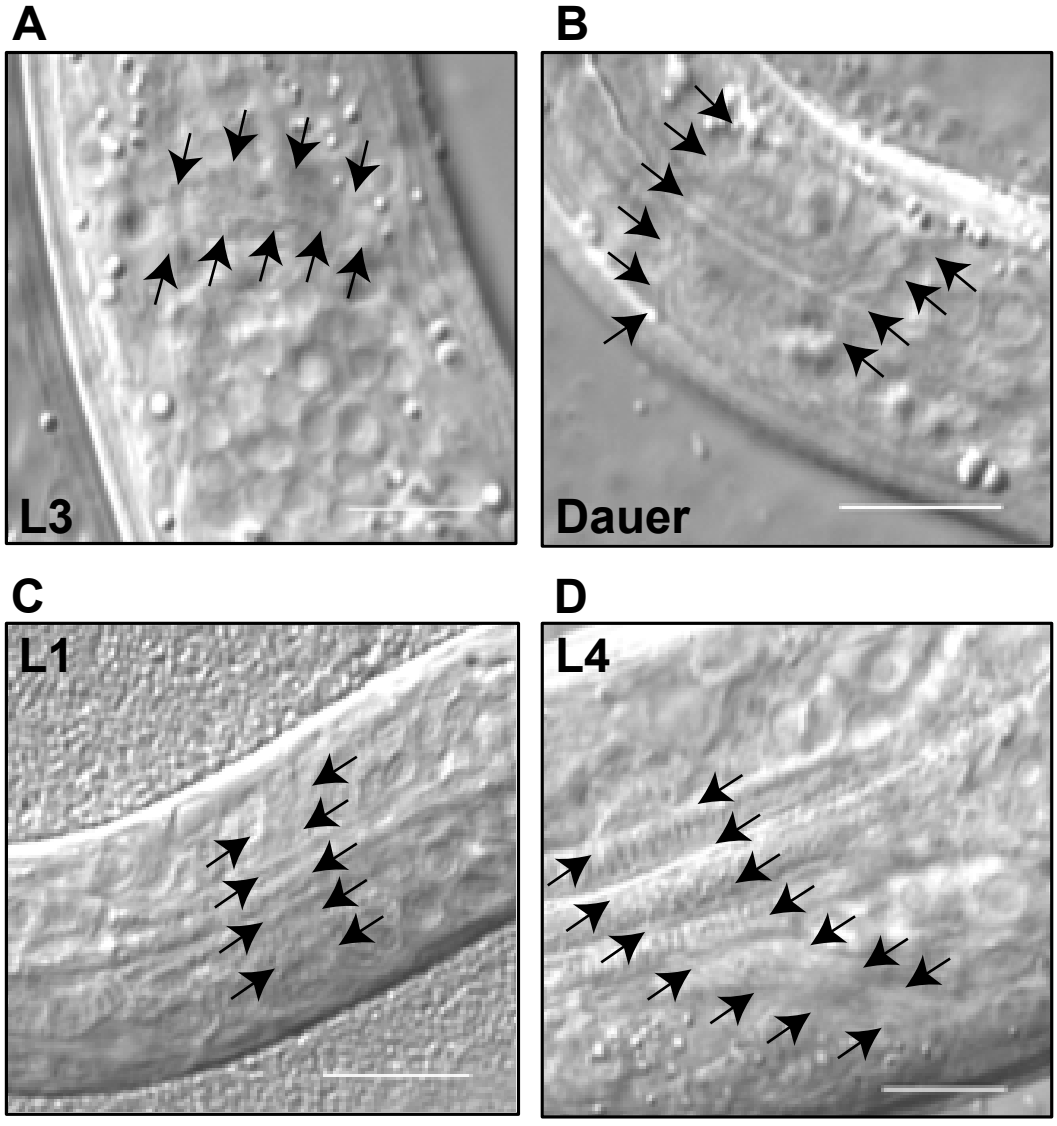

Fig. 6.1: Stress changes nerve ring (NR) morphology. The edges of the NR structure are indicated by arrows. The concave round structures beyond the arrows are a cluster of neuronal nuclei that are adjacent to the NR in that same focal plane. Scale bar, 10 microns. (A and B) Compared to an L3 larva, a dauer has a wider NR. (C) An L1 has a narrower NR compared to an L3 and a dauer. (D) An L4 has a wider nerve ring compared to an L1, despite having a narrower NR than the dauer NR.

neuropil is known as the nerve ring that consists of 180 axonal projections and their associated electrical and chemical synapses [Fig. 6.1; (Ware et al., 1975)]. Interestingly, I found that the nerve ring of dauers widened along the anterior-posterior axis, compared to that of its unstressed larval counterpart, L3 (Fig. 6.1 A-B), or of any other larval stages, such as L1s and L4s (Fig. 6.1 C-D).

To understand if this stress-induced structural alteration is plastic in nature, I measured the width of the NR at all stages under unstressed, stressed, and post-stressed conditions (Fig. 6.2). I found that as the worm developed through the larval stages, the width of the NR increased until the L3 stage, after which the NR width remained the same till the last larval stage (L4; Fig. 6.2). However, as soon as L1s sense stressful situations, the NR further widened, as evident in the NR width of pre-dauers and the subsequent dauers (Fig. 6.2). The broadening of the NR in pre-dauers and dauers was quite distinct from the increase in NR width from L1 to L3 (Fig. 6.2), which suggests that the centrally located neuropil of *C. elegans* is structurally very different under stressful situations. Consistent with this idea, when dauers sensed the return of optimal conditions and exited into the post-dauer L4 stage, the NR started to narrow (Fig. 6.2).

As dauer formation is a conscious response to overcrowding and food scarcity during development (Golden and Riddle, 1984), I explored the effect of starvation alone on the NR. Interestingly, I found that starvation not only was insufficient to broaden the NR, but it also caused stunted NR development, based on the reduced NR width of starved L3s (Fig. 6.3). Since dauers are longer and thinner than their developmental counterpart, L3 (Albert and Riddle, 1983; Golden and Riddle, 1984; Swanson and Riddle, 1981), it is possible that the increase in NR width is due to an increase in the length and/or decrease in the diameter of dauers. Thus, I measured the lengths of the pharyngeal isthmuses,

which position the nerve rings and are reflections of the animals' lengths, as well as the diameters of the different larvae. First, I found that pre-dauers have a similar

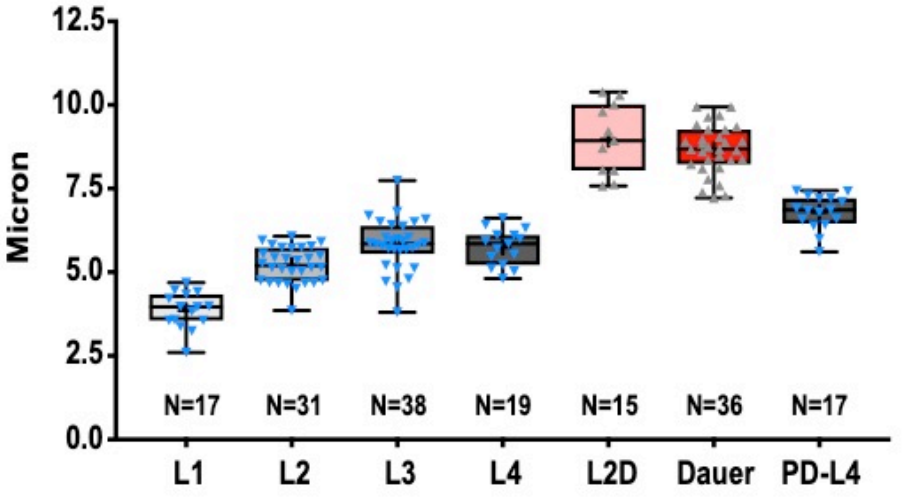

Bonferroni's test	Significant?	Summary	Adjusted P Value
L1 vs. L2	Yes	****	<0.0001
L1 vs. L3	Yes	****	<0.0001
L1 vs. L4	Yes	****	<0.0001
L1 vs. L2D	Yes	****	<0.0001
L1 vs. Dauer	Yes	****	<0.0001
L1 vs. PD-L4	Yes	****	<0.0001
L2 vs. L3	No	ns	0.591
L2 vs. L4	Yes	ns	0.294
L2 vs. L2D	Yes	****	<0.0001
L2 vs. Dauer	Yes	****	<0.0001
L2 vs. PD-L4	Yes	***	<0.001
L3 vs. L4	No	ns	>0.9999
L3 vs. L2D	Yes	****	<0.0001
L3 vs. Dauer	Yes	****	<0.0001
L3 vs. PD-L4	Yes	**	0.002
L4 vs. L2D	Yes	****	<0.0001
L4 vs. Dauer	Yes	****	<0.0001
L4 vs. PD-L4	Yes	**	0.007
L2D vs. Dauer	No	ns	>0.9999
L2D vs. PD-L4	Yes	**	0.002
Dauer vs. PD-L4	Yes	****	<0.0001

Fig. 6.2: Quantification of changes in NR width along the anterior-posterior axis during development. (A) The NR width is plotted graphically with individual values represented in blue (non-dauer or post-dauer larvae) and gray (pre-dauer or dauer larvae) triangles. The number of animals assayed (N) are mentioned for each stage. (B) Bonferroni tests for the NR widths are tabulated. Pre-dauers (L2Ds) and dauers have significantly greater NR width compared to any other developmental stage, suggesting that the dauer program alters NR structure.

A

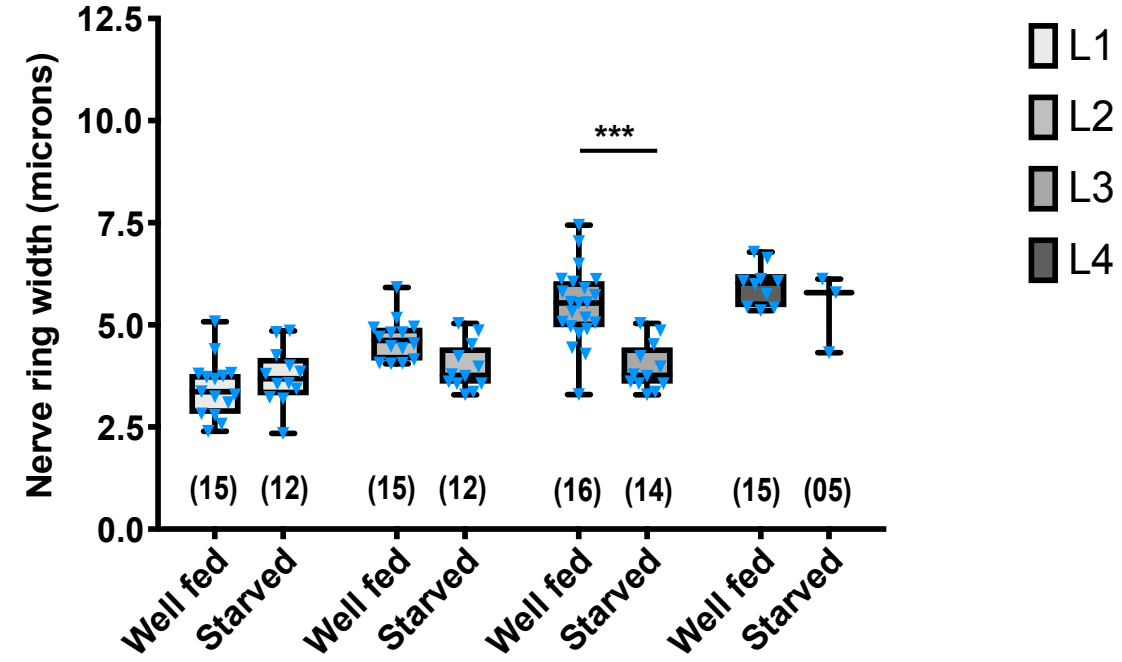

B

Bonferroni's test	Significant?	Summary	Adjusted P Value
L1 vs. L2	Yes	**	<0.01
L1 vs. L3	Yes	****	<0.0001
L1 vs. L4	Yes	****	<0.0001
L2 vs. L3	No	ns	>0.0.05
L2 vs. L4	Yes	****	<0.0001
L3 vs. L4	Yes	**	<0.01

Fig. 6.3: Starvation is not sufficient to change NR width. (A) Graphical plots of the NR width of all four larval stages reared in starvation versus well-fed conditions. Individual values are represented in blue triangles. The NR width of well-fed L3 is significantly higher than starved L3s. The number of animals assayed (N) are mentioned for each stage. (B) Bonferroni tests for the NR widths are tabulated for well-fed larvae. Each stage shows a significant increase in NR width as the animal develops to the L3 stage. (C) Unlike the well-fed state, starved larvae do not show significant changes the early larval stages and differ only between the earlier larval stages and the last larval stage.

A

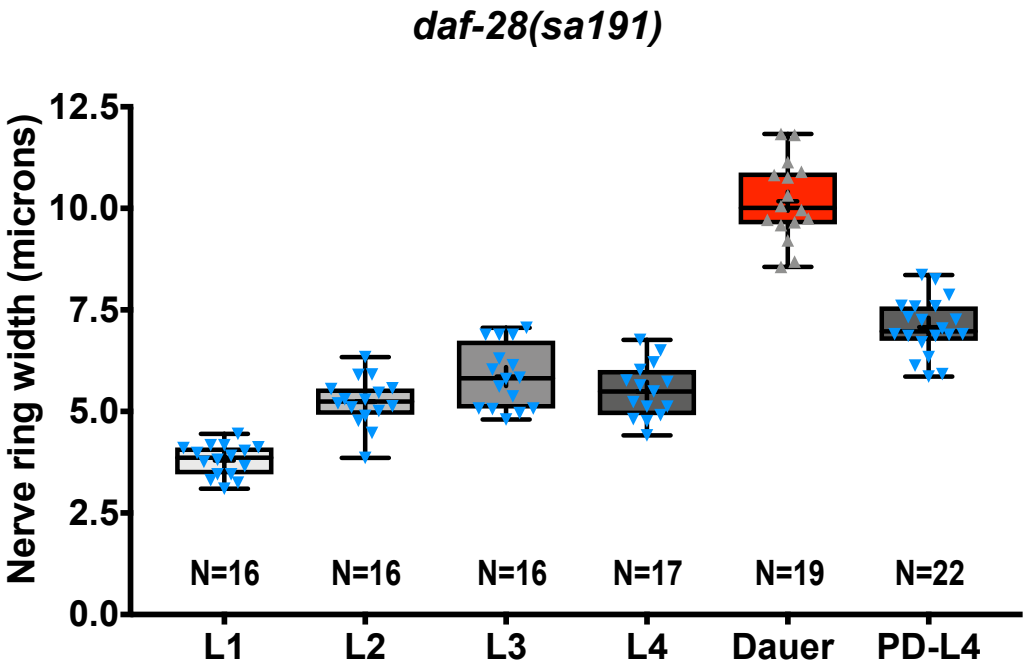

B

Bonferroni's test	Significant?	Summary	Adjusted P Value
L1 vs. L2	Yes	****	<0.0001
L1 vs. L3	Yes	****	<0.0001
L1 vs. L4	Yes	****	<0.0001
L1 vs. Dauer	Yes	****	<0.0001
L1 vs. PD-L4	Yes	****	<0.0001
L2 vs. L3	No	ns	0.211
L2 vs. L4	No	ns	>0.9999
L2 vs. Dauer	Yes	****	<0.0001
L2 vs. PD-L4	Yes	***	<0.001
L3 vs. L4	No	ns	>0.9999
L3 vs. Dauer	Yes	****	<0.0001
L3 vs. PD-L4	Yes	***	<0.001
L4 vs. Dauer	Yes	****	<0.0001
L4 vs. PD-L4	Yes	****	<0.0001
Dauer vs. PD-L4	Yes	****	<0.0001

Fig. 6.4: Quantification of changes in NR width along the anterior-posterior axis during development of *daf-28* dominant-negative mutants. (A) The NR width is plotted graphically with individual values represented in blue (non-dauer or post-dauer larvae) and gray (dauer larvae) triangles. The number of animals assayed (N) are mentioned for each stage. (B) Bonferroni tests for the NR widths are tabulated. Dauers have significantly greater NR width compared to any other developmental stage, suggesting that dauers have altered NR structures.

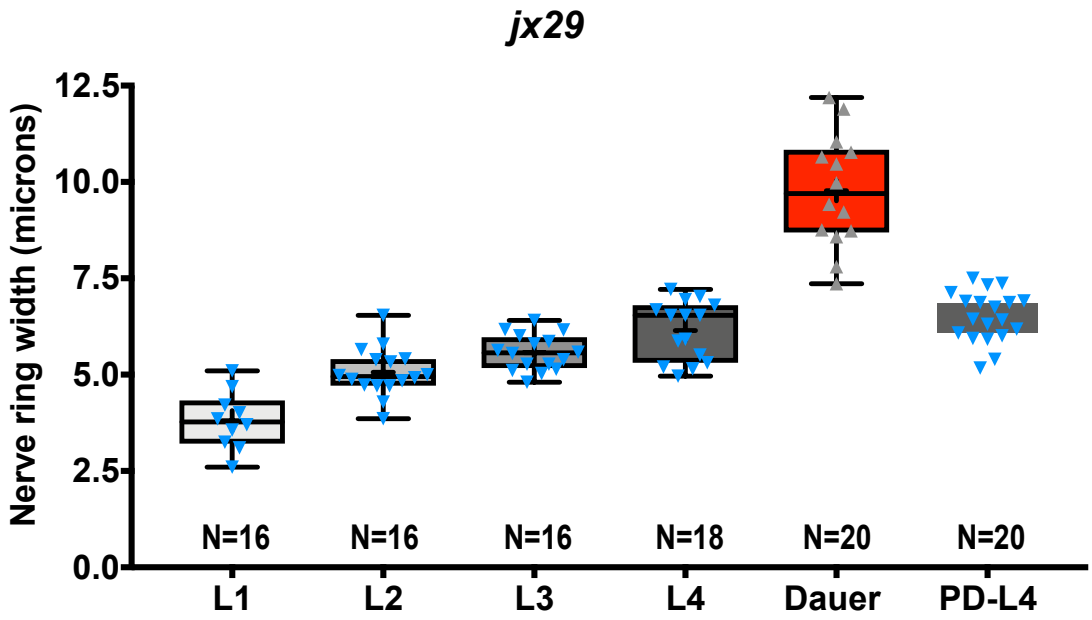

B

Bonferroni's test	Significant?	Summary	Adjusted P Value
L1 vs. L2	Yes	**	<0.01
L1 vs. L3	Yes	****	<0.0001
L1 vs. L4	Yes	****	<0.0001
L1 vs. Dauer	Yes	****	<0.0001
L1 vs. PD-L4	Yes	****	<0.0001
L2 vs. L3	No	ns	0.911
L2 vs. L4	No	**	<0.01
L2 vs. Dauer	Yes	****	<0.0001
L2 vs. PD-L4	Yes	****	<0.0001
L3 vs. L4	No	ns	>0.9999
L3 vs. Dauer	Yes	****	<0.0001
L3 vs. PD-L4	Yes	*	0.022
L4 vs. Dauer	Yes	****	<0.0001
L4 vs. PD-L4	No	ns	>0.9999
Dauer vs. PD-L4	Yes	****	<0.0001

Fig. 6.5: Quantification of changes in NR width along the anterior-posterior axis during development of *jx29* mutants. (A) The NR width is plotted graphically with individual values represented in blue (non-dauer or post-dauer larvae) and gray (dauer larvae) triangles.. The number of animals assayed (N) are mentioned for each stage. (B) Bonferroni tests for the NR widths are tabulated. Dauers have significantly greater NR width compared to any other developmental stage, again suggesting dauers have altered NR structures.

A

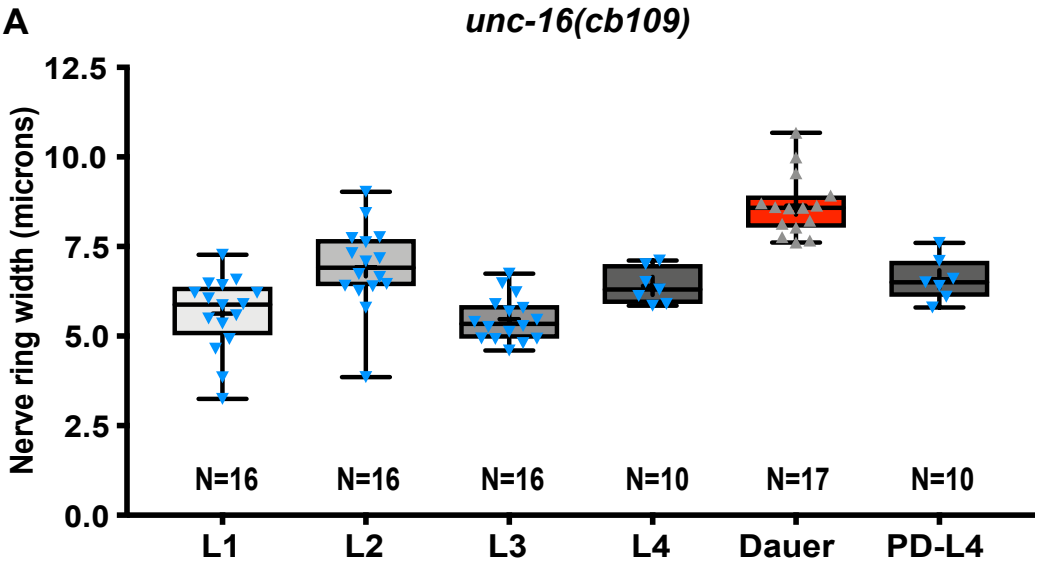

B

Bonferroni's test	Significant?	Summary	Adjusted P Value
L1 vs. L2	Yes	**	0.0018
L1 vs. L3	No	ns	>0.9999
L1 vs. L4	No	ns	0.982
L1 vs. Dauer	Yes	****	<0.0001
L1 vs. PD-L4	Yes	****	0.320
L2 vs. L3	Yes	**	0.003
L2 vs. L4	No	ns	>0.9999
L2 vs. Dauer	Yes	****	<0.0001
L2 vs. PD-L4	No	ns	>0.9999
L3 vs. L4	No	ns	>0.9999
L3 vs. Dauer	Yes	****	<0.0001
L3 vs. PD-L4	No	ns	0.118
L4 vs. Dauer	Yes	****	<0.0001
L4 vs. PD-L4	No	ns	>0.9999
Dauer vs. PD-L4	Yes	****	<0.0001

Fig. 6.6: Quantification of changes in NR width along the anterior-posterior axis during development of *unc-16* mutants. (A) The NR width is plotted graphically with individual values represented in blue (non-dauer or post-dauer larvae) and gray (dauer larvae) triangles. The number of animals assayed (N) are mentioned for each stage. (B) Bonferroni tests for the NR widths are tabulated. Dauers again have significantly greater NR widths than any other developmental stage.

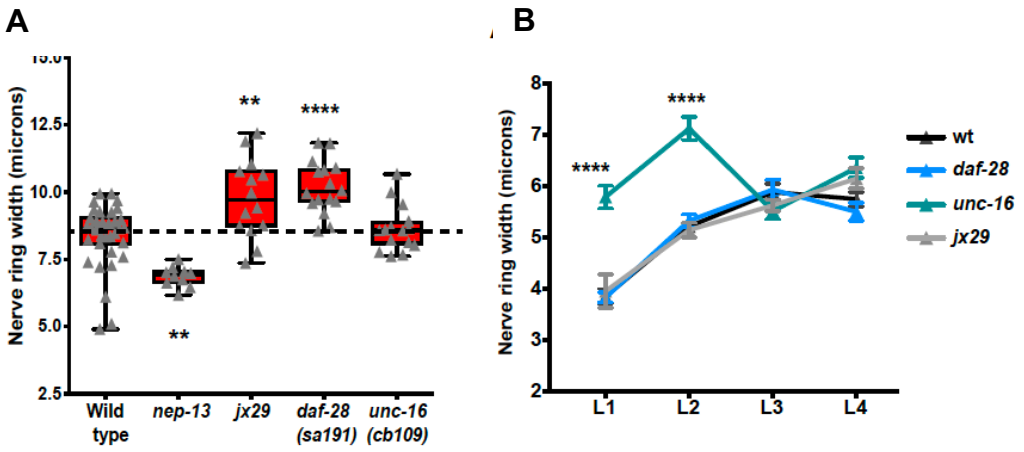

Fig. 6.7: Regulators of NR morphology. (A) Comparisons of NR widths between wild-type and mutant dauers. While the *unc-16* mutation has no effect on dauer NR width, the *daf-28* dominant-negative mutation and the *jx29* mutation further widened the dauer NR. In contrast, *nep-13* narrowed the dauer NR. (B) Comparisons of NR widths between wild-type and mutant well-fed larvae. L1s and L2s of *unc-16* mutants have much wider NR compared to wild-type and other mutant larvae under well-fed conditions.

isthmus length as L3s (pre-dauers, 26.6 ± 0.4 μm, n = 15; L3, 26.1 ± 0.7 μm, n = 15, P = 0.14), although pre-dauers have a much wider NR than L3s. Second, I found that pre-dauers have a similar diameter as L1s (pre-dauers, 11.3 ± 0.8 μm, n = 10; L1, 10.7 ± 0.6 μm, n = 10, P = 0.99), although again pre-dauers have a much wider NR than L1s. Together my data suggest that NR changes in dauers are not dependent on the changes in body dimensions. They also suggest that starvation versus stress-induced dauer formation have distinct effects on NR morphology, which means that the brain of the worm is equipped to respond to different kinds of stress through specific alterations of the NR structure. In the future, it will be interesting to note if the morphological changes observed in the NR region also affect neurotransmission and/or exchange of information at the neuropil.

Molecular regulators of nerve ring morphology

The influence of insulin signaling on the dauer program [(Cornils et al., 2011) and references therein] and on the rodent brain circuitry in response to stress (Bibollet-Bahena

et al., 2009) next led me to test if insulin signaling affects the NR structure (Fig. 6.4). Like wild type (Fig. 6.2), *daf-28(sa191)* mutants follow a similar pattern in NR growth from L1 to L3 and broadening of the NR in dauers (Fig. 6.4). The *ins-6* regulator and potential inter-ILP network regulator *jx29* mutant (Figs. 4.3 and 4.4) also showed similar growth in NR width and dauer NR morphology (Fig. 6.5). However, the dauer NR width of *daf-28(sa191)* and *jx29* are much wider than the wild-type dauer NR (Fig. 6.7A), which suggests that insulin signaling regulates the broadening of the NR.

Since changes in axonal activities could influence NR morphology, I also tested if a mutation in the axonal gatekeeper *unc-16*, *cb109*, which affects synaptic transmission (Byrd et al., 2001; Edwards et al., 2013), affects NR morphology (Fig. 6.6). During optimal reproductive development, *unc-16* mutants have a wider NR morphology compared to wild-type animals at the L1 and L2 stages (Fig. 6.2 versus Fig. 6.6). The broad NR of *unc-16* mutants at the early larval stages did not further grow at the later stages, in contrast to wild-type animals (Fig. 6.7B), which suggests that wild-type UNC-16 might slow NR development during reproductive growth. However, *unc-16* mutants have no effect on dauer NR, unlike the above insulin signaling mutants (Fig. 6.7A). Because insulin signaling only affects NR morphology of dauers and *unc-16* only affects NR morphology of L1s and L2s (Fig. 6.7), my data suggest that different molecular mechanisms might be responsible for the morphology of the NR neuropil during specific stages of development.

The extracellular matrix (ECM) also likely plays an important role in NR morphology by acting as a substrate on which the axons grow, develop and form connections. Therefore, the molecules that maintain ECM integrity may affect NR development and morphology. A mutation in *nep-13*, which is predicted to encode a matrix metalloproteinase called neprilysin that can degrade proteins and plaques in healthy and Alzheimer's-affected brains (Grimm et al., 2013), shrank the width of the dauer NR (Fig. 6.7A). This suggests that extracellular endopeptidases, like neprilysins, might have an

opposite effect on NR morphology, when compared to intracellular endopeptidases that are predicted to be impaired in the *daf-28(sa191)* mutants (Fig. 6.7A). This is also consistent with the idea that ECM structure will affect NR structure.

Discussion

Depression, anxiety, and post-traumatic stress disorders are only a few among many symptoms of an improper transit from stress (Breslau, 2002; Flory and Yehuda, 2015; McEwen and Morrison, 2013). These pathological conditions exhibit altered brain function and connectivity (McEwen and Morrison, 2013; Shin and Liberzon, 2010). Stress affects the brain circuitry as a part of the animal's physiological responses, and these altered structures in the brain presumably assist animals to endure stressful situations (McEwen and Morrison, 2013; Selye, 1950, 1993; Shin and Liberzon, 2010). The problem arises when the animal is unable to exit from stress.

Here I show that similar structural alterations are found in the *C. elegans* NR, when the worms undergo dauer development and exit to L4 to become adults (Fig. 6.2). The plasticity of the NR suggests that the neuropil of stressed *C. elegans* follow different trajectories compared to the neuropil of their unstressed counterparts. These altered trajectories in dauers could be due to ectopic axonal branching or some axons defasciculating and other axons fasciculating, which will lead to changed connectivity. The narrowing of the NR in post-dauers (Fig. 6.2) also raises the possibility that at least some of the NR changes are reversible.

Starvation is also a form of stress. In contrast to the dauer program (Fig. 6.2), starvation led to narrowing of the NR (Fig. 6.3), which might be due to stunted development. While these data show that the NR responds to the animal's environment, future experiments are needed to determine whether (i) starvation-induced changes in NR structure are reversible and (ii) the starvation-dependent and dauer-dependent NR plasticity share molecular mechanisms.

To provide molecular insight into the mechanisms behind the structural alterations in the NR, the findings that defective insulin signaling widens the dauer NR (Figs. 6.4, 6.5 and 6.7) suggest a starting point. It will be intriguing to find if insulin signaling differentially modulates NR structure in response to starvation versus the dauer-inducing cues. In humans, ILPs, such as insulins and IGF-1, maintain both neuronal plasticity and structural integrity and are found aberrant in many neurological pathologies that bear alterations in brain connectivities (Bibollet-Bahena et al., 2009). Therefore, the knowledge gained using the *C. elegans* NR on how ILPs modulate its structure and function during stress recovery remains of utmost importance.

The axonal gatekeeper UNC-16, which restricts organellar and vesicular transport (Edwards et al., 2013), also influences how axons form their trajectories during early development, but not in the later stages of development (Figs. 6.6 and 6.7). This suggests that NR structure formation under optimal environment involves a different mechanism than that required for NR structure during stress, such as the dauer stage of development.

One of the mechanisms responsible for inducing such diverse and specific structural changes might be the mobilization of specific mRNAs of different ILPs or other neuropeptides. In support of this hypothesis, I found that the ILP *ins-6* and *daf-28* mRNAs are transported to the NR in response to stress, *i.e.*, in dauers, but not in non-dauers (Chapter 3). In parallel, I report that the defective ILP-processing *sa191* mutation, which prevents *ins-6* mRNA transport in dauers (Chapter 5), also widens the dauer NR (this Chapter). In addition, Bhattacharya et al. (2019) showed through a systematic analysis of the *C. elegans* nervous system that the dauer electrical connectivity is altered, compared to non-dauers, in a manner that depends on *daf-16*, a downstream effector of insulin signaling (Bhattacharya et al., 2019). Thus, my findings and Bhattacharya et al's data (2019) are consistent with the idea that insulin signaling plays a crucial role in maintaining dauer neural connectivity at the NR. Because *jx29*, which might affect the gap junction

protein CHE-7 (Fig. 4.4), regulates both dauer NR morphology (Figs. 6.5 and 6.7) and dauer *ins-6* expression (Fig. 4.3), this suggests that feedback regulation might also exist between ILPs and electrical signaling at the dauer NR. Therefore, the remodeling of the *C. elegans* primitive brain likely involves several layers of regulation that range from transcription and post-transcriptional mechanisms to feedback regulatory loops.

The regulation at the NR might differ from the regulation at the dendritic processes during dauer development, since I have found that the dendrites of GFP-marked ASJ neurons can arborize under certain conditions (Fig. 5.6), but not the axons, which enter the NR. While this suggests that the neurites of a single neuron can respond differentially to stress, ultimately the *C. elegans* NR emerges as a powerful model to study how stress alters axonal morphology in the stressed nervous system. Because at least some of the dauer-associated alterations are reversible, the toolboxes available for *C. elegans* study (Allen et al., 2015) facilitate the dissection of the mechanisms underlying neurite plasticity. The future identification of the molecules that regulate this plasticity could serve as a basis for future therapies in humans suffering from impaired neural circuit plasticity.

CHAPTER 7 CONCLUSIONS AND PERSPECTIVES

Humans can exist in two different physiological states, homeostasis and allostasis, depending on the amount of stress we encounter every day. For instance, a student taking an exam undergoes allostasis, but will return to homeostasis once the stress of the exam ends. However, failure to exit from the stressed mental state caused by the exam can lead to chronic stress, a sustained allostatic physiological state (McEwen, 1998). Constant allostasis leads to chronic stress and increases the risk of insulin resistance (McEwen, 2003), which predisposes us to many different diseases, such as Alzheimer's Disease (type III diabetes), type II diabetes and even several metabolic diseases (Baker et al., 2011). Thus, insulin signaling plays a major role in dictating how we will adapt and recover from stress (Blázquez et al., 2014; McEwen, 1998, 2003; Selye, 1950, 1993). Since allostasis represents an altered state of physiology, the *C. elegans* dauer state fits the classical definition of allostatic physiology (Blázquez et al., 2014; Golden and Riddle, 1984; McEwen, 1998, 2003; Riddle and Albert, 1997; Riddle et al., 1981; Selye, 1950, 1993). Thus, I dissected the role of the insulin-like peptides (ILPs) during the transition from allostasis to homeostasis in *C. elegans*.

The existing literature shows that insulin signaling is decreased during allostasis across many species, including *C. elegans*, based on the decrease in insulin receptor signaling at the time of stress (Gems et al., 1998; McEwen, 2003; Pierce et al., 2001; Riddle and Albert, 1997; Riddle et al., 1981; Selye, 1950). Now, if *C. elegans* needs optimal insulin signaling to control the transition from allostasis to homeostasis, then how do worms exit from dauer to L4 when insulin signaling is reduced? First, the proper subcellular localization of insulin-like peptide mRNAs could compensate for low insulin receptor activity, *e.g.*, when dauer exit- or stress recovery-promoting ILP mRNAs are transported to the axonal compartments of neurons (Chapters 3 and 5). The presence of the ILP mRNAs at the axons should facilitate the processing and secretion of the

corresponding peptide products from the crucial subcellular compartments, once the animal does

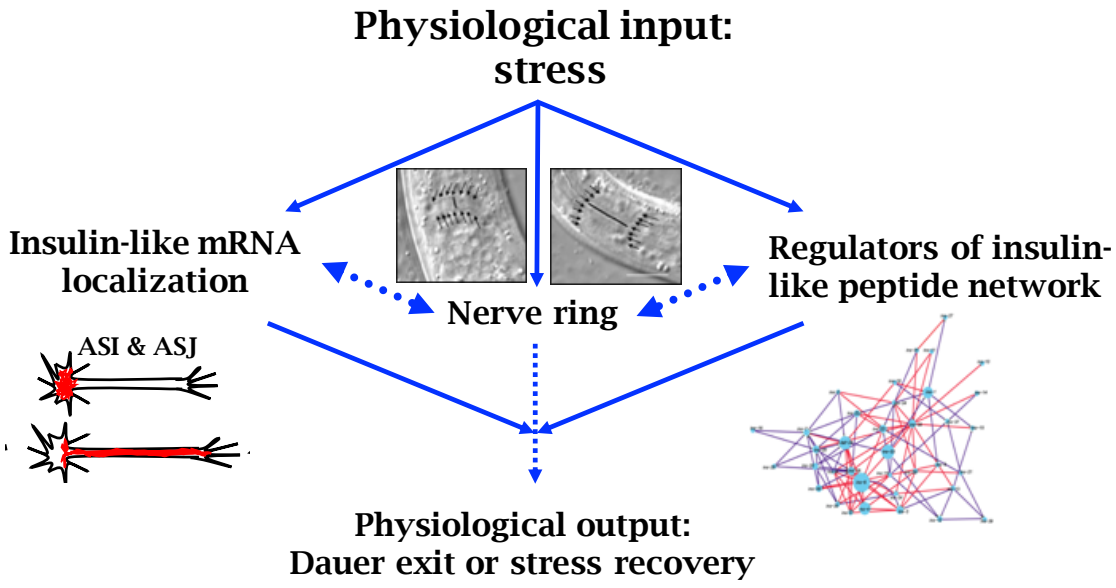

Fig. 7.1: The mechanisms *C. elegans* uses to transition from allostasis to homeostasis. Chapters 3 and 5 of this thesis describe one mechanism the animal uses to recover from stress: how the mRNAs of specific DAF-2 ligands, the ILPs *ins-6* and *daf-28*, are localized to the axons of neurons. Since I observe that Golgi is also mobilized to the axons, I hypothesize that these ILP mRNAs are transported for local translation at the axons, where the nascent peptides are packaged for secretion to act on post-synaptic DAF-2 receptors. Another mechanism the worm uses to regulate insulin signaling during dauer allostasis could be through altered electrical synaptic activities [Chapter 4 and (Bhattacharya et al., 2019)]. Changes in the electrical synapses could also alter the structure of the nerve ring axon bundle (denoted by black arrows), which I have shown is again regulated by insulin signaling (Chapter 6). Therefore, I propose the following model. Low insulin signaling during dauer allostasis transforms electrical signaling between axons, which also changes axonal morphology. These in turn will regulate insulin signaling through a feedback loop, which includes the localization of specific ILP mRNAs to the axons, thereby enhancing survival during stress.

receive the dauer exit-inducing cues. Second, lowered insulin signaling alters the electrical synapses and connectivities in the nerve ring (NR) axon bundle of stressed dauers [Chapter 6; (Bhattacharya et al., 2019)], which in turn could regulate insulin signaling through a feedback loop (Chapter 4). Thus, this thesis highlights two new mechanisms

through which lowered insulin signaling compensates for itself and modulate the transition from stressful to non-stressful situations (Fig. 7.1).

Allostasis and insulin signaling

During dauer, *i.e.*, when worms are in allostasis, expression of the insulin receptor DAF-2 is low and certain ILP mRNAs are transported to the axonal bundle as a preemptive measure for stress recovery as soon as the environment improves. However, it is possible that there are different levels of DAF-2 activities needed for different processes. Namely, a specific low level of insulin signaling promotes ILP mRNA transport, whereas any level of signaling below this threshold hinders transport, since a weaker hypomorphic allele of *daf-2* reduces the axonal transport of the ILP *ins-6* mRNA (Chapter 3). Consistent with the idea that the optimal levels of DAF-2 activity vary for each process, a stronger hypomorphic allele of *daf-2* affects both *ins-6* mRNA transport and stability (Chapter 3). Indeed, as dauers age, DAF-2 activity further decreases and ILP mRNA levels throughout the whole cell are further diminished (Chapter 3). Because the longer an animal stays in dauer makes the return to homeostasis difficult and this coincides with ILP mRNA decay, this suggests that insulin signaling is an important component of the transition from allostasis to homeostasis.

I have found that ILP mRNA transport is specific to the axonal compartments of wild-type dauer populations. However, why are the ILP mRNAs mobilizing toward the axons, instead of the dendrites? I speculate that in dauers most of the neurotransmission occurs in the NR area. Therefore, to save time and energy, the ILP mRNAs are shunted to these synapse-rich regions of the worm, which should promote efficient communication between neurons through a structure that is comprised of the majority of axons within the animal's nervous system. The axonal localization of the ILP mRNAs during allostasis (Chapters 3 and 5) suggests that ILP mRNAs are locally translated. This is consistent with the presence of both the rough endoplasmic reticulum (Edwards et al., 2015) and Golgi

bodies in *C. elegans* axons (Chapter 3), since nascent ILPs require packaging through Golgi bodies to prepare them for secretion (Edwards et al., 2015).

Allostasis will involve both ILP mRNA transport and stability (Chapter 3).Through bioinformatic approaches, I have predicted multiple structures based on the absence versus presence of specific UTRs (Figs. 5.7-5.11), which can stabilize mRNAs. Not surprisingly, I find that the UTRs of three ILPs*, ins*-6*, daf*-28 *and ins-1*, alter mRNA stability (Chapter 5), which I have confirmed experimentally for *ins-6* (Chapter 3). However, the physiological roles of the UTRs of all ILP mRNAs have yet to be tested in mRNA stability, subcellular localization or translation. Therefore, it will be interesting to note how the dynamics of the inter-ILP network change, when the UTRs of the 40 ILPs are systematically ablated or swapped with other ILP UTRs that have opposing functions. By establishing the role of UTRs in stabilizing the ILP network during the transition from allostasis to homeostasis, one might reveal another layer of regulation that focuses on mRNA structures and/or efficient translation.

Allostasis, insulin signaling and the structure of the NR

Allostasis alters the structure of our brain (Bloss et al., 2010; Cordero et al., 2003; Esch et al., 2002; McEwen and Morrison, 2013; Shin and Liberzon, 2010). Again, how our brain changes its circuits due to environmental stress is difficult to understand. Therefore, simpler model organisms that provide a window into how a whole brain changes during stress are important. With this idea in mind, I have explored whether the main centralized neuropil, the NR, in *C. elegans* alters its structure during the switches between homeostasis and allostasis (Chapter 6). I have found that the *C. elegans* brain exhibits plasticity in its anatomical structures under simple differential-interference contrast microscopy. To gain insight into the mechanism of this plasticity, I find that the *daf-28(sa191)* mutation, which is predicted to impair ILP processing (Li et al., 2003), increases NR plasticity (Fig. 6.7). Moreover, the *ins-6* regulator *jx29*, which potentially impairs the

function of the gap junction CHE-7 (Chapter 4), changes the dauer NR structure in a similar manner (Chapter 6; Fig. 6.7). Because the two mutations, *daf-28(sa191)* and *jx29*, have the capability to regulate the inter-ILP network and the dauer NR structure, I conclude that insulin signaling modulates the structure of the *C. elegans* brain during allostasis. The fact that *daf-28(sa191)* affects *ins-6* mRNA transport at the same time the NR structure is altered (Figs. 5.1A and 6.7A), I propose that ILP mRNA transport contributes to the plasticity of the NR structure and/or vice versa.

Allostasis, NR structure, insulin signaling and consciousness

Under stress, our conscious choices change. For example, sports-persons agree that under stress their performance decreases compared to the times when they do not face stress (Bryant et al., 2008; Hardy et al., 1996). Therefore, does allostatic physiology, a stress response that exhibits physiological plasticity, also retain the plasticity of consciousness?

Clinical theories about people suffering from post-traumatic stress disorders (PTSDs) suggest that intrusive memories trigger stress responses (Marie Hall and Berntsen, 2008). This implies that even though the traumatic event has passed, the trauma still lingers and the stress responses remain heightened. Recent studies have shown that brains suffering from PTSD exhibit altered neural connectivities (Cisler et al., 2013; MacNamara et al., 2016). This is reminiscent of the altered anatomy of the post-dauer L4 (PD-L4) NR, which does not return to the exact same structure as the NR of an L4 that has never experienced stress (Fig. 6.2). Thus, do PD-L4s also exhibit altered physiological outputs later in life? Will *C. elegans* post-dauer adults exhibit heightened responses to different stressors, such as starvation, high population density or other forms of stress? What would the molecular mechanisms be behind such responses?

Structural changes in the brain have been observed during altered states of consciousness, but the mechanism behind these changes have not been explored (Crick

and Koch, 1990, 1995; Hurley and Noë, 2003). It is safe to assume that *C. elegans* can serve as a model organism to study the mechanisms behind altered consciousness (see Chapter 1), as exemplified during PTSDs. In this thesis, I report that the modified state of animal consciousness in invertebrates, which is the decision to become a dauer, depends on various aspects of insulin signaling. In other words, insulin signaling influences the ability of the worm to make conscious choices by modifying the structure of its brain, *i.e.*, the NR. This is consistent with the fact that during stressful situations many animals, including humans, exhibit changes in both insulin signaling and brain structure. Since experiments on animal consciousness should not be subject to human bias, it will be fascinating to observe in the future the natural changes happening in the realm of the other mind, whether these involve or do not involve insulin signaling.

REFERENCES

Aerts, S., Lambrechts, D., Maity, S., Van Loo, P., Coessens, B., De Smet, F., Tranchevent, L.-C., De Moor, B., Marynen, P., and Hassan, B. (2006). Gene prioritization through genomic data fusion. Nature biotechnology *24*, 537.

Ailion, M., Inoue, T., Weaver, C.I., Holdcraft, R.W., and Thomas, J.H. (1999). Neurosecretory control of aging in Caenorhabditis elegans. Proc Natl Acad Sci U S A *96*, 7394-7397.

Ailion, M., and Thomas, J.H. (2000). Dauer formation induced by high temperatures in Caenorhabditis elegans. Genetics *156*, 1047-1067.

Albert, P.S., Brown, S.J., and Riddle, D.L. (1981). Sensory control of dauer larva formation in Caenorhabditis elegans. J Comp Neurol *198*, 435-451.

Albert, P.S., and Riddle, D.L. (1983). Developmental alterations in sensory neuroanatomy of the Caenorhabditis elegans dauer larva. J Comp Neurol *219*, 461-481.

Alcedo, J., and Kenyon, C. (2004). Regulation of C. elegans longevity by specific gustatory and olfactory neurons. Neuron *41*, 45-55.

Alcedo, J., and Zhang, Y. (2013). Molecular and cellular circuits underlying Caenorhabditis elegans olfactory plasticity. In Invertebrate Learning and Memory, R. Menzel, and P. Benjamin, eds. (San Diego, CA: Elsevier Academic Press, Inc), pp. 112-123.

Allen, E., Ren, J., Zhang, Y., and Alcedo, J. (2015). Sensory systems: their impact on C. elegans survival. Neuroscience *296*, 15-25.

Apfeld, J., and Kenyon, C. (1998). Cell nonautonomy of C. elegans daf-2 function in the regulation of diapause and life span. Cell *95*, 199-210.

Arendt, D., Tosches, M.A., and Marlow, H. (2016). From nerve net to nerve ring, nerve cord and brain--evolution of the nervous system. Nat Rev Neurosci *17*, 61-72.

Artan, M., Jeong, D.E., Lee, D., Kim, Y.I., Son, H.G., Husain, Z., Kim, J., Altintas, O., Kim, K., Alcedo, J.*, et al.* (2016). Food-derived sensory cues modulate longevity via distinct neuroendocrine insulin-like peptides. Genes Dev *30*, 1047-1057.

Baker, L.D., Cross, D.J., Minoshima, S., Belongia, D., Watson, G.S., and Craft, S. (2011). Insulin resistance and Alzheimer-like reductions in regional cerebral glucose metabolism for cognitively normal adults with prediabetes or early type 2 diabetes. Archives of neurology *68*, 51-57.

Ball, N.J., Mercado, E., III, and Orduña, I. (2019). Enriched Environments as a Potential Treatment for Developmental Disorders: A Critical Assessment. Frontiers in Psychology *10*, 466.

Bargmann, C.I. (1998). Neurobiology of the Caenorhabditis elegans genome. Science (New York, NY) *282*, 2028-2033.

Bargmann, C.I., Hartwieg, E., and Horvitz, H.R. (1993). Odorant-selective genes and neurons mediate olfaction in C. elegans. Cell *74*, 515-527.

Bargmann, C.I., and Horvitz, H.R. (1991). Control of larval development by chemosensory neurons in Caenorhabditis elegans. Science *251*, 1243-1246.

Bathgate, R.A., Halls, M.L., van der Westhuizen, E.T., Callander, G.E., Kocan, M., and Summers, R.J. (2013). Relaxin family peptides and their receptors. Physiol Rev *93*, 405-480.

Bathgate, R.A., Samuel, C.S., Burazin, T.C., Layfield, S., Claasz, A.A., Reytomas, I.G., Dawson, N.F., Zhao, C., Bond, C., Summers, R.J.*, et al.* (2002). Human relaxin gene 3 (H3) and the equivalent mouse relaxin (M3) gene. Novel members of the relaxin peptide family. J Biol Chem *277*, 1148-1157.

Bedarkar, S., Turnell, W., Blundell, T., and Schwabe, C. (1977). Relaxin has conformational homology with insulin. Nature *270*, 449.

Bertrand, E., Chartrand, P., Schaefer, M., Shenoy, S.M., Singer, R.H., and Long, R.M. (1998). Localization of ASH1 mRNA particles in living yeast. Mol Cell *2*, 437-445.

Bhattacharya, A., Aghayeva, U., Berghoff, E.G., and Hobert, O. (2019). Plasticity of the Electrical Connectome of C. elegans. Cell *176*, 1174-1189 e1116.

Bibollet-Bahena, O., Cui, Q.L., and Almazan, G. (2009). The insulin-like growth factor-1 axis and its potential as a therapeutic target in central nervous system (CNS) disorders. Cent Nerv Syst Agents Med Chem *9*, 95-109.

Bickle, J. (2007). Who says you can't do a molecular biology of consciousness? (Oxford: Blackwell Publishers).

Blázquez, E., Velázquez, E., Hurtado-Carneiro, V., and Ruiz-Albusac, J.M. (2014). Insulin in the brain: its pathophysiological implications for states related with central insulin resistance, type 2 diabetes and Alzheimer's disease. Front Endocrinol *5*, 161.

Bloss, E.B., Janssen, W.G., McEwen, B.S., and Morrison, J.H. (2010). Interactive effects of stress and aging on structural plasticity in the prefrontal cortex. The Journal of neuroscience : the official journal of the Society for Neuroscience *30*, 6726-6731.

Boly, M., Massimini, M., Tsuchiya, N., Postle, B.R., Koch, C., and Tononi, G. (2017). Are the Neural Correlates of Consciousness in the Front or in the Back of the Cerebral Cortex? Clinical and Neuroimaging Evidence. The Journal of neuroscience : the official journal of the Society for Neuroscience *37*, 9603-9613.

Bosch, T.C.G., Klimovich, A., Domazet-Loso, T., Grunder, S., Holstein, T.W., Jekely, G., Miller, D.J., Murillo-Rincon, A.P., Rentzsch, F., Richards, G.S.*, et al.* (2017). Back to the Basics: Cnidarians Start to Fire. Trends Neurosci *40*, 92-105.

Brenner, S. (1974). The genetics of Caenorhabditis elegans. Genetics *77*, 71-94.

Breslau, N. (2002). Epidemiologic studies of trauma, posttraumatic stress disorder, and other psychiatric disorders. Canadian journal of psychiatry Revue canadienne de psychiatrie *47*, 923-929.

Brown, H., Sanger, F., and Kitai, R. (1955). The structure of pig and sheep insulins. The Biochemical journal *60*, 556-565.

Brown, H.M., Van Epps, H.A., Goncharov, A., Grant, B.D., and Jin, Y. (2009). The JIP3 scaffold protein UNC-16 regulates RAB-5 dependent membrane trafficking at C. elegans synapses. Dev Neurobiol *69*, 174-190.

Browning, H., and Strome, S. (1996). A sperm-supplied factor required for embryogenesis in C. elegans. Development *122*, 391-404.

Bryant, R.A., Felmingham, K., Kemp, A., Das, P., Hughes, G., Peduto, A., and Williams, L. (2008). Amygdala and ventral anterior cingulate activation predicts treatment response to cognitive behaviour therapy for post-traumatic stress disorder. Psychological Medicine *38*, 555-561.

Burkhardt, P., and Sprecher, S.G. (2017). Evolutionary origin of synapses and neurons - Bridging the gap. Bioessays *39*.

Burnell, A.M., Houthoofd, K., O'Hanlon, K., and Vanfleteren, J.R. (2005). Alternate metabolism during the dauer stage of the nematode Caenorhabditis elegans. Experimental gerontology *40*, 850-856.

Butcher, R.A., Fujita, M., Schroeder, F.C., and Clardy, J. (2007). Small-molecule pheromones that control dauer development in Caenorhabditis elegans. Nat Chem Biol *3*, 420-422.

Byrd, D.T., Kawasaki, M., Walcoff, M., Hisamoto, N., Matsumoto, K., and Jin, Y. (2001). UNC-16, a JNK-signaling scaffold protein, regulates vesicle transport in C. elegans. Neuron *32*, 787-800.

Cajal, S.R.y. (1906). Nobel Lecture: The structure and connexions of neurons. wwwnobelprizeorg.

Campbell, J. (2002). Reference and consciousness.

Cao, J., Ni, J., Ma, W., Shiu, V., Milla, L.A., Park, S., Spletter, M.L., Tang, S., Zhang, J., Wei, X.*, et al.* (2014). Insight into insulin secretion from transcriptome and genetic analysis of insulin-producing cells of *Drosophila*. Genetics *197*, 175-192.

Cassada, R.C., and Russell, R.L. (1975). The dauerlarva, a post-embryonic developmental variant of the nematode Caenorhabditis elegans. Dev Biol *46*, 326-342.

Cazzolla Gatti, R. (2016). Self-consciousness: beyond the looking-glass and what dogs found there. Ethology Ecology & Evolution *28*, 232-240.

Chalasani, S.H., Chronis, N., Tsunozaki, M., Gray, J.M., Ramot, D., Goodman, M.B., and Bargmann, C.I. (2007). Dissecting a circuit for olfactory behaviour in Caenorhabditis elegans. Nature *450*, 63-70.

Chandler, K. (2011). Modern science and Vedic science: An introduction. Consciousness-Based Education and Computer Science, 289.

Chen, B.L., Hall, D.H., and Chklovskii, D.B. (2006). Wiring optimization can relate neuronal structure and function. Proceedings of the National Academy of Sciences of the United States of America *103*, 4723-4728.

Chen, Z., Hendricks, M., Cornils, A., Maier, W., Alcedo, J., and Zhang, Y. (2013). Two insulin-like peptides antagonistically regulate aversive olfactory learning in C. elegans. Neuron *77*, 572-585.

Cheng, K.C.-C., Klancer, R., Singson, A., and Seydoux, G. (2009). Regulation of MBK-2/DYRK by CDK-1 and the pseudophosphatases EGG-4 and EGG-5 during the oocyte-to-embryo transition. Cell *139*, 560-572.

Chisholm, A.D., Hutter, H., Jin, Y., and Wadsworth, W.G. (2016). The genetics of axon guidance and axon regeneration in *Caenorhabditis elegans*. Genetics *204*, 849-882.

Cisler, J.M., Scott Steele, J., Smitherman, S., Lenow, J.K., and Kilts, C.D. (2013). Neural processing correlates of assaultive violence exposure and PTSD symptoms during

implicit threat processing: A network-level analysis among adolescent girls. Psychiatry Research: Neuroimaging *214*, 238-246.

Clark, E.G., Kanauchi, D., Kano, T., Aonuma, H., Briggs, D.E.G., and Ishiguro, A. (2019). The function of the ophiuroid nerve ring: how a decentralized nervous system controls coordinated locomotion. J Exp Biol *222*.

Colón-Ramos, D.A., Margeta, M.A., and Shen, K. (2007). Glia promote local synaptogenesis through UNC-6 (Netrin) signaling in *C. elegans*. Science (New York, NY) *318*, 103-106.

Consortium, G.O. (2004). The Gene Ontology (GO) database and informatics resource. Nucleic acids research *32*, D258-D261.

Cordero, M.I., Venero, C., Kruyt, N.D., and Sandi, C. (2003). Prior exposure to a single stress session facilitates subsequent contextual fear conditioning in rats. Evidence for a role of corticosterone. Hormones and behavior *44*, 338-345.

Cornils, A., Gloeck, M., Chen, Z., Zhang, Y., and Alcedo, J. (2011). Specific insulin-like peptides encode sensory information to regulate distinct developmental processes. Development *138*, 1183-1193.

Costales, J., and Kolevzon, A. (2016). The therapeutic potential of insulin-like growth factor-1 in central nervous system disorders. Neurosci Biobehav Rev *63*, 207-222.

Crick, F., and Koch, C. (1990). Towards a neurobiological theory of consciousness. Paper presented at: Seminars in the Neurosciences (Saunders Scientific Publications).

Crick, F., and Koch, C. (1995). Are we aware of neural activity in primary visual cortex? Nature *375*, 121-123.

Crick, F., and Koch, C. (1998). Consciousness and neuroscience. Cereb Cortex *8*, 97-107.

Dalley, B.K., and Golomb, M. (1992). Gene expression in the *Caenorhabditis elegans* dauer larva: Developmental regulation of Hsp90 and other genes. Dev Biol *151*, 80-90.

De Sousa, A. (2013). Towards an integrative theory of consciousness: part 1 (neurobiological and cognitive models). Mens Sana Monogr *11*, 100-150.

Doitsidou, M., Jarriault, S., and Poole, R.J. (2016). Next-Generation Sequencing-Based Approaches for Mutation Mapping and Identification in Caenorhabditis elegans. Genetics *204*, 451-474.

Duret, L., Guex, N., Peitsch, M.C., and Bairoch, A. (1998). New insulin-like proteins with atypical disulfide bond pattern characterized in Caenorhabditis elegans by comparative sequence analysis and homology modeling. Genome Res *8*, 348-353.

Edelman, G.M., Gally, J.A., and Baars, B.J. (2011). Biology of consciousness. Frontiers in psychology *2*, 4-4.

Edwards, S.L., Morrison, L.M., Yorks, R.M., Hoover, C.M., Boominathan, S., and Miller, K.G. (2015). UNC-16 (JIP3) Acts Through Synapse-Assembly Proteins to Inhibit the Active Transport of Cell Soma Organelles to Caenorhabditis elegans Motor Neuron Axons. Genetics *201*, 117-141.

Edwards, S.L., Yu, S.-c., Hoover, C.M., Phillips, B.C., Richmond, J.E., and Miller, K.G. (2013). An organelle gatekeeper function for Caenorhabditis elegans UNC-16 (JIP3) at the axon initial segment. Genetics *194*, 143-161.

Elahi, D., Nagulesparan, M., Hershcopf, R.J., Muller, D.C., Tobin, J.D., Blix, P.M., Rubenstein, A.H., Unger, R.H., and Andres, R. (1982). Feedback inhibition of insulin secretion by insulin: relation to the hyperinsulinemia of obesity. N Engl J Med *306*, 1196-1202.

Erkut, C., and Kurzchalia, T.V. (2015). The C. elegans dauer larva as a paradigm to study metabolic suppression and desiccation tolerance. Planta *242*, 389-396.

Esch, T., Stefano, G.B., Fricchione, G.L., and Benson, H. (2002). The role of stress in neurodegenerative diseases and mental disorders. Neuro Endocrinol Lett *23*, 199-208.

Eskridge, E.M., and Shields, D. (1983). Cell-free processing and segregation of insulin precursors. J Biol Chem *258*, 11487-11491.

Fang-Yen, C., Wasserman, S., Sengupta, P., and Samuel, A.D. (2009). Agarose immobilization of C. elegans. The Return of The Worm Breeder's Gazette.

Feller, M.B. (1999). Spontaneous correlated activity in developing neural circuits. Neuron *22*, 653-656.

Fernandes de Abreu, D.A., Caballero, A., Fardel, P., Stroustrup, N., Chen, Z., Lee, K., Keyes, W.D., Nash, Z.M., Lopez-Moyado, I.F., Vaggi, F.*, et al.* (2014). An insulin-to-insulin regulatory network orchestrates phenotypic specificity in development and physiology. PLoS Genet *10*, e1004225.

Fernandez, A.M., and Torres-Aleman, I. (2012). The many faces of insulin-like peptide signalling in the brain. Nat Rev Neurosci *13*, 225-239.

Flory, J.D., and Yehuda, R. (2015). Comorbidity between post-traumatic stress disorder and major depressive disorder: alternative explanations and treatment considerations. Dialogues in clinical neuroscience *17*, 141-150.

Frey, W.H., 2nd (2013). Intranasal insulin to treat and protect against posttraumatic stress disorder. J Nerv Ment Dis *201*, 638-639.

Frye, M.A. (2013). Visual attention: a cell that focuses on one object at a time. Curr Biol *23*, R61-63.

Fu, Z., Gilbert, E.R., and Liu, D. (2013). Regulation of insulin synthesis and secretion and pancreatic Beta-cell dysfunction in diabetes. Curr Diabetes Rev *9*, 25-53.

Gems, D., Sutton, A.J., Sundermeyer, M.L., Albert, P.S., King, K.V., Edgley, M.L., Larsen, P.L., and Riddle, D.L. (1998). Two pleiotropic classes of *daf-2* mutation affect

larval arrest, adult behavior, reproduction and longevity in *Caenorhabditis elegans*. Genetics *150*, 129-155.

Golden, J.W., and Riddle, D.L. (1984). The Caenorhabditis elegans dauer larva: developmental effects of pheromone, food, and temperature. Dev Biol *102*, 368-378.

Grimm, M.O.W., Mett, J., Stahlmann, C.P., Haupenthal, V.J., Zimmer, V.C., and Hartmann, T. (2013). Neprilysin and Aβ Clearance: Impact of the APP Intracellular Domain in NEP Regulation and Implications in Alzheimer's Disease. Front Aging Neurosci *5*, 98-98.

Gujar, M.R., Stricker, A.M., and Lundquist, E.A. (2017). Flavin monooxygenases regulate *Caenorhabditis elegans* axon guidance and growth cone protrusion with UNC-6/Netrin signaling and Rac GTPases. PLoS Genet *13*, e1006998.

Gunkel, N., Yano, T., Markussen, F.-H., Olsen, L.C., and Ephrussi, A. (1998). Localization-dependent translation requires a functional interaction between the 5′ and 3′ ends of *oskar* mRNA. Genes Dev *12*, 1652-1664.

Hameroff, S.R. (1994). Quantum coherence in microtubules: A neural basis for emergent consciousness? Journal of consciousness studies *1*, 91-118.

Hannan, A.J. (2014). Environmental enrichment and brain repair: harnessing the therapeutic effects of cognitive stimulation and physical activity to enhance experience-dependent plasticity. Neuropathology and applied neurobiology *40*, 13-25.

Hardy, L., Mullen, R., and Jones, G. (1996). Knowledge and conscious control of motor actions under stress. British Journal of Psychology *87*, 621-636.

Hirokawa, N., Noda, Y., Tanaka, Y., and Niwa, S. (2009). Kinesin superfamily motor proteins and intracellular transport. Nat Rev Mol Cell Biol *10*, 682-696.

Holt, Christine E., and Schuman, Erin M. (2013). The central dogma decentralized: new perspectives on RNA function and local translation in neurons. Neuron *80*, 648-657.

Hubbard, E.J., and Greenstein, D. (2005). Introduction to the germ line. WormBook, 1-4.

Hung, W.L., Wang, Y., Chitturi, J., and Zhen, M. (2014). A Caenorhabditis elegans developmental decision requires insulin signaling-mediated neuron-intestine communication. Development (Cambridge, England) *141*, 1767-1779.

Hurley, S., and Noë, A. (2003). Neural plasticity and consciousness. Biology and philosophy *18*, 131-168.

Husson, S.J., Clynen, E., Baggerman, G., Janssen, T., and Schoofs, L. (2006). Defective processing of neuropeptide precursors in Caenorhabditis elegans lacking proprotein convertase 2 (KPC-2/EGL-3): mutant analysis by mass spectrometry. Journal of neurochemistry *98*, 1999-2012.

Iversen, J., and Miles, D.W. (1971). Evidence for a feedback inhibition of insulin on insulin secretion in the isolated, perfused canine pancreas. Diabetes *20*, 1-9.

Jacob, T.C., and Kaplan, J.M. (2003). The EGL-21 carboxypeptidase E facilitates acetylcholine release at Caenorhabditis elegans neuromuscular junctions. The Journal of neuroscience : the official journal of the Society for Neuroscience *23*, 2122-2130.

Jansen, R.P. (2001). mRNA localization: message on the move. Nat Rev Mol Cell Biol *2*, 247-256.

Jeong, P.Y., Jung, M., Yim, Y.H., Kim, H., Park, M., Hong, E., Lee, W., Kim, Y.H., Kim, K., and Paik, Y.K. (2005). Chemical structure and biological activity of the Caenorhabditis elegans dauer-inducing pheromone. Nature *433*, 541-545.

Johnstone, I.L. (2000). Cuticle collagen genes: expression in Caenorhabditis elegans. Trends in Genetics *16*, 21-27.

Jorgensen, E.M., and Mango, S.E. (2002). The art and design of genetic screens: Caenorhabditis elegans. Nature Reviews Genetics *3*, 356.

Kak, S.C. (1997). On the science of consciousness in ancient India. Indian Journal of History of Science *32*, 105-120.

Kanai, Y., Dohmae, N., and Hirokawa, N. (2004). Kinesin transports RNA: isolation and characterization of an RNA-transporting granule. Neuron *43*, 513-525.

Kao, G., Nordenson, C., Still, M., Rönnlund, A., Tuck, S., and Naredi, P. (2007). ASNA-1 positively regulates insulin secretion in *C. elegans* and mammalian cells. Cell *128*, 577-587.

Kaplan, R.E.W., Maxwell, C.S., Codd, N.K., and Baugh, L.R. (2019). Pervasive positive and negative feedback regulation of insulin-like signaling in *Caenorhabditis elegans*. Genetics *211*, 349-361.

Kass, J., Jacob, T.C., Kim, P., and Kaplan, J.M. (2001). The EGL-3 proprotein convertase regulates mechanosensory responses of Caenorhabditis elegans. J Neurosci *21*, 9265-9272.

Kenyon, C. (2005). The plasticity of aging: insights from long-lived mutants. Cell *120*, 449-460.

Kim, S., and Paik, Y.-K. (2008). Developmental and reproductive consequences of prolonged non-aging dauer in *Caenorhabditis elegans*. Biochem Biophys Res Commun *368*, 588-592.

Kimble, J., and White, J. (1981). On the control of germ cell development in Caenorhabditis elegans. Developmental biology *81*, 208-219.

Kimura, K.D., Tissenbaum, H.A., Liu, Y., and Ruvkun, G. (1997). *daf-2*, an insulin receptor-like gene that regulates longevity and diapause in Caenorhabditis elegans. Science *277*, 942-946.

Koch, C., Massimini, M., Boly, M., and Tononi, G. (2016). Neural correlates of consciousness: progress and problems. Nat Rev Neurosci *17*, 307-321.

Lee, R.C., and Ambros, V. (2001). An Extensive Class of Small RNAs in Caenorhabditis elegans. Science *294*, 862-864.

Li, C., Nelson, L.S., Kim, K., Nathoo, A., and Hart, A.C. (1999). Neuropeptide gene families in the nematode Caenorhabditis elegans. Ann N Y Acad Sci *897*, 239-252.

Li, W., Kennedy, S.G., and Ruvkun, G. (2003). daf-28 encodes a C. elegans insulin superfamily member that is regulated by environmental cues and acts in the DAF-2 signaling pathway. Genes & development *17*, 844-858.

Liberzon, I., and Sripada, C.S. (2007). The functional neuroanatomy of PTSD: a critical review. In Progress in Brain Research, E.R. De Kloet, M.S. Oitzl, and E. Vermetten, eds. (Elsevier), pp. 151-169.

Lipton, D.M., Maeder, C.I., and Shen, K. (2018). Rapid assembly of presynaptic materials behind the growth cone in dopaminergic neurons is mediated by precise regulation of axonal transport. Cell Rep *24*, 2709-2722.

MacNamara, A., DiGangi, J., and Phan, K.L. (2016). Aberrant spontaneous and task-dependent functional connections in the anxious brain. Biological Psychiatry: Cognitive Neuroscience and Neuroimaging *1*, 278-287.

Malaisse, W.J., Malaisse-Lagae, F., Lacy, P.E., and Wright, P.H. (1967). Insulin secretion by isolated islets in presence of glucose, insulin and anti-insulin serum. Proc Soc Exp Biol Med *124*, 497-500.

Mandolesi, L., Gelfo, F., Serra, L., Montuori, S., Polverino, A., Curcio, G., and Sorrentino, G. (2017). Environmental Factors Promoting Neural Plasticity: Insights from Animal and Human Studies. Neural Plast *2017*, 7219461.

Marcovecchio, M.L., and Chiarelli, F. (2012). The effects of acute and chronic stress on diabetes control. Sci Signal *5*, pt10.

Marie Hall, N., and Berntsen, D. (2008). The effect of emotional stress on involuntary and voluntary conscious memories. Memory *16*, 48-57.

Maya-Vetencourt, J.F., Baroncelli, L., Viegi, A., Tiraboschi, E., Castren, E., Cattaneo, A., and Maffei, L. (2012). IGF-1 restores visual cortex plasticity in adult life by reducing local GABA levels. Neural Plast *2012*, 250421.

McEwen, B.S. (1998). Stress, adaptation, and disease: Allostasis and allostatic load. Annals of the New York academy of sciences *840*, 33-44.

McEwen, B.S. (2003). Interacting mediators of allostasis and allostatic load: towards an understanding of resilience in aging. Metabolism *52*, 10-16.

McEwen, B.S., and Morrison, J.H. (2013). The brain on stress: vulnerability and plasticity of the prefrontal cortex over the life course. Neuron *79*, 16-29.

Messitt, T.J., Gagnon, J.A., Kreiling, J.A., Pratt, C.A., Yoon, Y.J., and Mowry, K.L. (2008). Multiple kinesin motors coordinate cytoplasmic RNA transport on a subpopulation of microtubules in *Xenopus* oocytes. Dev Cell *15*, 426-436.

Mignone, F., Gissi, C., Liuni, S., and Pesole, G. (2002). Untranslated regions of mRNAs. Genome Biol *3*, REVIEWS0004-REVIEWS0004.

Minevich, G., Park, D.S., Blankenberg, D., Poole, R.J., and Hobert, O. (2012). CloudMap: a cloud-based pipeline for analysis of mutant genome sequences. Genetics *192*, 1249-1269.

Miranda-Vizuete, A., Fierro Gonzalez, J.C., Gahmon, G., Burghoorn, J., Navas, P., and Swoboda, P. (2006). Lifespan decrease in a Caenorhabditis elegans mutant lacking TRX-1, a thioredoxin expressed in ASJ sensory neurons. FEBS Lett *580*, 484-490.

Morest, D.K. (1971). Dendrodendritic synapses of cells that have axons: the fine structure of the Golgi type II cell in the medial geniculate body of the cat. Z Anat Entwicklungsgesch *133*, 216-246.

Mori, I., and Ohshima, Y. (1997). Molecular neurogenetics of chemotaxis and thermotaxis in the nematode Caenorhabditis elegans. BioEssays *19*, 1055-1064.

Mukhopadhyay, A., Oh, S.W., and Tissenbaum, H.A. (2006). Worming pathways to and from DAF-16/FOXO. Experimental gerontology *41*, 928-934.

Murphy, C.T.a.H., Patrick J. (2013). Insulin/insulin-like growth factor signaling in C. elegans. The C elegans Research Community, WormBook *10.1895/wormbook.1.164.1*, 1551-8507.

National_Research_Council (1989). Opportunities in Biology. Book *The nervous system and behaviour*.

Nonet, M.L., Saifee, O., Zhao, H., Rand, J.B., and Wei, L. (1998). Synaptic transmission deficits in Caenorhabditis elegans synaptobrevin mutants. J Neurosci *18*, 70-80.

Oh, S.W., Mukhopadhyay, A., Svrzikapa, N., Jiang, F., Davis, R.J., and Tissenbaum, H.A. (2005). JNK regulates lifespan in Caenorhabditis elegans by modulating nuclear translocation of forkhead transcription factor/DAF-16. Proceedings of the National Academy of Sciences of the United States of America *102*, 4494.

Parry, J.M., Velarde, N.V., Lefkovith, A.J., Zegarek, M.H., Hang, J.S., Ohm, J., Klancer, R., Maruyama, R., Druzhinina, M.K., and Grant, B.D. (2009). EGG-4 and EGG-5 link events of the oocyte-to-embryo transition with meiotic progression in C. elegans. Current Biology *19*, 1752-1757.

Pawley, J.B. (2006). Handbook of biological confocal microscopy, 3rd edn (New York, NY: Springer).

Peden, E.M., and Barr, M.M. (2005). The KLP-6 kinesin is required for male mating behaviors and polycystin localization in *Caenorhabditis elegans*. Curr Biol *15*, 394-404.

Pierce, S.B., Costa, M., Wisotzkey, R., Devadhar, S., Homburger, S.A., Buchman, A.R., Ferguson, K.C., Heller, J., Platt, D.M., Pasquinelli, A.A.*, et al.* (2001). Regulation of

DAF-2 receptor signaling by human insulin and ins-1, a member of the unusually large and diverse C. elegans insulin gene family. Genes Dev *15*, 672-686.

Plotnik, J.M., de Waal, F.B., Moore, D., 3rd, and Reiss, D. (2010). Self-recognition in the Asian elephant and future directions for cognitive research with elephants in zoological settings. Zoo Biol *29*, 179-191.

Plotnik, J.M., de Waal, F.B., and Reiss, D. (2006). Self-recognition in an Asian elephant. Proc Natl Acad Sci U S A *103*, 17053-17057.

Procko, C., Lu, Y., and Shaham, S. (2011). Glia delimit shape changes of sensory neuron receptive endings in C. elegans. Development *138*, 1371-1381.

Quinault, A., Leloup, C., Denwood, G., Spiegelhalter, C., Rodriguez, M., Lefebvre, P., Messaddeq, N., Zhang, Q., Dacquet, C., Penicaud, L.*, et al.* (2018). Modulation of large dense core vesicle insulin content mediates rhythmic hormone release from pancreatic beta cells over the 24h cycle. PLoS One *13*, e0193882.

Raj, A., and Tyagi, S. (2010). Detection of individual endogenous RNA transcripts in situ using multiple singly labeled probes. Methods Enzymol *472*, 365-386.

Rees, G., Kreiman, G., and Koch, C. (2002). Neural correlates of consciousness in humans. Nat Rev Neurosci *3*, 261-270.

Riddle, D.L., and Albert, P.S. (1997). Genetic and Environmental Regulation of Dauer Larva Development. In C elegans II, nd, D.L. Riddle, T. Blumenthal, B.J. Meyer, and J.R. Priess, eds. (Cold Spring Harbor (NY)).

Riddle, D.L., Swanson, M.M., and Albert, P.S. (1981). Interacting genes in nematode dauer larva formation. Nature *290*, 668-671.

Rinderknecht, E., and Humbel, R.E. (1978). The amino acid sequence of human insulin-like growth factor I and its structural homology with proinsulin. J Biol Chem *253*, 2769-2776.

Sakamoto, R., Byrd, D.T., Brown, H.M., Hisamoto, N., Matsumoto, K., and Jin, Y. (2005a). The Caenorhabditis elegans UNC-14 RUN domain protein binds to the kinesin-1 and UNC-16 complex and regulates synaptic vesicle localization. Mol Biol Cell *16*, 483-496.

Sakamoto, R., Byrd, D.T., Brown, H.M., Hisamoto, N., Matsumoto, K., and Jin, Y. (2005b). The *Caenorhabditis elegans* UNC-14 RUN domain protein binds to the Kinesin-1 and UNC-16 complex and regulates synaptic vesicle localization. Mol Biol Cell *16*, 483-496.

Schackwitz, W.S., Inoue, T., and Thomas, J.H. (1996). Chemosensory neurons function in parallel to mediate a pheromone response in C. elegans. Neuron *17*, 719-728.

Schindelin, J., Arganda-Carreras, I., Frise, E., Kaynig, V., Longair, M., Pietzsch, T., Preibisch, S., Rueden, C., Saalfeld, S., Schmid, B.*, et al.* (2012). Fiji: an open-source platform for biological-image analysis. Nature Methods *9*, 676.

Schneeberger, K. (2014). Using next-generation sequencing to isolate mutant genes from forward genetic screens. Nature Reviews Genetics *15*, 662.

Scholey, J.M. (2013). Kinesin-2: a family of heterotrimeric and homodimeric motors with diverse intracellular transport functions. Annu Rev Cell Dev Biol *29*, 443-469.

Schroeder, N.E., Androwski, R.J., Rashid, A., Lee, H., Lee, J., and Barr, M.M. (2013). Dauer-specific dendrite arborization in *C. elegans* is regulated by KPC-1/Furin. Curr Biol *23*, 1527-1535.

Sega, G.A. (1984). A review of the genetic effects of ethyl methanesulfonate. Mutation research *134*, 113-142.

Selye, H. (1950). Stress and the general adaptation syndrome. British medical journal *1*, 1383.

Selye, H. (1993). History of the stress concept.

Seth, A.K., Dienes, Z., Cleeremans, A., Overgaard, M., and Pessoa, L. (2008). Measuring consciousness: relating behavioural and neurophysiological approaches. Trends in cognitive sciences *12*, 314-321.

Shaham, S. (2006). Glia–neuron interactions in the nervous system of Caenorhabditis elegans. Current Opinion in Neurobiology *16*, 522-528.

Shen, K., and Bargmann, C.I. (2003). The immunoglobulin superfamily protein SYG-1 determines the location of specific synapses in *C. elegans*. Cell *112*, 619-630.

Shin, L.M., and Liberzon, I. (2010). The neurocircuitry of fear, stress, and anxiety disorders. Neuropsychopharmacology : official publication of the American College of Neuropsychopharmacology *35*, 169-191.

Sibarita, J.B. (2005). Deconvolution microscopy. Adv Biochem Eng Biotechnol *95*, 201-243.

Siddiqui, S.S. (2002). Metazoan motor models: kinesin superfamily in *C. elegans*. Traffic *3*, 20-28.

Simpkin, K.G., and Coles, G.C. (1981). The use of Caenorhabditis elegans for anthelmintic screening. J Chem Technol Biotechnol *31*, 66-69.

Singh, R., and Sulston, J. (1978). Some observations on molting in C. elegans. Nematologica *24*, 63-71.

Smith, H.E., and Yun, S. (2017). Evaluating alignment and variant-calling software for mutation identification in C. elegans by whole-genome sequencing. PLoS One *12*, e0174446.

Snutch, T.P., and Baillie, D.L. (1983). Alterations in the pattern of gene expression following heat shock in the nematode Caenorhabditis elegans. Can J Biochem Cell Biol *61*, 480-487.

Spaulding, E.L., and Burgess, R.W. (2017). Accumulating evidence for axonal translation in neuronal homeostasis. Front Neurosci *11*, 312.

Steiner, D.F. (1998). The proprotein convertases. Current Opinion in Chemical Biology *2*, 31-39.

Stewart, J.C., Villasmil, M.L., and Frampton, M.W. (2007). Changes in fluorescence intensity of selected leukocyte surface markers following fixation. Cytometry A *71*, 379-385.

Sumakovic, M., Hegermann, J., Luo, L., Husson, S.J., Schwarze, K., Olendrowitz, C., Schoofs, L., Richmond, J., and Eimer, S. (2009). UNC-108/RAB-2 and its effector RIC-19 are involved in dense core vesicle maturation in *Caenorhabditis elegans*. J Cell Biol *186*, 897-914.

Swanson, M.M., and Riddle, D.L. (1981). Critical periods in the development of the Caenorhabditis elegans dauer larva. Dev Biol *84*, 27-40.

Tabish, M., Kidwai Siddiqui, Z., Nishikawa, K., and Siddiqui, S.S. (1995). Exclusive expression of *C. elegans osm-3* kinesin gene in chemosensory neurons open to the external environment. J Mol Biol *247*, 377-389.

Tautz, D., and Pfeifle, C. (1989). A non-radioactive in situ hybridization method for the localization of specific RNAs in Drosophila embryos reveals translational control of the segmentation gene hunchback. Chromosoma *98*, 81-85.

Thacker, C., and Rose, A.M. (2000). A look at the Caenorhabditis elegans Kex2/Subtilisin-like proprotein convertase family. Bioessays *22*, 545-553.

Thio, G.L., Ray, R.P., Barcelo, G., and Schupbach, T. (2000). Localization of *gurken* RNA in Drosophila oogenesis requires elements in the 5' and 3' regions of the transcript. Developmental biology *221*, 435-446.

Tie, M. (1997). The problem of simple minds: Is there anything it is like to be a honey bee? Philosophical Studies *88*, 289-317.

Tiengo, M. (2003). Pain perception, brain and consciousness. Neurol Sci *24 Suppl 2*, S76-79.

Tiffin, N., Kelso, J.F., Powell, A.R., Pan, H., Bajic, V.B., and Hide, W.A. (2005). Integration of text-and data-mining using ontologies successfully selects disease gene candidates. Nucleic acids research *33*, 1544-1552.

Tononi, G., and Koch, C. (2008). The neural correlates of consciousness: an update. Ann N Y Acad Sci *1124*, 239-261.

Van Auken, K., Weaver, D., Robertson, B., Sundaram, M., Saldi, T., Edgar, L., Elling, U., Lee, M., Boese, Q., and Wood, W.B. (2002). Roles of the Homothorax/Meis/Prep homolog UNC-62 and the Exd/Pbx homologs CEH-20 and CEH-40 in C. elegans embryogenesis. Development *129*, 5255-5268.

Van Nostrand, E.L., Sánchez-Blanco, A., Wu, B., Nguyen, A., and Kim, S.K. (2013). Roles of the developmental regulator unc-62/Homothorax in limiting longevity in Caenorhabditis elegans. PLoS genetics *9*, e1003325-e1003325.

Wadsworth, W.G., and Riddle, D.L. (1989). Developmental regulation of energy metabolism in Caenorhabditis elegans. Dev Biol *132*, 167-173.

Wang, J., and Kim, S.K. (2003). Global analysis of dauer gene expression in Caenorhabditis elegans. Development *130*, 1621-1634.

Wang, Y., Ezemaduka, A.N., Tang, Y., and Chang, Z. (2009). Understanding the mechanism of the dormant dauer formation of C. elegans: from genetics to biochemistry. IUBMB life *61*, 607-612.

Ward, S., Thomson, N., White, J.G., and Brenner, S. (1975). Electron microscopical reconstruction of the anterior sensory anatomy of the nematode Caenorhabditis elegans.?2UU. J Comp Neurol *160*, 313-337.

Ware, R.W., Clark, D., Crossland, K., and Russell, R.L. (1975). The nerve ring of the nematode Caenorhabditis elegans: Sensory input and motor output. Journal of Comparative Neurology *162*, 71-110.

White, J.G., Albertson, D.G., and Anness, M.A.R. (1978). Connectivity changes in a class of motoneurone during the development of a nematode. Nature *271*, 764-766.

White, J.G., Southgate, E., Thomson, J.N., and Brenner, S. (1986). The structure of the nervous system of the nematode Caenorhabditis elegans. Philos Trans R Soc Lond B Biol Sci *314*, 1-340.

Wiederman, S.D., and O'Carroll, D.C. (2013). Selective attention in an insect visual neuron. Curr Biol *23*, 156-161.

Wigglesworth, V.B. (1960). Axon structure and the dictyosomes (Golgi bodies) in the neurones of the cockroach, *Periplaneta americana*. J Cell Sci *s3-101*, 381-388.

Wilkinson, T.N., Speed, T.P., Tregear, G.W., and Bathgate, R.A. (2005). Evolution of the relaxin-like peptide family: from neuropeptide to reproduction. Ann N Y Acad Sci *1041*, 530-533.

Willis, D.E., Xu, M., Donnelly, C.J., Tep, C., Kendall, M., Erenstheyn, M., English, A.W., Schanen, N.C., Kirn-Safran, C.B., Yoon, S.O.*, et al.* (2011). Axonal localization of transgene mRNA in mature PNS and CNS neurons. J Neurosci *31*, 14481-14487.

Wojnarowicz, M.W., Fisher, A.M., Minaeva, O., and Goldstein, L.E. (2017). Considerations for Experimental Animal Models of Concussion, Traumatic Brain Injury, and Chronic Traumatic Encephalopathy-These Matters Matter. Frontiers in neurology *8*, 240-240.

Xia, X., Lessmann, V., and Martin, T.F.J. (2009). Imaging of evoked dense-core-vesicle exocytosis in hippocampal neurons reveals long latencies and kiss-and-run fusion events. Journal of Cell Science *122*, 75-82.

Zeng, Y., Zhang, L., and Hu, Z. (2016). Cerebral insulin, insulin signaling pathway, and brain angiogenesis. Neurol Sci *37*, 9-16.

Zhang, Y., Lu, H., and Bargmann, C.I. (2005). Pathogenic bacteria induce aversive olfactory learning in Caenorhabditis elegans. Nature *438*, 179.

Zhao, H., and Nonet, M.L. (2000). A retrograde signal is involved in activity-dependent remodeling at a *C. elegans* neuromuscular junction. Development *127*, 1253-1266.

Zuker, M. (2003). Mfold web server for nucleic acid folding and hybridization prediction. Nucleic acids research *31*, 3406-3415.

Zuryn, S., Le Gras, S., Jamet, K., and Jarriault, S. (2010). A strategy for direct mapping and identification of mutations by whole-genome sequencing. Genetics *186*, 427-430.

ABSTRACT

STRESS-DEPENDENT REGULATION OF A MAJOR NODE OF THE INSULIN-LIKE PEPTIDE NETWORK THAT MODULATES SURVIVAL

by

RASHMI CHANDRA

August 2019

Advisor: Dr. Joy Angelie Alcedo

Major: Biological Sciences

Degree: Doctor of Philosophy

Chronic stress disrupts insulin signaling, predisposing human populations to diabetes, cardiovascular disease, Alzheimer's Disease, and other metabolic and neurological disorders, including post-traumatic disorders (PTSD). Thus, efficient recovery from stress optimizes survival. However, stress recovery in humans is difficult to study, but is much easier to dissect in model organisms. The worm genetic model *Caenorhabditis elegans* can switch between stressed and non-stressed states, and this switch is largely regulated by insulin signaling. Previously, the Alcedo lab proposed that insulin-like peptides (ILPs), which exist as multiple members of a protein family in both *C. elegans* and humans, implements a combinatorial coding strategy to control the switch between the two physiological states. The concept of combinatorial coding has led to the identification of an inter-ILP network, where one ILP, *ins-6*, is a major node of the network. This is consistent with *ins-6* as the most pleotropic of all ILPs that have been tested. *ins-6* has also been shown to be the most important ILP in promoting stress recovery in *C. elegans*. Because of its central role in the ILP network and in stress recovery, for my thesis I identified mechanisms through which INS-6 regulates the network and an animal's recovery from stress.

Under optimal environments, *ins-6* mRNA is endogenously expressed in the cell

bodies of one or two chemosensory neurons, ASI and ASJ, in the developing animal. However, upon stress-induced developmental arrest, known as dauer, *ins-6* mRNA is only limited to the ASJ sensory neurons. I discovered that *ins-6* mRNA from ASJ is also surprisingly transported to the axonal nerve ring bundle of stressed animals, but lost from the nerve ring after recovery from stress. Consistent with the existence of an inter-ILP network, insulin signaling regulates *ins-6* mRNA transport, which also requires the activities of specific kinesins. This transport additionally depends on the untranslated regions of *ins-6* mRNA, but these regions are insufficient for transport. More importantly and in collaboration with other members of the Alcedo lab, we showed that axonal *ins-6* mRNA facilitates stress recovery, where high axonal *ins-6* mRNA promotes faster recovery and low axonal *ins-6* mRNA delays recovery. Moreover, I demonstrated the existence of axonal Golgi bodies, whose mobilization are enhanced during stress. Together my data suggest that stress stimulates the axonal transport of ILP mRNAs, which are then locally translated and packaged for secretion--a mechanism that promotes plasticity during stress and optimal stress recovery.

To identify additional regulators of *ins-6* mRNA, I also performed, together with other members of the lab, a forward genetic screen for mutants that alter *ins-6* transcription during stress. Through whole-genome sequencing, one of the five mutants we isolated is potentially a mutation in an innexin gap junction protein. Since innexins have been shown to regulate neural activity, I tested the hypothesis that neural activity will also affect axonal *ins-6* mRNA transport. Interestingly, I found that a synaptic transmission mutant, which should have low neural activity, increases axonal *ins-6* mRNA and alters neurite morphology.

My thesis study raises an intriguing hypothesis: stress modulates neurite activity and morphology, which in turn promote ILP mRNA transport to the axons. The axonal localization of an ILP mRNA also uncovers a novel mechanism of insulin signaling during

stress. Because of the high degree of conservation between *C. elegans* and humans and the effects of altered insulin signaling in stressed brains, my findings should advance our understanding of how a nervous system recovers from stress. The work described in this thesis should lead to potential therapies for stress management to promote better health.

AUTOBIOGRAPHICAL STATEMENT

RASHMI CHANDRA

EDUCATION

2019 Ph.D., Department of Biological Sciences, Wayne State University, USA
2008 M.Sc., Department of Biochemistry, University of Calcutta, India
2006 B.Sc., Department of Human Physiology, University of Calcutta, India
(Honors with distinction)

FELLOWSHIP

2018-2019 Thomas C. Rumble Fellowship, Graduate School, Wayne State University

HONORS/AWARDS

06/2019 Genetics Society of America's Travel Award, 22nd International C. elegans Conference, University of California Los Angeles
03/2018 Poster Prize in Graduate and Post-Doctoral Research Symposium, Wayne State University
06/2017 Travel award, Gordon Research Conference on Modulation of Neural Circuits and Behavior
06/2016 Travel award, Workshop on Applications of Microfluidics in C. elegans at Georgia Institute of Technology
03/2014 P. Dennis Smith Genetics Research Award, Department of Biological Sciences, Wayne State University, Michigan, USA
10/2013 Poster Prize, Annual Departmental Retreat, Department of Biological Sciences, Wayne State University
06/2010. National Merit Scholarship, University of Calcutta, University Grants Commission, Government of India
06/2008 Shanti Bhakta Award (M.Sc.), University of Calcutta, National Assessment and Accreditation Council, Government of India

PUBLICATIONS

1. Ostojic, I., Boll, W., Waterson, M. J., Chan, T., Chandra, R., Pletcher, S. D., & Alcedo, J. (2014).. Proc Natl Acad Sci USA 111(22), 8143–8148. doi:10.1073/pnas
2. Singh AS, Chandra R, Guhathakurta S, Sinha S, Chatterjee A, Ahmed S, Ghosh S, Rajamma U. (2013). Prog Neuropsychopharmacol Biol Psychiatry 45, 131-143. doi: 10.1016/j.pnpbp.2013.04.015. Epub 2013 Apr 2

SELECTED ORAL PRESENTATIONS

06/2019 22nd International *C. elegans* Conference, "Axonal transport of an insulin-like peptide mRNA promotes stress recovery in *C. elegans*", University of California Los Angeles (Platform talk)
06/2019 Workshop on Career Success: Strategies to Develop Visibility When You Prefer to be a Wallflower, 22nd International *C. elegans* Conference, University of California Los Angeles (Moderator)
06/2018 *C. elegans* topic meeting: Neuronal Development, Synaptic Function and Behavior, Ce Neuro 2018, University of Wisconsin
04/2018 6th Midwest C. elegans meeting, Eastern Michigan University
05/2016 Workshop: Applications of Microfluidics in *C. elegans*, Georgia Institute of Technology